

**IDENTIFICATION AND CHARACTERIZATION OF BIOACTIVE
LEADS FROM MANGROVE SEDIMENT
ASSOCIATED BACTERIA AND ASSESSMENT OF THEIR
THERAPEUTIC POTENTIAL**

By

**LAKSHMI RAJAN
(2014-09-103)**

THESIS

Submitted in partial fulfilment of the requirement for the degree of

B. Sc. - M. Sc. (INTEGRATED) BIOTECHNOLOGY

**Faculty of Agriculture
Kerala Agricultural University, Thrissur**



**DEPARTMENT OF PLANT BIOTECHNOLOGY
COLLEGE OF AGRICULTURE
VELLAYANI, THIRUVANANTHAPURAM - 695 522
KERALA, INDIA**

2019

DECLARATION

I, hereby declare that this thesis entitled “**IDENTIFICATION AND CHARACTERIZATION OF BIOACTIVE LEADS FROM MANGROVE SEDIMENT ASSOCIATED BACTERIA AND ASSESSMENT OF THEIR THERAPEUTIC POTENTIAL**” is a bonafide record of research work done by me during the course of research and the thesis has not previously formed the basis for the award to me of any degree, diploma, associateship, fellowship or other similar title, of any other University or Society.

Place: Kochi

Date: 22.11.19



LAKSHMI RAJAN

(2014-09-103)

CERTIFICATE

Certified that this thesis entitled **“IDENTIFICATION AND CHARACTERIZATION OF BIOACTIVE LEADS FROM MANGROVE SEDIMENT ASSOCIATED BACTERIA AND ASSESSMENT OF THEIR THERAPEUTIC POTENTIAL ”** is a record of research work done independently by Ms. Lakshmi Rajan (2014-09-103) under my guidance and supervision and that it has not previously formed the basis for the award of any degree, diploma, fellowship or associateship to her.

Place: Kochi
Date: 22-11-2019

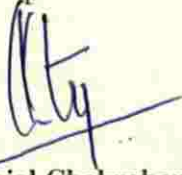


Dr. Kajal Chakraborty
(Chairman, Advisory Committee)
Senior scientist
Marine Biotechnology Division
ICAR-CMFRI,
Ernakulam North P. O.
Kochi – 682 018

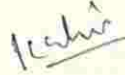
DR. KAJAL CHAKRABORTY
Senior Scientist (Marine Bio technology Division)
Central Marine Fisheries Research Institute
P B No. 1603, Ernakulam North P.O.
Cochin-682018, Kerala

CERTIFICATE

We, the undersigned members of the advisory committee of Ms. Lakshmi Rajan (2014-09-103), a candidate for the degree of B.Sc.-M.Sc. (Integrated) Biotechnology, agree that the thesis entitled “IDENTIFICATION AND CHARACTERIZATION OF BIOACTIVE LEADS FROM MANGROVE SEDIMENT ASSOCIATED BACTERIA AND ASSESSMENT OF THEIR THERAPEUTIC POTENTIAL” may be submitted by Ms. Lakshmi Rajan in partial fulfilment of the requirement for the degree.



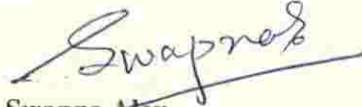
Dr. Kajal Chakraborty
(Chairman, Advisory Committee)
Senior Scientist
Marine Biotechnology Division
ICAR-CMFRI,
Ernakulam North P.O.,
Kochi-682 018



Dr. K. B. Soni
(Member, Advisory Committee)
Professor and Head
Department of Plant Biotechnology
College of Agriculture, Vellayani
Thiruvananthapuram-695 522



Dr. P. Vijayagopal
(Member, Advisory Committee)
Principal Scientist and Head
Marine Biotechnology Division
ICAR-CMFRI
Ernakulam North P. O.,
Kochi-682 018



Dr. Swapna Alex
(Member, Advisory Committee)
Professor and Course Director
B. Sc.-M. Sc. (Int.) Biotechnology
Department of Plant Biotechnology
College of Agriculture, Vellayani
Thiruvananthapuram-695 522



Dr. Veena S. S.
(External Examiner)
Principal Scientist (Plant Pathology)
Division of Crop Protection
Central Tuber Crops Research Institute
Sreekariyam, Thiruvananthapuram- 695 017

ACKNOWLEDGEMENT

On this occasion of my masters degree thesis, I realize that the successful completion of any task would be incomplete without acknowledging the people whose constant guidance and encouragement has crowned all the efforts with success. I am thankful to many people who have helped me through the completion of this thesis. With profound sense of gratitude, I express my utmost indebtedness to Dr. Kajal Chakraborty, Senior Scientist, (Marine Biotechnology Division of ICAR-Central Marine Fisheries Research Institute) who has been supportive throughout the work and for his excellent guidance, valuable suggestions, constant encouragement and support in preparation and compilation of the thesis.

I express my deepest gratitude to the advisory committee members, Dr. Swapna Alex (Professor and Head, Department of Plant Biotechnology, CoA), Dr. K. B. Soni (Professor, Department of Plant Biotechnology, CoA) for all their help and encouragement during my work. I sincerely express my gratitude to Dr. P. Vijayagopal, Principal Scientist and Head (Marine Biotechnology Division, ICAR-CMFRI) for providing me an opportunity and making available the department facilities.

I would like to express my sincere gratitude to Dr. Rekha Devi Chakraborty, Scientist, ICAR- CMFRI for her continuous support, patience and motivation. I am totally indebted to the help and suggestions, as well as her valuable advice in every aspect.

I take immense pleasure to express my deep sense of gratitude to Dr. A. Anilkumar (Dean, CoA, Vellayani) and Dr. A. Gopalakrishnan (Director, ICAR- CMFRI) for providing me the opportunity to embark on this project. I express my gratitude to Dr. Sumitra T. G. (Scientist, Marine Biotechnology Division) and all my dear teachers for their meaningful suggestions and inspirational words.

I express my sincere gratitude to all the staff and students of Marine Biotechnology Division who rendered their help during the period of my project work. I express my deep sense of gratitude to Prima Francis for

her valuable suggestions, support and help extended towards compiling my spectroscopic studies. I am very much obliged to Ms. Vinaya K. K. for her talented guidance, valuable suggestions, thoughtful criticism and constant encouragement throughout my project. I would like to thank Sumayya Asharaf and Mr. Chandru who helped me in sample collection. A special word of gratitude is due to Dr. Bini Thilakan who shared her valuable experience and knowledge for molding the project. I am thankful to, Mrs. Archana, Dr. Minju Joy, Ms. Tima Antony, Ms. Silpa K. P., Ms. Vishnupriya, Anjali Thambi, Subhajith Dhara, Ms. Haripriya, Dr. Aswathy Elizabeth Mani, Mr. Purushothaman and Mr. Kuber Vijay for their consistent support and suggestions.

Last but not the least, I thank my entire family for their support and encouragement. I would like to thank my father, Rajan A. K. and mother, Swapna Rajan for their selfless sacrifice and great efforts with pain and tears and unceasing prayers which enabled me to successfully complete the research work. My special gratitude towards my sister Parvathy Rajan and grandmothers for their support and motivation. I would also like to extend my gratitude towards my classmates, cousins, relatives, neighbors and room mates

Above all, I bow before your Almighty.

Lakshmi Rajan

**DEDICATED TO
MY FAMILY**

TABLE OF CONTENTS

| Sl. No. | Chapters | Page No. |
|----------------|-----------------------|-----------------|
| 1 | INTRODUCTION | 1-4 |
| 2 | REVIEW OF LITERATURE | 5-24 |
| 3 | MATERIALS AND METHODS | 25-43 |
| 4 | RESULTS | 44-100 |
| 5 | DISCUSSION | 101-112 |
| 6 | SUMMARY | 113-117 |
| 7 | REFERENCES | 118-140 |
| 8 | ABSTRACT | 141-142 |

LIST OF TABLES

| Table No. | Title | Page No. |
|-----------|-----------------------------------------------------------------------------------------------|----------|
| 3.1 | Primer sequences used for 16S rRNA sequencing | 36 |
| 4.1 | Antimicrobial activity of isolates from samples S1 to S10 | 48 |
| 4.2 | Biochemical characteristics of the selected Isolates | 51-52 |
| 4.3 | Morphological characters of the selected isolates | 53 |
| 4.4 | Quality of DNA at absorbance 260/ 280 nm and quantity of DNA | 57 |
| 4.5 | GenBank accession numbers of the strains identified by NCBI | 60 |
| 4.6 | Antioxidant and anti-inflammatory activities of the crude bacterial extract | 68 |
| 4.7 | Inhibition zone diameter exhibited by the intracellular organic extract | 69 |
| 4.8 | Inhibition zone diameter exhibited by the extracellular organic extract | 70 |
| 4.9 | Structural characterization of polyketide compound (1) | 72 |
| 4.10 | NMR spectroscopic data of polyketide (1) in MeOD ^a | 74 |
| 4.11 | Structural characterization of polyketide compound (2) | 86 |
| 4.12 | NMR spectroscopic data of polyketide (2) in MeOD ^a | 88 |
| 4.13 | <i>In vitro</i> bioactive potentials (antioxidant and anti-inflammatory) of polyketides (1-2) | 100 |

LIST OF FIGURES

| Figure No. | Title | Between pages |
|------------|-------------------------------------------------------------------------------------------------------------------------------------------------------------------------------------------------------------------------------------------------------------------------------------------------------------------------------------------------------------------------------------------------------------------------------------------------------------------------------------------------------|---------------|
| 2.1 | (A) Mangrove sediments of Mangalavanam mangrove ecosystem at Kochi. (B) Soil sediment of Mangalavanam mangrove ecosystem used to isolate <i>B. licheniformis</i> MTCC 6824 | 8 |
| 2.2 | Bioactive compounds associated with <i>Bacillus</i> species | 12 |
| 2.3 | (A) Spot over lawn assay of <i>B. subtilis</i> MTCC 10403 culture against pathogenic <i>V. parahaemolyticus</i> MTCC 451 (B) Polyketide furanoterpenoids (1-4) isolated from <i>B. subtilis</i> MTCC 10403 and their antibacterial activities against <i>V. parahaemolyticus</i> MTCC 451 (C) Biosynthetic gene clusters (BGCs) in heterotrophic <i>B. subtilis</i> MTCC 10403 (D-F) The array of events in biosynthetic route of homologous furanoterpenoids with characteristic polyketide | 21-22 |
| 3.1 | (A) <i>A. officinalis</i> and (B) <i>A. ilicifolius</i> (C) Mangrove sediments of Mangalavanam (D) mangrove sediment associated bacteria | 27 |
| 4.1 | Serially diluted and spread plated nutrient agar plates from dilutions ranging from 10^{-1} and 10^{-7} from 1 to 7, respectively. | 46 |
| 4.2 | The streak cultures of bacteria from S1 to S9 in nutrient agar Plates from 1 to 9 respectively | 47 |
| 4.3 | Gram stained <i>Bacillus</i> isolates, S1A, S1C, S2A, S2B, S2C, S2D, S4A, S10B and S10C (1-9). | 49 |
| 4.4 | Control of biochemical characterization | 50 |
| 4.5 | Biochemical characterization of S2A (A), S4A (B), S10C (C), S1C(D) and S2D (E) | 50 |
| 4.6 | Catalase test for S2A (A) and catalase test of S10B (B) | 50 |
| 4.7 | Pie diagram representing the percentage of isolates which exhibited an inhibition zone ≥ 10 mm against various pathogens | 55 |

| | | |
|------|------------------------------------------------------------------------------------------------------------------------------------------------------|-------|
| 4.8 | Zone of clearance produced by S2A (A) and S10B (B) in DPPH sprayed filter papers incubated with bacteria | 55 |
| 4.9 | Gel profiles of the isolated DNA samples | 58 |
| 4.10 | Gel profile of the amplified, 16S rRNA gene of bacteria | 58-59 |
| 4.11 | Polyketide synthase product of <i>B. amyloliquefaciens</i> MK765025 | 59 |
| 4.12 | Phylogenetic analysis of isolated strains | 61 |
| 4.13 | Bacterial growth curve of <i>B. amyloliquefaciens</i> MK765025 at 660 nm | 62 |
| 4.14 | TLC chromatogram of the extracellular compounds from <i>B. amyloliquefaciens</i> MK765025 at 254 nm | 64 |
| 4.15 | TLC chromatogram of the extracellular compounds from <i>B. amyloliquefaciens</i> MK765025 at 365 nm | 65 |
| 4.16 | (A)TLC chromatogram of the extracellular compounds from <i>B. amyloliquefaciens</i> MK765025 stained with vanillin-sulphuric acid | 65 |
| | (B) TLC chromatogram of the extracellular compounds from <i>B. amyloliquefaciens</i> MK765025 stained with iodine | 65 |
| 4.17 | TLC chromatogram of the extracellular compounds from <i>B. amyloliquefaciens</i> MK765025 stained with DPPH | 66 |
| 4.18 | TLC chromatogram of the intracellular compounds from <i>B. amyloliquefaciens</i> MK765025 | 66 |
| 4.19 | TLC chromatogram of the intracellular compounds from <i>B. amyloliquefaciens</i> MK765025 stained with (A) iodine and (B) vanillin-sulphuric acid | 66 |
| 4.20 | HPTLC chromatogram of the extracellular compounds | 67 |
| 4.21 | The antimicrobial activity of the crude extract of <i>B. amyloliquefaciens</i> MK765025 against pathogenic bacteria | 70 |

| | | |
|------|------------------------------------------------------------------------------------------------------------------------|----|
| 4.22 | Absorption maxima of polyketide (1) | 73 |
| 4.23 | HPLC chromatogram of polyketide (1) | 73 |
| 4.24 | ^1H - ^1H COSY (bold-face red-bonds), selected HMBC double-barbed arrows) correlations of compound 1 | 74 |
| 4.25 | NOESY (coloured arrows) cross-peaks of the polyketide (1) | 75 |
| 4.26 | ^1H NMR spectrum of polyketide (1) | 76 |
| 4.27 | ^{13}C NMR spectrum of polyketide (1) | 77 |
| 4.28 | $^{135}\text{DEPT}$ NMR spectrum of polyketide(1) | 78 |
| 4.29 | ^1H - ^1H COSY NMR spectrum of polyketide (1) | 79 |
| 4.30 | HSQC NMR spectrum of polyketide (1) | 80 |
| 4.31 | HMBC NMR spectrum of polyketide (1) | 81 |
| 4.32 | NOSEY spectrum of polyketide (1) | 82 |
| 4.33 | FT-IR spectrum of polyketide (1) | 83 |
| 4.34 | GCMS spectrum of polyketide (1) | 84 |
| 4.35 | Mass fragmentation pattern of polyketide (1) | 85 |
| 4.36 | Absorption maximum of polyketide (2) | 87 |
| 4.37 | HPLC chromatogram of polyketide (2) | 87 |
| 4.38 | ^1H - ^1H COSY (bold-face red-bonds), selected HMBC double-barbed arrows) correlations of compound 2 | 89 |
| 4.39 | NOESY (coloured arrows) cross-peaks of the polyketide (2) | 89 |
| 4.40 | ^1H NMR spectrum of polyketide (2) | 90 |
| 4.41 | ^{13}C NMR spectrum of polyketide (2) | 91 |
| 4.42 | $^{135}\text{DEPT}$ NMR spectrum of polyketide (2) | 92 |

| | | |
|------|-----------------------------------------------------------------|-----|
| 4.43 | ^1H - ^1H COSY NMR spectrum of polyketide (2) | 93 |
| 4.44 | HSQC NMR spectrum of polyketide (2) | 94 |
| 4.45 | HMBC NMR spectrum polyketide (2) | 95 |
| 4.46 | NOSEY spectrum of polyketide (2) | 96 |
| 4.47 | FT-IR spectrum of compound of polyketide (2) | 97 |
| 4.48 | GCMS spectrum of polyketide (2) | 98 |
| 4.49 | Mass fragmentation pattern of polyketide (2) | 99 |
| 5.1 | Polyketide compounds isolated from <i>B. amyloliquefaciens</i> | 111 |

LIST OF ABBREVIATIONS

| | |
|--------------------|---------------------------------------------------------|
| % | Percentage |
| °C | Degree Celsius |
| μL | Microlitre |
| μM | Micromolar |
| ABTS | 2,2'-Azino-bis(3-ethylbenzothiazoline-6-sulphonic acid) |
| BLAST | Basic Local Alignment Search Tool |
| bp | Basepair |
| CDCl ₃ | Deuterated chloroform |
| cm | Centimetre |
| DEPT | Distortionless Enhancement by Polarization Transfer |
| DNA | Deoxyribo Nucleic Acid |
| DPPH | 2, 2-Diphenyl-1-picrylhydrazyl |
| EtOH | Ethanol |
| G | Gram |
| GCMS | Gas Chromatography Mass Spectrometry |
| ¹ H NMR | Proton Nuclear Magnetic Resonance Spectroscopy |
| h | Hour |
| HMBC | Heteronuclear Multiple Bond Correlation |
| HPLC | High Performance Liquid Chromatography |
| HSQC | Heteronuclear Single Quantum Coherence |
| IC ₅₀ | Half Maximal Inhibitory Concentration of the Population |
| IR | Infra Red |
| LOX | Lipoxygenase |
| MeOH | Methanol |
| mg | Milligram |
| MgCl ₂ | Magnesium Chloride |
| MIC | Minimum Inhibitory Concentration |
| Min | Minute |
| mL | Millilitre |
| mm | Millimetre |

| | |
|-------|-----------------------------------------|
| mM | Millimolar |
| m/z | Mass to charge ratio |
| ng | Nanogram |
| nm | Nanometre |
| NMR | Nuclear Magnetic Resonance Spectroscopy |
| no. | Number |
| nos | Numbers |
| NOESY | Nuclear Overhauser Effect Spectroscopy |
| PCR | Polymerase Chain Reaction |
| PVP | Polyvinyl pyrrolidone |
| Rf | Retention factor |
| RNase | Ribonuclease |
| ROS | Reactive Oxygen Species |
| Rpm | Revolution Per Minute |
| s | Seconds |
| sp | Species |
| TE | Tris EDTA |
| TLC | Thin Layer Chromatography |
| U | Enzyme Unit |
| UV | Ultra Violet |
| V | Volt |

INTRODUCTION

1.INTRODUCTION

Mangroves are woody halophytes, which have been traditionally used for food, fuel, timber and medicine, were reported to occur in the tropical and sub-tropical latitudes exhibiting a marked degree of tolerance to high salt concentrations and soil anoxia. (Kathiresan and Bingham, 2001; Alongi, 2002; Saenger, 2013). They are called as 'coastal woodlands', 'tidal forests' or 'mangals' in Sanskrit (Saenger, 2013). They were reported to cover between 60 and 75% of the world's tropical and sub-tropical coastlines (Holguin *et al.*, 2001). India has a total mangrove cover of 4628 sq. km, which is 0.14% of the country's total geographical area.

Despite being fragile and sparsely distributed, continuous changes in salinity, inter-tidal fluctuations and anoxygenic conditions make a mangrove ecosystem highly productive (Thatoi and Biswal, 2008; Hong *et al.*, 2009; Youssef and Saenger, 1998; 1999; Lee *et al.*, 2014). A large number of bacteria with high diversity survive under such conditions and produce fascinating and structurally complex natural products, which could be isolated and evaluated for possible drug development with suitable biotechnology tools (Zhang *et al.* 2009). The continuous quest for natural compounds for treating human diseases have paved way for the discovery of drugs and high-value pharmacophore leads from the microbes especially from marine environment. The explorations of previously unfathomed spaces are required for finding novel therapeutic candidates, and the advances are quite promising.

During the recent years, the bacterial communities associated with mangroves have sought the attention of natural product discoverers mainly due to the polyketide type of compounds produced by them due to their biomedical and agricultural importance (Uzair *et al.*, 2008). To date, only a small range of bacteria are investigated for bioactive compounds, yet a huge number of active substances have been isolated that could be used as anticancer, anti-inflammatory and antimicrobial agents. A significant diversity of natural compounds is derived

from bacteria, which are an unlimited source of potential drugs and they were more accessible in industrial quantities as compared to plant derived metabolites. Many important groups of pharmaceutical compounds were found to be associated with Firmicutes, such as *Bacillus subtilis* and *Bacillus amyloliquefaciens* (Armstrong *et al.*, 2001; Goecke *et al.*, 2010; Thilakan *et al.*, 2016). Lipopeptides such as iturin in *Bacillus subtilis* exhibited significant antibacterial, antiviral, anti-inflammatory and anticancer activities (Zhao *et al.*, 2017; 2018). Surfactin and fengycin are other lipopeptides associated with *Bacillus* species showing significant anticancer activities (Kim *et al.*, 2007; Yin *et al.*, 2013).

The investigations of mangrove associated bacteria for bioactive compounds are higher in *Streptomyces* species worldwide, even though there have been focuses on other less explored strains to develop high-value products (Ser *et al.*, 2015). The mangrove associated bacteria were characterized based on microbiological, molecular and biochemical tools. The potential antibacterial and antioxidant strains were selected by preliminary screening methods. The organic extracts prepared from *B. amyloliquefaciens* was further screened for potential antimicrobial, antioxidant and anti-inflammatory compounds.

The mangrove associated bacterial communities, particularly *B. amyloliquefaciens* were potential sources of bioactive metabolites with pharmacological significance. However, there were meager reports on the bioactive compounds isolated from *B. amyloliquefaciens*, and no extensive studies were performed on their therapeutic potentials. Therefore, in the current scenario of increasing lethal diseases, further investigation of bioactive leads from this group of bacteria is essential. Thus, the present study aimed to develop the culture-dependent methods to assess the cultivable bacterial communities associated with mangrove ecosystem, and to explore them as a source for potentially useful pharmaceutically active compounds. The potential of the bacterial communities associated with mangrove ecosystem to produce bioactive metabolites were phylogenetically analyzed by polymerase chain reaction

employing the amplifying gene encodings for functional gene. The bioactive compounds were characterized by exhaustive spectroscopic techniques and evaluated for antibacterial, anti-inflammatory and anti-oxidant properties. Consequently, the objectives of the current study on “identification and characterization of bioactive leads from mangrove sediment associated bacteria and assessment of their therapeutic potential” were envisaged as follows:

- (1) To evaluate mangrove sediment-associated bacterial phyla and their pharmaceutical potential for antioxidant, antibacterial and anti-inflammatory properties.
- (2) To identify the microbial diversity of mangrove sediment associated bacteria by microbiological, molecular and chemical characterization.
- (3) To isolate and characterize bioactive leads with selective pharmacological properties.
- (4) *In vitro* validation of the target bioactive properties of the pharmacologically active leads.

The research programme would help to identify the therapeutic potential of mangrove sediment associated bacteria and pool of bioactive pharmacophores for future use.

REVIEW OF LITERATURE

2. REVIEW OF LITERATURE

2.1. MANGROVES

Mangroves are tropical and subtropical shrubs or trees that occur in the coastal areas. They tolerate high stress conditions like salinity, low oxygen conditions and inter-tidal fluctuations (ISFR, 2017). The term “mangrove” is also utilized to designate halophytic (salt tolerant) and salt-resistant marine tidal forests comprising of shrubs, ground ferns, palms, trees, epiphytes and grasses, which are associated in stands or groves. These unique ecological constraints prevailing in the ecosystem would make them highly productive (Wu *et al.*, 2008; Tomlinson, 2016). The mangroves are distributed in 123 countries globally, mostly flanked by latitudes 30° N and 30° S (ISFR, 2017; Ancheeva *et al.*, 2018). Asia sheltered the largest mangroves in the world and especially India alone contributes over 3 % of the global mangrove habitat. The total mangrove cover in the world is about 1, 50, 000 sq. km. where India contributes 3.3 % of the total mangrove coverage (Ashokkumar and Irfan, 2018). The mangrove forest distributed in India is about 4921 sq. km, where Gujarat covers the highest area of mangrove forest, followed by Maharashtra, West Bengal and Odisha (FSOI, 2015; Ashokkumar and Irfan, 2018). In Kerala, the mangroves are spread mainly in Kannur, Ernakulam and Kasaragod in which Ernakulam contributes 22 % of the total mangrove cover in the state (ISFR, 2017). Ernakulam was found to host a total of 10 mangrove species, which has been the maximum number among the 10 coastal districts of Kerala (Nambudiri, 2018). The most abundant species identified was *Avicennia officinalis* L. (35 %) followed by *Acanthus ilicifolius* (20 %) and *Rhizophora mucronata* (18 %) by a survey conducted by Cochin University of Science and Technology in Ernakulam mangrove ecosystem.

2.2. MANGROVES AND MANGROVE SEDIMENT ASSOCIATED BACTERIA AS BIOACTIVE SOURCES

Mangroves are widely known as medicinal plants for various human diseases from the ancient period, due to the presence of the biologically active novel compounds present in them (Bhimba *et al.*, 2010), and these were proved to have traditional and medicinal uses (Bandaranayake, 2002; Cragg and Newman, 2011). These species were used as traditional medicine in the treatment of diabetes, diarrhea, dysentery, blood in urine, fever, angina, diabetes and hemorrhage. In India, the

bark of mangrove plants were used for diabetes and old leaves as decoction at child birth (Kusuma *et al.*, 2011). These plants were found to be rich sources of secondary metabolites, such as triterpens, alkaloids, saponins, steroids, flavonoids and tannins. The extracts prepared from the mangrove plants were reported to possess diverse medicinal properties with activity against human, plant and animal pathogens (Bandaranayake, 2002). More specifically, *Rhizophoraceae* and *Acanthaceae* family were well documented for their phytochemical properties (Nebula *et al.*, 2013).

Mangrove and mangrove associates including the sediment associated bacterial flora were reported to contain biologically active compounds, such as triterpenes, saponins, flavonoids, alkaloids and tannins (Bandaranayake, 1995). These adverse biochemical conditions also necessitate to enable these plants to generate various biologically active metabolites (Nebula *et al.*, 2013), which protect them from these destructive elements. This might explain the utilization potential of salt marsh mangrove plants as renewable sources to offer excellent package of 'natural' bioactive molecules for use in food supplements for increasing the shelf-life of food products, and for use as medication against oxidative stress induced degenerative diseases and inflammatory disorders.

Mangroves are biochemically unique, and the mangrove sediment associated bacterial flora were found to produce a wide array of natural products with unique bioactivities. They were reported to possess active metabolites with novel chemical structures, which belong to diverse chemical classes, such as alkaloids, phenol, steroids, terpenoids, tannins, etc. However, the extensive scientific information about the biological effects of bacterial species associated with the sediments of mangrove plants and active substances has been scarce and poorly documented.

2.3. MANGALAVANAM MANGROVE ECOSYSTEM

Mangalavanam mangrove forest and bird sanctuary is located on Dr. Salim Ali road near the High Court of Kerala . Mangroves of Mangalavanam are regarded as a secondary growth flourished after the closing of a log depot. *Avicennia officinalis* L. was the most abundant species followed by *Acanthus ilicifolius* L., *Rhizophora mucronata* Lamk. and *Bruguiera gymnorhyza* Lamk. The species that are more resistant to the adverse ecological conditions were eventually colonized in the harsh environment. Mangrove ecosystem is a habitat for many species like shrimps, crabs

and fishes. They feed on the rich organic matter released by decomposition of the mangrove foliage.

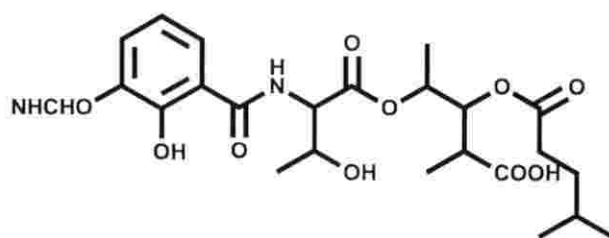


Figure 2.1. (A) Mangrove sediments of Mangalavanam mangrove ecosystem at Kochi. (B) Soil sediment of Mangalavanam mangrove ecosystem used to isolate *Bacillus licheniformis* MTCC 6824 (Paulraj, Joseph and Chakraborty, 2019, Indian Patent Grant Number: 302657)

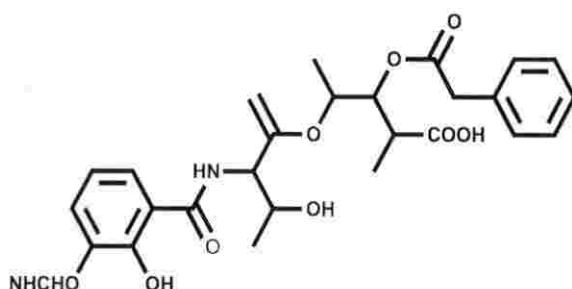
2.4. MANGROVE ASSOCIATED MICROBES

The discovery of bioactive compounds, such as di and triterpenoids, iridoids and tetranorterprenoids (limonoids) from mangroves like *Avicennia*, *Xylocarpus*, *Bruguiera* and *Rhizophora* spp. further attracted the attention of marine natural product discoverers (Wu *et al.*, 2008). Salinosporamide A derived from mangrove bacterium *Salinosporatropica* and xyloketals gained from *Xylaria* sp. made the attention deep-rooted (Lin *et al.*, 2001; Feling *et al.*, 2003). Mangroves and mangrove associated microorganisms were proved to be a rich source of bioactive natural products and the natural products derived from mangrove associated microbes have displayed potential antibacterial, antioxidant, anti-inflammatory, antiviral, antifungal activities, tyrosine phosphatase B inhibitory activities and α -glucosidase inhibitory properties (Ancheeva *et al.*, 2018). Several classes of bacteria were isolated from the mangrove sediments exhibiting prominent bioactivities. There were reports of novel strains being isolated from mangrove sediments like *Mangrovitalea sediminis* sp. nov. from Yunxiavo Mangrove National Nature Reserve in China (Liao *et al.*, 2017). The exopolysaccharide derived from mangrove associated bacteria, *Paenibacillus lactes* NRC1 was found to exhibit potential anti-inflammatory activity against cyclooxygenases (Mahmoud *et al.*, 2016).

Two actinomycins, A₁ (1) and B₂ (2) were isolated from *Streptomyces lucitanus* associated with *Avicennia mariana* in China (Han *et al.*, 2012). Actinomycin B₁ exhibited activity against pathogenic *Laribacter hongkongensis* and *Staphylococcus aureus*.



1

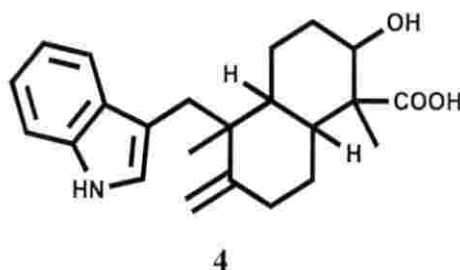
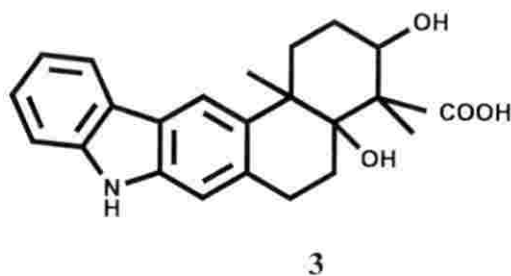


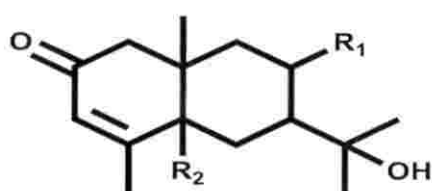
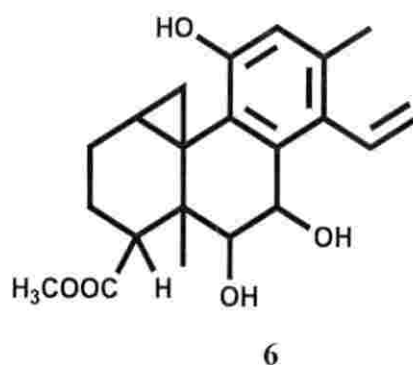
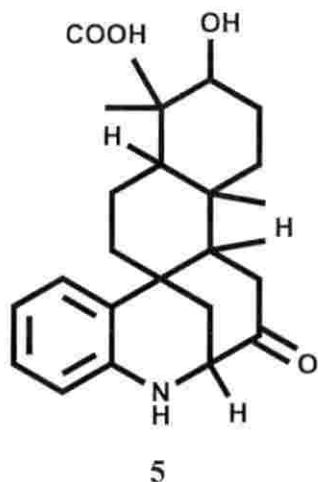
2

Ser *et al.* (2016) proposed a novel species of *Streptomyces malasiense* sp. nov. from Malaysian mangrove forest. This strain exhibited significant cytotoxicity against the HCT-116 cells. Gas chromatography-mass spectrometry (GC-MS) data further confirmed that the compounds were interrelated with chemopreventive metabolites. *Streptomyces* species, such as *Streptomyces tanashiensis*, *Streptomyces bacillaris* and *Streptomyces viridobrunneus* isolated from the Mangalavanam ecosystem along the south west coast of India have exhibited potential antimicrobial activities against pathogenic bacteria, such as *Aeromonas hydrophila*, *Vibrio vulnificus* 1145, *V. parahemolyticus*, *V. alginolyticus*, *V. anguillarum* O1 and *V. anguillarum* A1 (Chakraborty *et al.*, 2015).

2.5. BIOACTIVE COMPOUNDS FROM MANGROVE SEDIMENT ASSOCIATED MICROBES

Natural products are valuable resources of diverse structural compounds with pharmaceutical, nutraceutical and cosmaceutical applications (Chauhan *et al.*, 2013). Microbes are the best sources of diverse bioactive compounds. The biosynthetic gene clusters, which encode biosynthetic enzymes would assist in biosynthesising the structurally and functionally diverse compounds (Katz and Baltz, 2016). They possess several advantages, such as easy growth and simple cultivation techniques as well as better alternatives to solve the environmental issues caused by chemical synthesis (Matassa *et al.*, 2016). The microbial products in the market were contributed mainly by the genus *Streptomyces* (Kim *et al.*, 2011; Sanjivkumar *et al.*, 2016; Zainal *et al.*, 2016; Biswas *et al.*, 2017; Dan and Sanavar, 2017; Tan *et al.*, 2017). Novel strains are being isolated from the mangrove ecosystems worldwide including *S. colonosanans*, *S. humi*, *S. euryhalinus* and *S. antioxidans* (Ser *et al.*, 2016; Law *et al.*, 2017). The mangrove associated microbes that were studied from countries like India, Brazil, China, Malaysia and Saudi Arabia were extremely diverse (Liang *et al.*, 2007; Mendes and Tsai, 2014; Simoes *et al.*, 2015; Basak *et al.*, 2016; Ser *et al.*, 2016; Loganathachetti *et al.*, 2017). The 16S rRNA sequences obtained from the bacterial consortia associated with the sediments of the mangrove forests of China have demonstrated the presence of novel bacterial strains, which were distinct from the present known bacterial isolates, whereas the fungal species of Brazilian mangrove ecosystem were of different genera that are previously undescribed (Liang *et al.*, 2007; De Souza Sebastianes *et al.*, 2013).



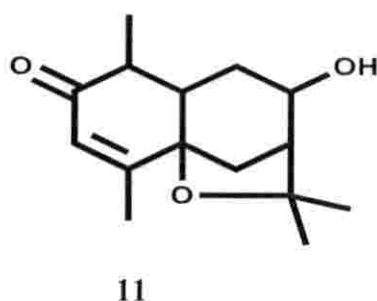


7. $R_1 = \text{OH}; R_2 = \text{H}$

8. $R_1 = R_2 = \text{OH}$

9. $R_1 = \text{OH}; R_2 = \text{OOH}$

10. $R_1 = \text{H}; R_2 = \text{OOH}$



Several indolosesquiterpenes, such as xiamycin (3), indospene (4), sespenine (5), and the previously known xiamycin (6), which exhibited potential antibacterial activity against vancomycin resistant *E. faecalis* and methicillin resistant *Staphylococcus aureus* were isolated from an endophytic *Streptomyces* associated with *Kandelia kandel* in China (Ding *et al.*, 2011). Kandenols (7-11), which belonged to the eudesmene type of sesquiterpene compounds showing moderate activity against *Mycobacterium vaccae* and *B. subtilis* were isolated from the mangrove province of China (Ding *et al.*, 2012). Cultivation-based studies remained essential for designing antibiotic screening assays and understanding the microbial ecology and physiology despite the limitations possessed by them (Ali *et al.*, 2012).

2.6. SECONDARY METABOLITES FROM MICROORGANISMS

Secondary metabolites are compounds produced in very low concentration by different groups of fungi, plants and bacteria. These metabolites are termed

secondary since they were not involved in the primary metabolic reactions like growth, but these compounds could provide an extra responsive mechanism against the pathogens. Almost thousand metabolites have been discovered from mangrove associated microorganisms; whereas 850 compounds were fungal derived and 120 were from bacteria (Blunt *et al.*, 2018).

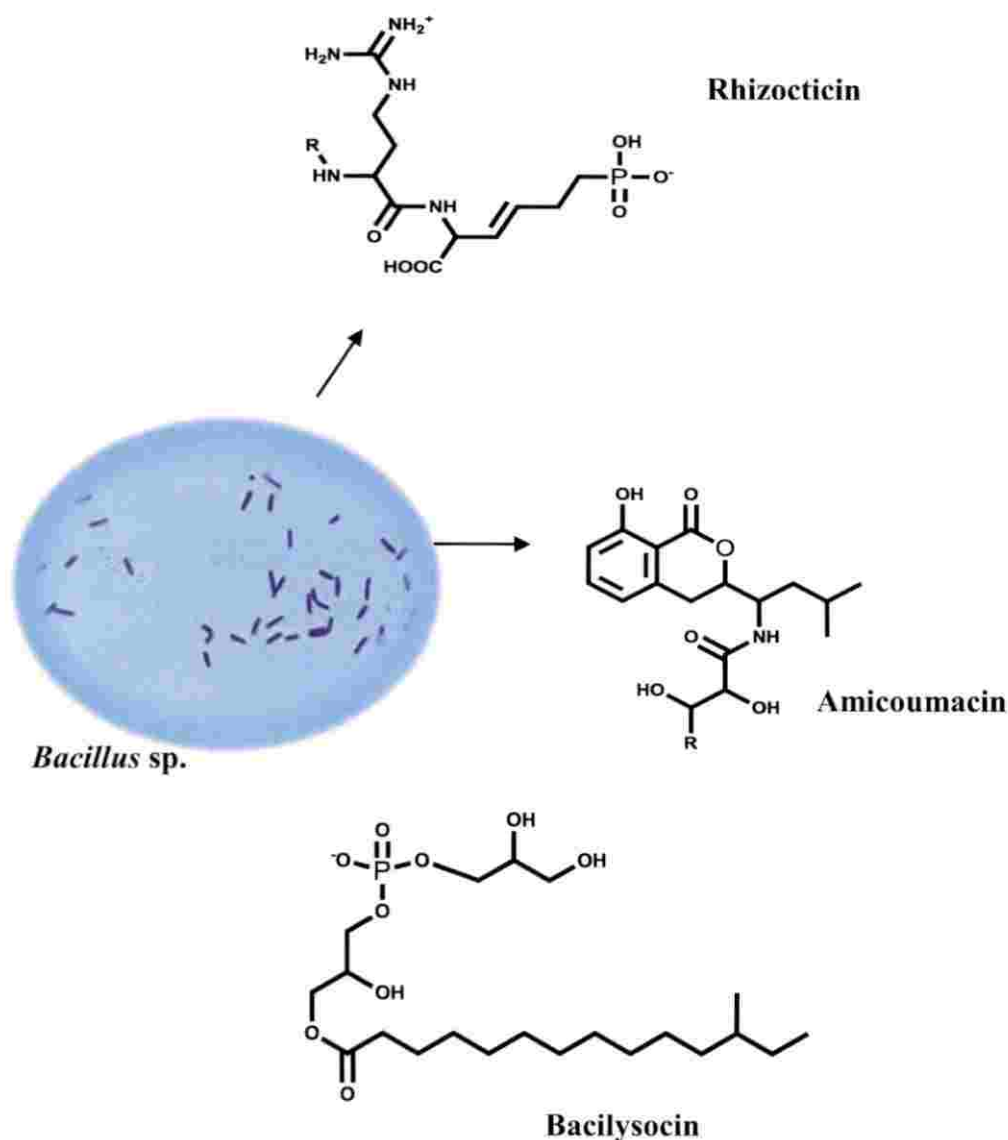


Figure 2.2. Bioactive compounds associated with *Bacillus* species

The well-known bioactive compound producing actinobacteria included *Streptomyces*, which belonged to the order Actinomycetales (Lechevalier and

Lechevalier, 1981). Tamehiro *et al.* (2002) have reported bacilysocin, a novel antibiotic from *B. subtilis* strain showing antifungal activity against *Saccharomyces cerevisiae* and *Candida pseudotropicalis* and antimicrobial activity against *S. aureus*. Kugler *et al.* (1990) have reported that Rhizocticin A derived from *B. subtilis* ATCC 6633 have showed significant antifungal activity against nematode *Caenorhabditis elegans*. The probiotic strain *B. subtilis* exhibited activity against *Helicobacter pylori* (Enterobacteriaceae family) along with anti-inflammatory activities ranging from 0.75-6.8 µg/mL, and one of the compounds was identified as amicoumacin (Pinchuk *et al.*, 2001). Prathiba and Jayaraman (2018) have reported the presence of compound squalene in *Bacillus* VITPS12 and *Planococcus maritimus* VITP21 and methyl hexadecanoate in another *Bacillus* strain. They concluded that the antioxidant and cytotoxic activities of the methanolic extracts could be attributed by the alkaloid, flavonoid and terpenoid compounds present in the extract. The free radical scavenging capabilities of flavonoids, such as rutin, quercetin and scutellarein, terpenoids such as geraniol, β-carotene and astaxanthin were previously reported (Ahmed *et al.*, 2016; Thoppil and Bishayee, 2011). Bacteria belonging to the phyla *Firmicutes* and *Gamma-proteobacteria* are being paid considerable attention as they represent an important source of previously undescribed bioactive substances, which were found to play important role in human health (Gomez *et al.*, 2010; El Bour *et al.*, 2013). A previous report of literature found that the minimum inhibitory concentration (MIC) of bacterial extracts lesser than 10 µg/mL constituted the best range of bioactivity (Ancheeva *et al.*, 2018). Characteristic antimicrobial, antifouling, and quorum sensing inhibiting features of *Firmicutes* and *Gamma-proteobacteria* made this group as highly successful agents to develop bioactive compounds and products (Goecke *et al.*, 2010, Kanagasabhpathy *et al.*, 2008; Fickers, 2012; Chakraborty *et al.*, 2018a-b; Kizhakkekalam and Chakraborty, 2019). Majority of the studies were conducted in actinomycetes belonging to the genera *Streptomyces* and fungus penicillin, even though a large number of bacterial and fungal genera still remained unexplored (Watve *et al.*, 2001).

2.7. SECONDARY METABOLITES FROM *Bacillus* genera

Lipopeptides, such as iturin and surfactin that were produced by *B. subtilis* were reported to possess significant antibiotic potential (Cao *et al.*, 2009; Meena *et*

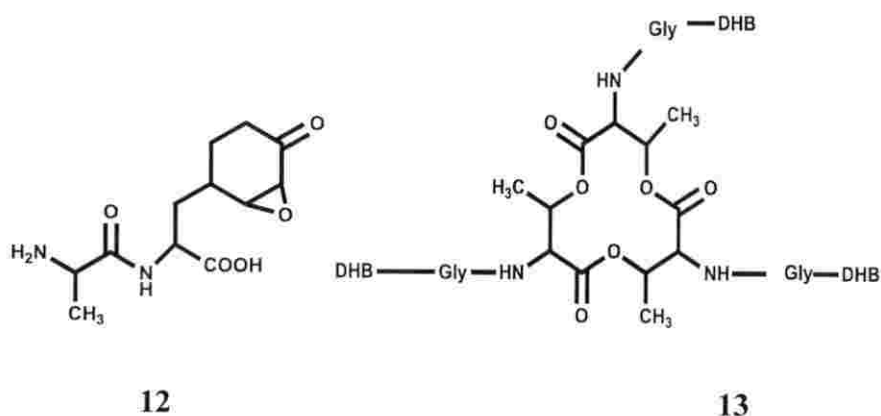
al., 2016). These compounds were promising agents for the pharmaceutical industry due to higher biodegradability, minimal toxicity and irritancy to human skin. These compounds were also found to possess potential antibacterial, antifungal, antiviral, antitumor, antithrombotic, and hypocholesterolemic activities. The wide range of applications of lipopeptides could pave way for deeper research in this field (Meena *et al.*, 2016). They were also found their applications in the field of nanotechnology (Plaza *et al.*, 2014).

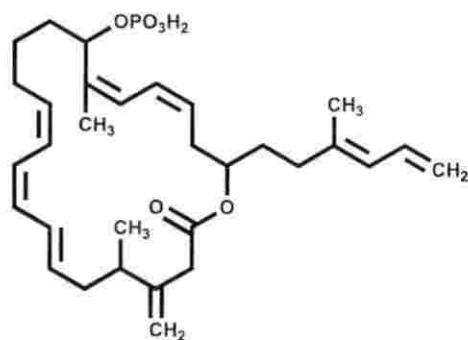
Surfactins are the first group of compounds produced during the bacterial growth (Cosby *et al.*, 1998). Iturin A has been produced when some of the nutrients got exhausted after the logarithmic growth phase (Mizumoto *et al.*, 2006). Mycosubtilisin compounds were found to be produced between log phase and stationary phase indicating that antibiotic compounds were produced in each step of growth and a strong antifungal activity was produced by a mixture of iturin and surfactin (Souto *et al.*, 2004).

Iturins are group of compounds constituted of a peptide and a β -amino fatty acid linked by amide bonds and they are grouped into iturin A, C, D and E, bacillomycin D, F and L, bacillopeptin and mycosubtilisin (Besson *et al.*, 1976; Vanittanakom, 1986; Ahimou *et al.*, 2000; Pathak and Keharia, 2014). Fengycin is another group of compounds in *Bacillus* species, which was found to be consisted of lipopeptides with 10 amino acids and a lipid linked to the N-terminal, and differed from the iturin class of compounds by the presence of ornithine and allothreonine (Vanittanakom, 1986). These compounds were deduced to act against phospholipase-A2 and filamentous fungi (Nishikori, 1986). They were also useful in controlling oil spills due to the ability to produce surfactants (Marti *et al.*, 2014).

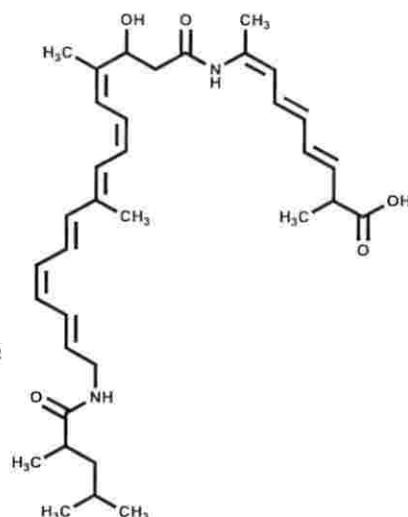
Surfactins are surface active agents with microbial origin, and has an amphipathic nature, and therefore, these classes of compounds were localized at the interface of two phases (Mulligan, 2005). They are cyclic lipopeptides with seven D- and L- amino acids and one β -hydroxy fatty acid residue (Kluge *et al.*, 1988). Surfactins obtained from *Bacillus* were the best of its kinds due to various industrial applications. Bacillibactin-13 were a group of compounds with metal chelating activity thus making them in controlling phytopathogens (May *et al.*, 2001). Bacilysin-12 is a simple peptide antibiotic composed of L-alanine and L-anticapsin. The antibacterial activity was due to its ability to inhibit, glucose amine-6-phosphate synthase, an essential enzyme required for cell wall synthesis.

Polyketide classes of compounds are structurally divergent molecules with potential pharmacological properties, and were reported to occur in microorganisms (Winter *et al.*, 2012; Chakraborty *et al.*, 2014; Chakraborty *et al.*, 2017a-b). This group of compounds can potentially bind to the target enzymes required to exhibit the bioactivities, and were therefore, found potential applications in the discovery of more effective pharmacophores (Driggers *et al.*, 2008; Thilakan *et al.*, 2016). Difficidin-14, bacillaene-15 and macrolactin A-16 were different types of polyketide compounds produced by wild strains of *B. amyloliquefaciens* (Maget-Dana and Peypoux, 1994). Difficidin possessed broad spectrum of antibacterial activities. Bacillaene was found to possess the ability to inhibit the protein synthesis of prokaryotes like *Klebsiella pneumoniae* and *S. aureus* (Patel *et al.*, 1995). Macrolactin was deduced to possess a 24-membered lactone ring and the compound was found to exhibit anticancer activity against murine melanoma cancer cells as well as antiviral activity against herpes simplex virus, HIV. The 24-membered macrolactin ring containing compound was also found to be active against gram positive strains, such as methicillin resistant *S. aureus* and vancomycin resistant *Enterococci* (Gustafson *et al.*, 1989).

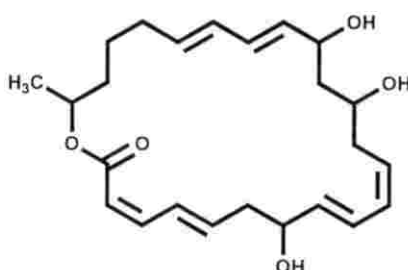




14



15



16

A previous report of literature (Wiese *et al.*, 2009; 2019) found the presence of more than 800 secondary metabolites with significant antibiotic potential from the *Bacillus* genera. Hu *et al.* (2010) have reported sequence variation in 16S rDNA sequences in several rRNA gene clusters.

7-O-Methyl-5'-hydroxy-3'-heptenoate-macrolactin, a seaweed associated *B. subtilis* derived bioactive compound was found to display potential antibacterial activities against human opportunistic pathogens such as *V. vulnificus*, *V. parahemolyticu* sand *A. hydrophila* and the antibacterial activities of the crude extract were more than the purified fraction indicating the presence of other bioactive compounds (Chakraborty *et al.*, 2014). There were distinctive reports on the anti-viral and anticancer activities of macrolactin group of compounds apart from their antibacterial activities (Gustafson *et al.*, 1989; Jaruchoktaweetchai *et al.*, 2000; Chakraborty *et al.*, 2014). Macrolactin A possessed higher activity when compared to the other chemically characterized macrolactins (Gustafson *et al.*, 1989; Jaruchoktaweetchai *et al.*, 2000). The macrolactins were initially characterized by

Gustafson *et al.* (1989) in a marine bacterium, whereas Nagao *et al.* (2001) claimed that the C-15 OH group in the structure was accounted for the bioactivity of the compound.

2.8. ANTIBACTERIAL ACTIVITIES OF THE SECONDARY METABOLITES FROM MANGROVE SEDIMENT ASSOCIATED BACTERIA

The ethyl acetate extracts of actinobacterial strains belonging to the *Streptomyces* genus isolated from mangrove sediments of Krishna district in Andhra Pradesh have exhibited significant antimicrobial activity against gram positive bacteria, such as *B. subtilis*, *B. megaterium* and *S. aureus* and gram negative bacterial isolates, such as *Pseudomonas aeruginosa*, *E. coli* and *Xanthomonas campestris* (Yasmeen *et al.*, 2016). The compounds, such as tetradecane, 1-tetradecene, octadecane and cyclotetracosane, which were derived from the extracts of *Streptomyces cheonanensis*, were found to display potential antimicrobial and antifungal activities (Naragani *et al.*, 2016). Thongjun *et al.* (2016) claimed that a Firmicute, *B. amyloliquefaciens* associated with mangrove soil have manifested antibacterial activities against *V. parahemolyticus* that has been a prominent food pathogen causing gastroenteritis. The active fractions were found to be surfactin, iturin A and mycosubtilisin through anion exchange chromatography, HPLC and mass spectrometry. The minimum bactericidal concentration exhibited was 512 µg/mL, and the minimum inhibitory concentration was found to be 256 µg/mL.

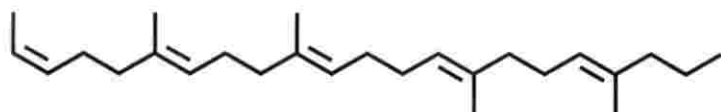
2.9. ANTI-INFLAMMATORY ACTIVITIES OF THE SECONDARY METABOLITES FROM MANGROVE SEDIMENT ASSOCIATED BACTERIA

According to Nathan (2002), inflammation is a response produced in association with infections, trauma, injury or toxicity. Inflammatory diseases, such as rheumatoid arthritis, chronic asthma, inflammatory bowel disease and multiple sclerosis were prevalent globally on a large scale (Mahmoud *et al.*, 2016). The inflammatory action includes preventing metastasis and killing of microbes, destruction of infected host cells and palliating the tissues impaired by trauma or host revulsion (Luft *et al.*, 1965). The molecules involved in the elevation of

inflammatory reactions included bradykinins, histamine, prostanoids, platelet activating factor and leucotrienes.

The inflammatory diseases were treated with two types of medications, non-steroidal and steroidal medication (Blumenthal *et al.*, 2008). Natural compounds for treating inflammation are being explored to reduce the side effects produced by many medications. Although non-steroidal anti-inflammatory medications (NSAIDs) have been used to deter the inflammatory pathophysiologicals, many side effects like kidney failure, gastro-intestinal bleeding, stroke, heart attacks, duodenal ulcers were reported to occur. These deleterious side-effects are liable for many instances of hospitalization and deaths (Sostres *et al.*, 2010).

Squalene (17), a bioactive compound extracted from *Bacillus sp.* has been proved to have inhibitory effect on major inflammatory pathways including P³⁸, COX, NF_κB, TNF- α , iNOS and IL-1 β (Kucharska-Newton *et al.*, 2009; Kavitha *et al.*, 2010; Thoppil and Bishayee, 2011).



17

Lipoxygenase is a category of non-heme containing, oxidative enzymes regulating the inflammatory response by generating leukotrienes that are pro-inflammatory mediators and lipoxins, which are a group of anti-inflammatory mediator (IA). They were found to yield hydroperoxyl derivatives like hydroperoxy-eicosatetraenoic acids by catalyzing the deoxygenation of polyunsaturated fatty acids (Miranda-Bautista *et al.*, 2017). The anti-inflammatory reaction could be assessed by inhibiting LOX.

2.10. ANTIOXIDANT ACTIVITIES OF THE SECONDARY METABOLITES FROM MANGROVE SEDIMENT ASSOCIATED BACTERIA

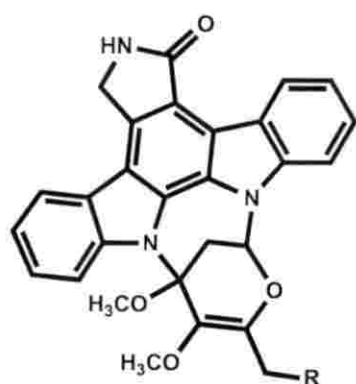
Antioxidants are compounds, which prevent the oxidative impairments caused by reactive oxygen species (ROS), such as superoxide, peroxide and hydroxyl radicals attacking deoxy ribonucleic acid (DNA), protein and membrane lipids (Federico *et al.*, 2007; Farinati *et al.*, 2010; Poljsak *et al.*, 2013; Rahal *et al.*, 2014). The

oxidative attacks by free radicals were found to lead towards crucial diseases like cancer, chronic inflammatory diseases and diabetes. The ROS also was found to cause lipid oxidation resulting in the deterioration of foods, and also the loss of some essential fatty acids and fat-soluble vitamins (Halliwell *et al.*, 1995; Shahidi, 2000; Falowo *et al.*, 2014). Some synthetic anti-oxidant compounds, such as butylated hydroxytoluene (BHT), propyl gallate (PG), tert-butyl hydroquinone (TBHQ) were used to stop food deterioration, even though these compounds could cause potential health hazards, such as carcinogenesis and liver damage (Shahidi, 2000). Since these compounds are toxic, there had been substantial interests in naturally derived antioxidant compounds. Marine sources were found to be promising source of antioxidant compounds, which are used for treating cancer by inhibiting the formation of free radicals. The Food and Drug Administration (FDA) approved drugs from marine sources, such as Trabectedin from *Ecteinascidia turbinata*, Cytarabine from *Cryptotheca crypt* are available in market for cancer treatment. Prathiba and Jayaraman (2018) reported significant antioxidant and cytotoxicity against HeLa cell lines by *Bacillus* VITPS7 isolated from soil samples of Pichavaram mangrove ecosystem and Marakkanam saltern region in South India. 2,2-Diphenyl-1-picrylhydrazyl (DPPH) is a stable free radical, which is used for estimating the antioxidant activity of many natural compounds. The free radicals can either hydrogen radical or an electron to develop into a diamagnetic molecule, which is stable and difficult to oxidize. It has an absorption maximum at 517 nm. The deep violet colored compound decolorizes according to the number of electrons gained. DPPH oxidizes natural compounds, such as ascorbic acid, cysteine, glutathione, polyhydroxy aromatic compounds and aromatic amines (Blois, 1958).

2.11. ANTI-CANCER ACTIVITIES OF THE SECONDARY METABOLITES FROM MANGROVE SEDIMENT ASSOCIATED BACTERIA

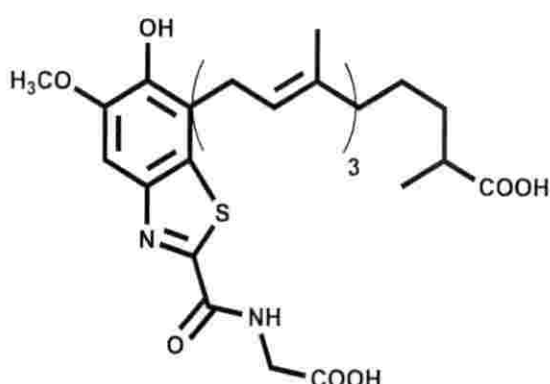
Several anticancer compounds were isolated from microbes ever since the characterisation of anticancer compounds actinomycin D, bleomycins, anthracyclins and mitosanes among other antitumor compounds extracted from *Streptomyces* sp. (Berdy, 2005; Newman and Cragg, 2014). A glycosylated 16 membered macrolide belonging to the family of elaiophylin with potential cytotoxic activity against HeLa and MCF-7 cell lines with IC₅₀ values ranging from 0.19 to 2.12 µM were derived

from a *Streptomyces* species from Hainan province, China (Han *et al.*, 2016). A new derivative of Bagremycin, Bagremycin C and a previously known Bagremycin B derived from mangrove sediments of Guangdong, China exhibited cytotoxicity against human glioma cells (Chen *et al.*, 2017). Sun *et al* (2018) claimed the presence of 4 new borrelidins, Borrelidin G, Borrelidin H, Borrelidin I, Borrelidin F and previously reported Borrelidin A from *S. rochei*, which showed cytotoxic activities on cancer cell lines, such as HeLa, MCF-7, HepG2, A549 and CNE2. Benzothiazole diterpenes, erythrazole A-20 and B-21 were derived from mangrove forests of U.S.A, where erythrazole-B was found to display potential activity against three HTCL cell lines (Hu and MacMillan, 2011).

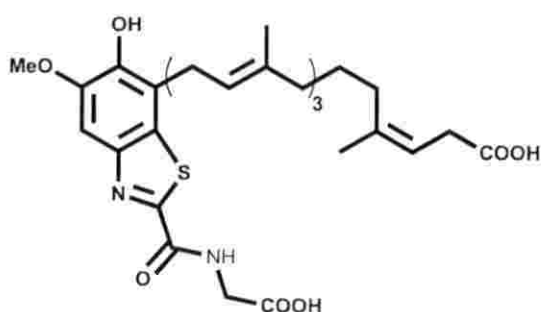


18. R=OH

19. R=H



20



21

Two streptocarbamazoles, streptocarbamazole A (18) and streptocarbamazole A (19) were isolated from mangrove province of China, whereas streptocarbamazole A (18) was found to display significant cytotoxic activity against HTCLs and arrested HeLa cells (Fu *et al.*, 2012).

2.12. BIOSYNTHETIC GENE CLUSTERS

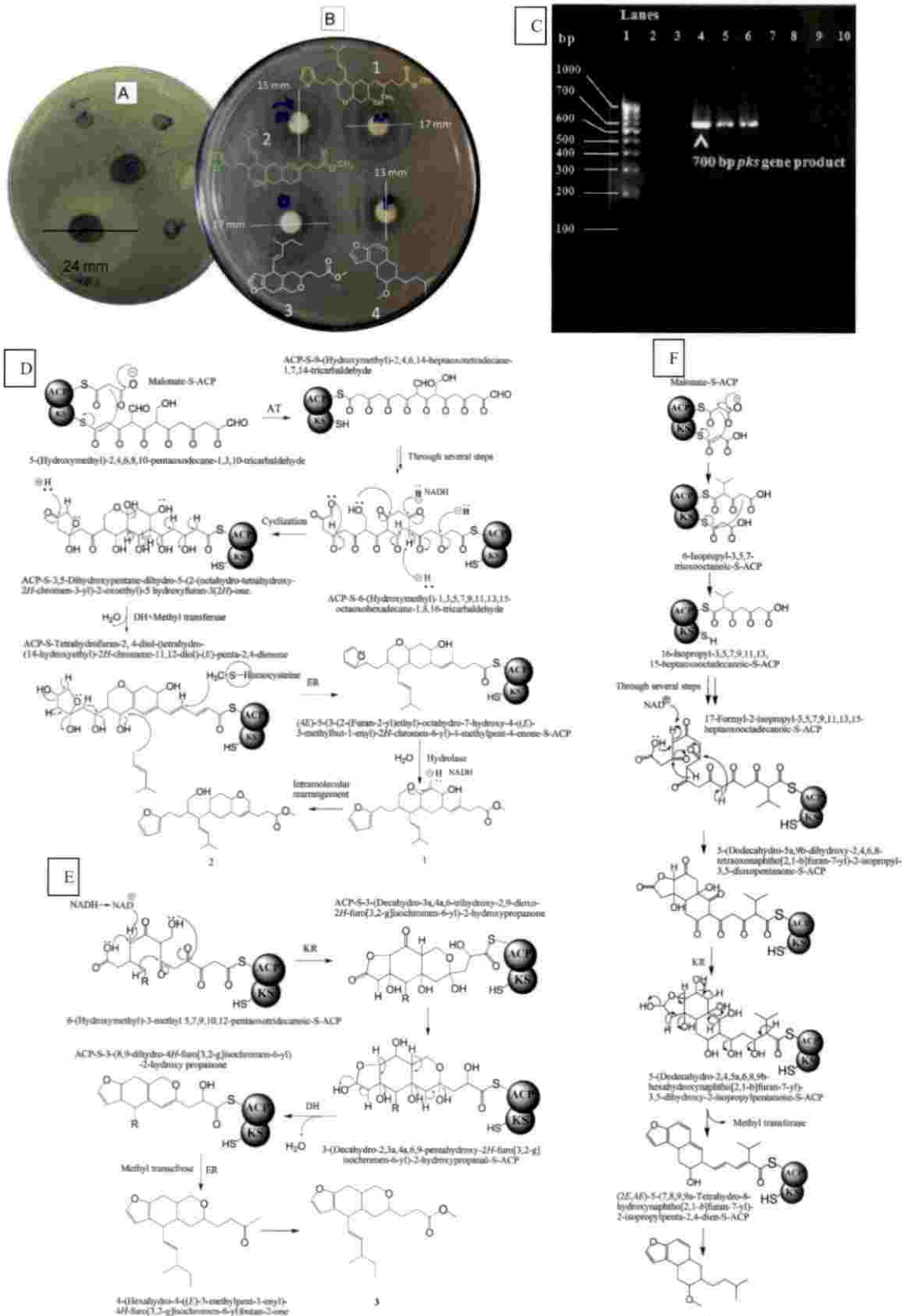


Figure 2.3. (A) Spot over lawn assay of *B. subtilis* MTCC 10403 culture against pathogenic *V. parahaemolyticus* MTCC 451. The plates were stained with MTT for visualization. (B) Polyketide furanoterpenoids (1-4) isolated from *B. subtilis* MTCC 10403 and their antibacterial activities against *V. parahaemolyticus* MTCC 451. (C) Biosynthetic gene clusters (BGCs) in heterotrophic *B. subtilis* MTCC 10403. Electrophoresis image of PKS gene profile (lane 4-6, showing positive hit) of the antagonistic isolates from heterotrophic *B. subtilis* MTCC 10403 on agarose gel. (D-F) The array of events in biosynthetic route of homologous furanoterpenoids with characteristic polyketide backbone (Chakraborty *et al.*, 2017a).

Advanced techniques in the field of molecular biology helped us to identify the secondary metabolite biosynthetic gene clusters (BGCs) in bacteria, and provide insights into certain compounds that could be produced by the particular genus of bacteria. The major biosynthetic gene clusters include polyketide synthase (PKS), nonribosomal peptide synthetase (NRPS), siderophore producing clusters and PKS-NRPS hybrid gene cluster (Thilakan *et al.*, 2016). These genes encode the enzymes, such as polyketide synthetase and nonribosomal peptide synthetase for the biosynthesis of bioactive secondary metabolites like polyketides and peptides (Chakraborty *et al.*, 2017a-b; Hu *et al.*, 2010). Hu *et al.* (2010) also revealed that the bacteriocin types of compounds were encoded either in chromosomes or plasmids. Various genes accountable for providing resistance to toxic compounds, such as mercury, arsenic, tellurium, cadmium and cobalt were also detected (Sengupta *et al.*, 2018). The production of secondary metabolites could occur only when the cryptic biosynthetic gene clusters are activated by specific environmental stimuli (Ludwig-muller, 2015; Katz and Baltz, 2016). The culture conditions like media, temperature, pH, light and elicitors could be altered for the better production of secondary metabolites (Tan and Zou, 2001).

Advances in the understanding of bacterial aromatic polyketide biosynthesis led to the identification of multifunctional polyketide synthase enzymes (PKSs) responsible for the construction of polyketide backbones of defined natural product drug discovery 13 chain lengths, the degree and regiospecificity of ketoreduction, and the regiospecificity of cyclizations and aromatizations, together with the genes encoding for the enzymes (Hutchinson, 1999). Since polyketides constituted a large number of structurally-diverse natural products exhibiting a broad range of biological activities (e.g., tetracyclines, doxorubicin, and avermectin), the potential for

generating novel molecules with enhanced known bioactivities, or even novel bioactivities, appeared to be high (Gokhale *et al.*, 1999).

In a report released by the American Academy of Microbiology entitled, "The Microbial World: Foundation of the Biosphere", it was estimated that "less than 1 % of bacterial species and less than 5 % of fungal species are currently known". Other evidences also indicated that millions of microbes were yet to be discovered (Young and Crawford, 2004). With less than 1 % of the microbial world currently known, advances in procedures for microbial cultivation and the extraction of nucleic acids from environmental samples from soil and marine habitats, would provide access to a vast untapped reservoir of genetic and metabolic diversity (Cragg *et al.*, 2011). Until recently, microbiologists were greatly limited in their study of natural microbial ecosystems due to an inability to cultivate most naturally occurring microorganisms (Cragg *et al.*, 2011). The recent development of procedures for cultivating and identifying microorganisms would aid microbiologists in their assessment of the earth's full range of microbial diversity. In addition, procedures based on the extraction of nucleic acids from environmental samples would permit the identification of microorganisms through the isolation and sequencing of ribosomal RNA or rDNA (genes encoding for rRNA). Samples from soils are currently being investigated, and the methods might be applied to other habitats, such as the microflora, insects, and marine animals (Handelsman *et al.*, 1998). Valuable products and information are certain to result from the cloning and understanding of the novel genes which will be discovered through these processes.

Extreme habitats harbor a host of extremophilic microbes (extremophiles), such as acidophiles (acidic sulfurous hot springs), alkalophiles (alkaline lakes), halophiles (salt lakes), baro- and thermophiles (deep-sea vents) and psychrophiles (arctic and antarctic waters, alpine lakes) (Persidis, 1998; Psenner & Sattler, 1998). While investigations thus far have focused on the isolation of thermophilic and hyperthermophilic enzymes, there were reports of useful enzymes being isolated from other extreme habitats (Adams & Kelly, 1998). These extreme environments would also undoubtedly yield novel bioactive chemotypes.

As Dr. Rita Colwell, Director of the United States National Science Foundation, “the microbes to be discovered would be the cure for many diseases, remedy for polluted environments and new sources of foods” (Colwell, 1997).

2.14. NATURAL ALTERNATIVES FROM THE MANGROVE-ASSOCIATED BACTERIAL FLORA

Keeping in mind the adverse effects of multi-drug resistant antibiotics including non-steroidal anti-inflammatory drugs and anti-oxidants, and the importance to explore novel sources to make health products, it is imperative to target naturally available renewable sources to harness bioactive molecules for use against various deleterious stress-induced diseases *viz.*, bacterial infection, inflammation and inflammation-induced oxidative stress without causing any serious adverse effects. Screening and development of ‘green’ and ‘environmentally safe’ chemicals from the sediment associated bacteria of mangrove plant species settled along the shoreline could be an effective and useful approach to produce these metabolites for use against bacterial infection, inflammation and oxidative stress.

With the richness of mangrove plant species and their sediment-associated microbial flora, there exists a definite need for bioprospecting these unexplored and potentially useful organisms to isolate natural alternatives to the synthetic antibacterial, anti-oxidant, and anti-inflammatory agents in combating infectious diseases, oxidative stress-induced and inflammatory diseases. This research work, therefore, envisages a systematic approach involving culture-dependent methods to assess the cultivable bacterial communities associated with mangrove rhizosphere of salt marsh mangrove plant species coupled with evaluation of biological activity by selected assays, and to explore them as a source for potentially useful pharmaceutically active compounds. Chromatographic procedures including preparatory HPLC were used to isolate and purify the target molecules (small molecular weight bioactives). Bioactive molecules were characterized using MS/IR/2D-NMR and novel leads would be validated through bioassay.

Thus, the present study was aimed to find bioactive leads from mangrove sediment-associated microbes, which survive in an extreme condition, and thereby, endowed with greater possibilities of the occurrences of highly active bioactive compounds, which could be used as potential therapeutic agents to combat diseases, such as microbial infections and inflammatory diseases.

MATERIALS AND METHODS

3. MATERIALS AND METHODS

3.1 ISOLATION, IDENTIFICATION AND CHARACTERIZATION OF MANGROVE SEDIMENT ASSOCIATED BACTERIA

3.1.1 Location

The study entitled 'Identification and characterization of bioactive leads from mangrove sediment associated bacteria and assessment of their therapeutic potential' was carried out at the Marine Natural Product Laboratory in Marine Biotechnology Division of ICAR-Central Marine Fisheries Research Institute, Kochi starting from 1st October 2018 to 5th August 2019. In this chapter, the materials and procedures employed in the study were explained in detail.

3.1.2 Sample collection

A total of ten mangrove sediments were collected from Mangalavanam Mangrove Ecosystem and Bird Sanctuary, located in Kochi, Kerala at 9°54'N 76°18'E. The samples were collected at a depth of 15 cm in sterile tubes. The sediment samples were associated with mangrove species, such as *Acanthus ilicifolius* and *Avicennia officinalis*.

3.1.3 Isolation of mangrove sediment associated bacteria

Isolation was carried out by conventional serial dilution and spread plate techniques (Lemos *et al.*, 1985; Behera *et al.*, 2014). Briefly, about 1 g of sediment sample was transferred to the test tube containing 10 mL sterilized distilled water to make the serial dilution 10^{-1} . Thereafter, 1 mL of the content from 10^{-1} dilution was transferred to a test tube with 9 mL autoclaved distilled water, making it 10^{-2} dilution, and likewise, the serial dilutions from 10^{-1} to 10^{-7} were prepared. About 0.1 mL of the serially diluted sample was poured into the centre of sterile solidified nutrient agar plates (NA-HIMEDIA) supplied with 0.5 % (w/v) of sodium chloride and 1% agar before being spread using an L rod to uniformity. The plates were incubated at a temperature of 34 °C for 1 week, and the plates were observed for visible growth in an interval of 24 h.

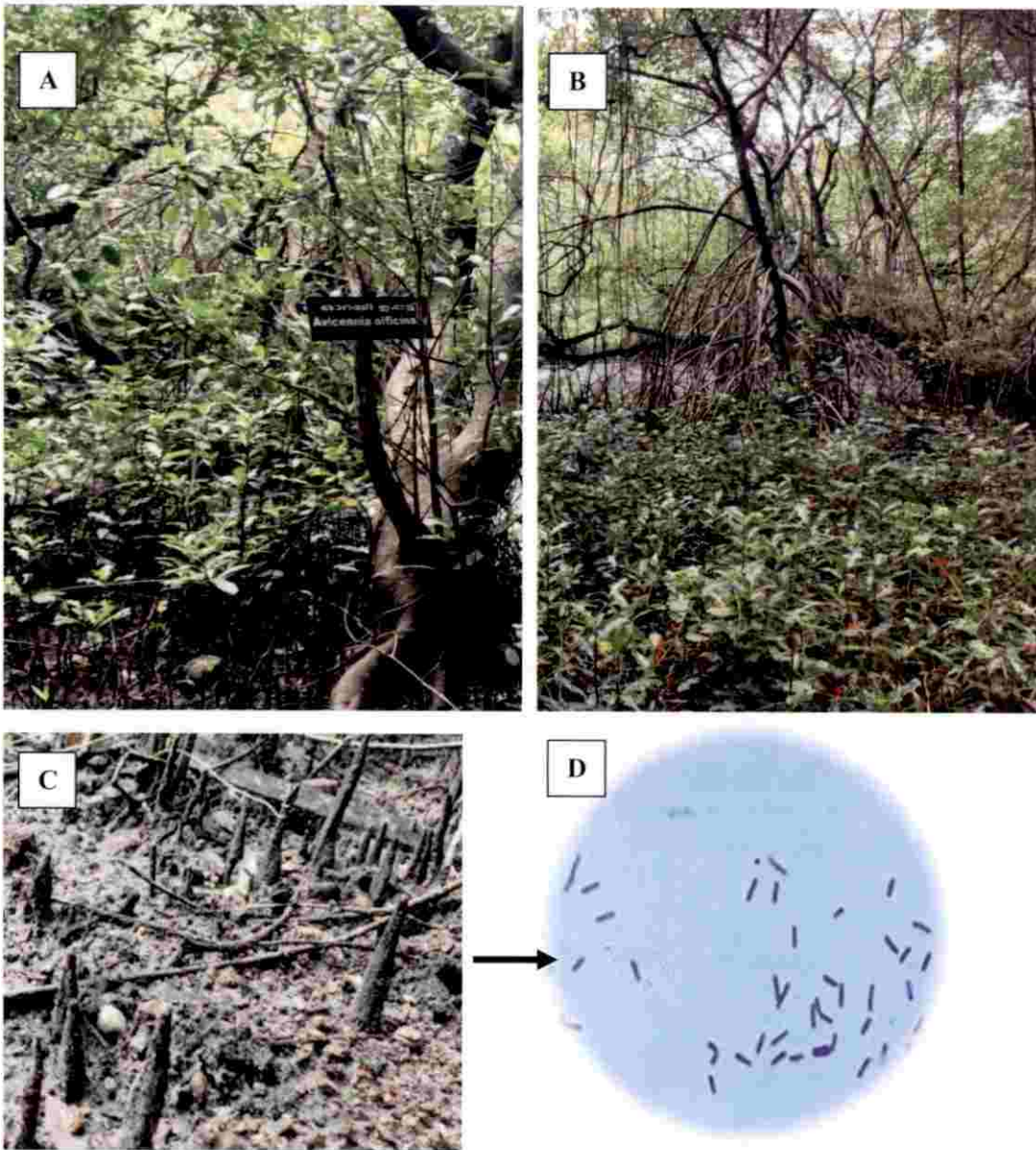


Figure 3.1. Representative photographs of (A) *A. officinalis* and (B) *A. ilicifolius*. (C) Mangrove sediments of Mangalavanam mangrove ecosystem and (D) Mangrove sediment associated bacteria

3.1.4 Subculturing of microbes

The microbes were transferred from one growth medium to another to keep them alive and for allowing the proper growth of microbes (Pelczar *et al.*, 1977). Four well

grown and morphologically distinct bacterial cultures from each sample were sub-cultured into sterile nutrient agar plates. The bacterial cultures were further quadrant streaked to obtain pure cultures and single colonies were picked and streaked in nutrient agar slants. The nutrient agar slants were incubated at 34 °C and further stored at 20 °C in BOD incubator (Labline). The pure cultures were inoculated into 10 mL sterile nutrient broth (HI MEDIA) and incubated at 34 °C for 18 h at 150 rpm in an incubator shaker (IKA KS 3000 I shaking incubator, Staufen, Germany). Glycerol stocks were prepared with 50 % of nutrient broth culture and stored at -80 °C for long term storage of the cultures. Slant cultures were prepared and stored the cultures in 20 °C.

3.1.5 Antibacterial activity of selected isolates by spot-over-lawn-assay

The antibacterial activity of the microbes were analysed by spot-over-lawn-assay (Chakraborty *et al.*, 2014). Mueller Hinton Agar (HI MEDIA) supplied with 1% agar was sterilized and allowed to solidify in petri-plates. The 18 h growth cultures of pathogenic bacteria *V. parahemolyticus*, *E. coli*, methicillin resistant *S. aureus* and *A. caviae* were prepared in nutrient broth (HI MEDIA). The pathogen cultures were swabbed in sterile Mueller Hinton agar plates and a loop-full of test cultures were spotted. The plates were incubated at 34 °C and the inhibition zone diameter was measured at an interval of 24, 48 and 72 h.

3.1.6 Biochemical characterization of bacteria

The biochemical characterization of the bacteria was performed according to Krieg and Holt (1984). The bacteria were biochemically characterized by several biochemical tests such as catalase, citrate, malonate, sugar utilization tests, motility tests after gram staining.

3.1.6.1 Gram staining

Gram staining was performed in glass slides, wherein a drop of distilled water was placed in the centre of the glass slide and a loop full of the test organism was smeared well along the marked area. It was air dried and the glass slides were heat fixed by passing

through flame and further started the staining procedure. Crystal violet was the primary stain, and the initial staining was performed for almost a minute. The stain was washed in running tap water, whereas proper care was taken so as to prevent the runaway of the culture on the plate. The primary stain was fixed with mordant, Gram's iodine for 1 min and washed with running tap water again. Thereafter, the primary stain was decolourised with ethanol for 1 to 3 seconds before being added with the counter stain saffranin for 45 seconds. The slide was washed again in running tap water and blotted with tissue paper before being allowed for air drying. The slide was observed under 10 X, 40 X and 100 X with an inverted microscope (LEICA). Oil immersion was performed with cedar wood oil for observing it at 100 X. The microbes, which appeared purple color, were characterized as Gram positive, whereas those appeared pink were attributed to Gram negative.

3.1.6.2 Motility test by Motility Indole Lysine Medium (MIL medium)

Briefly, 18-24 h old culture of bacteria inoculated in brain heart infusion broth was stabbed into the sterilized and solidified MIL medium (HiMedia) in test tubes. The stabbing was performed at a distance of 1-1.5 inch from the bottom of the tubes. The tubes were incubated at a temperature of 34 °C for 24 h, and the growth away from the stab line was considered as positive result towards the motility test.

3.1.6.3 Biochemical characterization of bacteria by Hibacillus identification kit

Biochemical characterization of 23 test strains was performed using HiBacillus identification kit (HIMEDIA, Mumbai, India). The test kit contained the media for malonate, Vogues Proskauer, citrate, ortho nitrophenyl β -galactoside (ONPG), nitrate reduction, catalase, arginine, sucrose, mannitol, glucose, arabinose and trehalose utilization tests, from well numbered as 1 to 12, respectively. The bacteria were inoculated in 5 mL of brain heart infusion broth (BHI) at 35 to 37 °C for 6-8 h until the turbidity was ≥ 1.0 at 620 nm. The kit was opened aseptically and inoculated 50 μ L of the test organism before being incubated at 35 to 37 °C for 24-48 h.

3.1.6.3.1 Malonate

The utilization of sodium malonate and ammonium sulfate in the medium by microbes resulted in the production of sodium hydroxide, which turn the medium alkaline. The pH indicator used in the medium was bromothymol blue, whereas the color of the medium changed from its original green to prussian blue color. The increase in acidity was indicated by yellow color in the medium.

3.1.6.3.2 Vogues Proskauer

About 1-2 drops of Barrit's reagent A (5 % α -naphthol) and 1-2 drops of Barrit's reagent B (40 % KOH) was added to the medium inoculated with the test bacteria. The fermentative degradation of glucose formed pyruvic acid, which in turns produced acetoin by various metabolic reactions. The α - naphthol would act as a catalyst to convert the acetoin to a red colored complex, diacetyl, in the presence of atmospheric oxygen and 40 % potassium hydroxide.

3.1.6.3.3 Citrate utilization

The microorganisms with the presence of citrate/ citrate permease would convert ammonium dihydrogen phosphate to ammonia and ammonium hydroxide, which turned the medium alkaline, and at pH greater than 7.5, bromothymol blue formed a navy blue color.

3.1.6.3.4 Ortho nitrophenyl β -galactoside (ONPG)

The microbes with enzyme β -galactosidase would convert ONPG to galactose and orthonitrophenol. The orthonitrophenol imparted an yellow color to the reaction.

3.1.6.3.5 Nitrate reduction

About 1-2 drops each of sulphanilic acid and N, N-dimethyl-1-naphthylamine reagent were added to the medium inoculated with the test bacteria. If the microorganism

would turn nitrate to nitrite, the latter in the medium could produce nitrous acid. The sulphanilic acid added to the medium would react with the nitrous acid to be diazotized, whereas α -naphthylamine reacted with the diazotized sulphanilic acid to yield a red colored complex.

3.1.6.3.6 Catalase

If the microorganisms have the ability to produce catalase, it could hydrolyze toxic oxygen compounds like hydrogen peroxide, causing the evolution of oxygen and bubbles. The presence of these bubbles would indicate that the reaction was catalase positive. A loopful of culture from the sixth well was spread in 2 or 3 drops of 3 % H_2O_2 . The reaction resulting in the formation of bubble was considered as positive, and those without a bubble formation were considered as negative.

3.1.6.3.7 Arginine

The microbes with arginine dihydrolase enzyme could utilize the arginine to increase the pH of the medium turning it into a violet colour (Sherris *et al.*, 1959).

3.1.6.3.8 Sugar utilization tests for sucrose, mannitol, glucose, arabinose and trehalose

The utilization of sugars would lead to the production of acid in the medium, thereby lowering the pH of the medium to acidic, which change the colour of the medium from red to yellow (Srinivas *et al.*, 1990). The pH indicator used in the medium was phenol red.

3.1.7 Preliminary screening of antioxidant activity

Antioxidants are substances that reduce damage due to oxygen, such as that caused by free radicals. 2,2-Diphenyl-1-picrylhydrazyl (DPPH), a free radical can be used for screening the antioxidant activity of bacteria. The antioxidant effect is directly proportional to the disappearance of DPPH and the neutralization of the free radical produces a zone of clearance (Velho-Pereira *et al.*, 2015).

The nutrient agar plates were spotted with a loopful of bacteria to be tested and incubated at 34 °C for 24 h. A sterile Whatman grade No.1 filter paper was placed with sterile forceps and incubated for 24 h so that the extracellular metabolites could get absorbed into it. The filter paper was then transferred to a petri-plate and sprayed with 0.2 mM of DPPH solution. The filter paper was then allowed to dry in room temperature and the zone of clearance was recorded.

3.1.8 Genomic DNA isolation of the selected bacteria

The genomic DNAs of the selected bacteria were extracted from 18 h old broth culture supplied with 0.5 % NaCl, incubated at 34 °C. The DNA was isolated by using GenElute bacterial genomic DNA kit (Sigma-Aldrich). The bacteria were pelleted at 12,000 X g for 2 min and 200 µL of 45 mg/mL lysozyme solution was added and vortexed (Spinix, Tarson). The lysed cells were incubated at a temperature of 37 °C for 30 min and another incubation was performed for 2 min after the addition of 20 µL RNase A. About 20 µL of proteinase K was added to remove protein contamination along with a lysis solution supplied with the kit before being incubated at 55 °C for 10 min. Further procedures were performed as per the manufacturer's protocol, and the DNA obtained was dissolved in Tris-EDTA buffer (pH 8) before being stored in -20 °C for further experiments.

3.1.9 Agarose gel electrophoresis

Agarose gel electrophoresis is a widely used technique for the analysis of deoxy ribonucleic acid (DNA). Briefly, 0.2 g of agarose (0.8 %) was poured into 25 mL Tris/Borate/ EDTA buffer (TBE) and it was heated in a microwave oven until the agarose was fully melted. The combs were inserted in the casting tray in appropriate positions. When the agarose came down at a temperature of 50 to 55 °C, about 0.2 µg-0.5 µg/mL of ethidium bromide (EtBr) was added for staining the DNA. The molten gel was thereafter mixed and poured into the casting tray, and the content was allowed to set. The combs were removed when the gel was set and the casting tray was placed in the electrophoresis

chamber. The chamber was filled with 1X TBE buffer, and 2 μL of DNA samples were mixed with 2 μL of gel loading dye. The DNA samples were thereafter loaded with a 1kb DNA ladder (New England Biolabs). The electrophoresis was carried out at 70 V and 35 mA for about 45 min to 1 h (Genei). Visualization of the DNA was performed under ultraviolet (UV) light and the images were documented in gel documentation system (Bio-Rad, USA). The DNA samples were stored in $-20\text{ }^{\circ}\text{C}$.

3.1.10 Quality check using nanodrop spectrophotometer

The quality and quantity of the DNA samples were assessed by using a nanodrop spectrophotometer (Eppendorf, Biospectrometer). The equipment was calibrated with Tris-EDTA (TE) buffer to zero absorbance or blank. Absorbance was checked at 260/280 nm, and the concentration ($\text{ng}/\mu\text{L}$) and the qualities of the samples were recorded.

3.1.11 Polymerase chain reaction of the DNA samples

The 16S region in the DNA was amplified using the forward primer, 8 F and the reverse primer, 1492 R (Sigma-Aldrich). Some reactions were performed with 27 F and reverse primer 1544 R (Sigma-Aldrich). The sequence of 16S forward primer used was AGAGTTTGATCCTGGCTCAG and the sequence of reverse primer used was GGTTACCTTGTTACGACTT. The PCR reaction was performed with a volume of 25 μL containing 12.5 μL of master mix (New England Biolabs), 10 μM forward primer (Sigma), 10 μM reverse primer (Sigma), 50-75 ng DNA and the remaining volume was constituted with nuclease-free water. The PCR cycling conditions performed were as follows, (1) an initial denaturation for 5 min at $94\text{ }^{\circ}\text{C}$, followed by 35 cycles of denaturation at $94\text{ }^{\circ}\text{C}$ for 30 s, (2) annealing reaction for 1 min at $52\text{ }^{\circ}\text{C}$, and (3) an extension step at $68\text{ }^{\circ}\text{C}$ for 1.5 min. A final extension for 10 min was performed at $68\text{ }^{\circ}\text{C}$ after these 35 cycles. Agarose gel electrophoresis was performed for the detection of the PCR products. The amplified products were run along with 1 kb DNA ladder (New England Biolabs) in 1.5 % agarose gel supplied with 2 μL EtBr at 70 V and 35 mA.

Table. 3.1. Primer sequences used for 16S rRNA sequencing

| Primer | Primer sequence | References |
|--------|--------------------------|---------------------------------|
| 27F | 5'GAGTTTGATCCTGGCTCAG3' | Suganthi <i>et al.</i> , 2013 |
| 1544 R | 3'AGAAAGGAGGTGATCCAGCC5' | El- Helow, 2001 |
| 8F | 5'AGAGTTTGATCCTGGCTCAG3' | Nandakumar <i>et al.</i> , 2007 |
| 1492 R | 3'GGTTACCTTGTTACGACTT5' | Abada <i>et al.</i> , 2019 |

3.1.12 16s sequencing of the PCR products and sequence analysis

The PCR products were sequenced at Agrigenome Labs Private Limited, Kochi, Kerala. Bio-Edit software was used to trim the sequence to remove low quality base pairs and for aligning the sequence. Basic Local Alignment Search Tool (BLAST_n) software of National Centre for Biotechnology Information (NCBI) was used for finding similar sequences in the database. The microbes were identified and further preceded the submission at GenBank for obtaining accession number for the sequences. A total of 9 sequences were submitted at GenBank for attaining the accession numbers for the sequences.

3.1.13 16S rRNA based phylogeny and phylogenetic tree construction

The 16S rRNA based phylogeny was carried out to confirm the biochemical tests. The sequences were aligned against reference sequences using CLUSTALW program of the BioEdit software. The phylogenetic tree was constructed to demonstrate the evolutionary relationship of the isolated strains against different species in the same genera and that of different genera by neighbor joining method (Kimura, 1980).

3.1.14 Polyketide synthase gene (*pks*) amplification and sequence analysis

The PCR reaction was performed with a volume of 25 μ L containing 0.25 μ L of PCR buffer (New England Biolabs), 5 μ M forward primer *gcf* (Sigma), 5 μ M reverse primer *gcr* (Sigma), 50-75 ng DNA, 0.3 μ L of Taq DNA polymerase (Sigma), 0.25 μ L of dNTP, and the remaining volume constituted by nuclease-free water. The PCR cycling conditions performed were as follows, (1) an initial denaturation for 5 min at 94 $^{\circ}$ C, followed by 35 cycles of denaturation at 94 $^{\circ}$ C for 30 s, (2) annealing reaction for 30 sec at 56 $^{\circ}$ C, and (3) an extension step at 72 $^{\circ}$ C for 1 min. A final extension for 5 min was performed at 72 $^{\circ}$ C after these 35 cycles (Applied biosystems).

Agarose gel electrophoresis was performed for the detection of polyketide synthase gene (*pks*) genes. The amplified products were run along with 1 kb DNA ladder (New England Biolabs) in 1.5 % agarose gel supplied with 2 μ L EtBr (0.2 μ g-0.5 μ g/mL) at 70 V and 35 mA. The nucleotide sequences were converted into peptide sequences using EMBOSS Transeq (EMBL-EBI), and the sequence was submitted in the GenBank, NCBI.

3.1.15 Bacterial growth curve

The bacteria were inoculated in a sterile 10 mL nutrient broth supplied with 0.5-1 % of NaCl for 18-24 h. A total amount of 100 mL sterile nutrient broth supplied with 0.5 % NaCl was prepared, and a 5 mL was removed to measure as blank. About 5 mL of inoculum was added to the remaining broth, and the absorbance was measured in a spectrophotometer (Varian Cary, USA) at 660 nm for 76 h (Monod, 1949).

3.2 BIOASSAY GUIDED ISOLATION AND CHARACTERIZATION OF BIOACTIVE COMPOUNDS FROM *B. AMYLOLIQUEFACIENS*

3.2.1 Extraction and concentration of bioactive compounds

A loopful of the isolate S2A was inoculated into the sterile nutrient broth supplied with 0.5 % NaCl, and it was incubated at 34 $^{\circ}$ C for 18 h. The nutrient agar plates supplied with 0.5 % NaCl were swabbed with the broth culture and incubated for 48-72 h at 34 $^{\circ}$ C

for the production of secondary metabolites. The surface layer of bacteria was scrapped out into 200 mL of ethyl acetate. The utilized agar was sliced and ethyl acetate was added with the contents for hot extraction. The spent agar was extracted by refluxing on a heating mantle for almost a week. The extracted solvent was filtered with a Whatman filter paper of grade 1, in every 7 h, and sodium sulphate was added to remove the moisture content. The filtrate was further concentrated and extraction was repeated with fresh solvent. Rotary vacuum evaporator (IKA) was used for distilling out the solvents from the samples. The concentration was carried out at a temperature not greater than 40 °C (Kizhakkekalam and Chakraborty, 2019).

3.2.2 Ultrasonication for bacterial cell lysis

The ultrasound sonication lysed the cell wall of bacteria to release the intracellular metabolites. The scrapped out bacterial cells from the nutrient agar surface was mixed in 200 mL of ethyl acetate. The cells were lysed at 37 % amplitude with a 10 s switch between pulse on and off cycle for 10 min in an ultrasound sonicator (Cole-Parmer) (Feliu *et al.*, 1998). The lysed cells were then extracted with ethyl acetate for 7 days. Fresh solvent was added each day prior to extraction and the extracted solvent was concentrated with a rotary vacuum evaporator (IKA) at a temperature not greater than 40 °C.

3.2.3 Thin layer chromatography (TLC) and documentation

Thin layer chromatography was performed for the preliminary detection of the types of various compounds in the crude. The concentrated extract was diluted and spotted at 1 cm away from the bottom of silica coated TLC plates (Silica gel 60, F₂₅₄, Merck) using a capillary tube. The TLC plates were run in a TLC chamber with 5 % methanol in dichloromethane. The plate was removed before it would reach the end line marked on it before being dried on a hot plate. The TLC plates were observed in UV light at the wavelengths of 254 nm and 365 nm. High performance thin layer chromatography and photo documentation was performed by ELITE-MINI LUMINOUS, AE-04 (Aetron, Mumbai, India). The retention factor or R_f is defined as the distance travelled by the

compound divided by the distance travelled by the solvent. The distance travelled by the solute from the origin and distance moved by the solvent was calculated and from those values the retention factor (R_f) of each separated compounds was calculated (Epifanio *et al.*, 2005).

3.2.4 Visualization of TLC plates with iodine

Most of the organic compounds form colorless spots in the TLC plates. Hence, visualizing reagents were used to locate the compounds. Iodine chamber was used for visualization of spots. The TLC plates were run initially in dichloromethane (DCM): methanol (19:1, v/v), before being placed in the iodine chamber for 20 min after air drying. The plates were observed for brown-coloured spots, which were related with the different components in the crude (Każmierczak *et al.*, 2004).

3.2.5 Visualization of TLC plates with vanillin-sulphuric acid

The TLC plates were run initially in DCM: methanol (19:1, v/v), air dried and placed in vanillin-sulphuric acid. The plates were taken out immediately and dried in hot plate for 3 min. The plates were observed for spots, which were related with the different components in the crude (Waldi, 1965).

3.2.6 Visualization of TLC plates with DPPH

The TLC plates were screened for antioxidant activity with the free radical DPPH. The TLC plates were run initially in DCM: methanol (19:1), air dried and placed in 0.1 mM DPPH solution under dark conditions (Takao *et al.*, 1994). The plates were removed from the solution and it was allowed to dry under the room temperature. The plates were observed further for the decolourization of spots from purple to white, whereas the decolourization of the spots on the TLC plate indicated the antioxidant activities of the compounds. The experiment was performed to test the ability of the compounds to scavenge the free radical.

3.2.7 Antioxidant assay with DPPH

DPPH is a free radical, which can either accept hydrogen radical or an electron to develop into a diamagnetic molecule, which is stable and difficult to oxidize. The deep violet colored compound decolourises according to the number of electrons gained. The extracts were prepared in the concentrations of 125, 250, 500, 1000 and 2000 ppm, and a 0.1 mM of DPPH solution was prepared in methanol (Blois, 1958; Brand-Williams *et al.*, 1995). The crude bacterial extract and DPPH solution were mixed in equal volumes, and a control was prepared with methanol and DPPH solution. The absorbance was recorded at 517 nm against methanol as blank in an interval of 20 min, 1 h and 2 h along with the reading of sample. The percentage inhibition was calculated using the following formula, $(A_0 - A_1)/A_0 \times 100$, where, A_0 = absorbance of control, A_1 = {(absorbance of sample + reagent) - absorbance of sample alone}. A graph was plotted with the concentrations in X axis and the percentage inhibition in Y axis. The IC_{50} value (the concentration at which the sample would inhibit 50% of its original activity) was calculated from the equation obtained from the graph.

3.2.8 Anti-inflammatory assay by lipoxygenase (5-LOX)

5-Lipoxygenase is an enzyme required for the synthesis of pro-inflammatory leukotrienes and lipoxins, whereas inhibition of 5-LOX demonstrated the anti-inflammatory activity of the test compound (Gilbert *et al.*, 2011). The assay was performed according to an earlier method of Baylac and Racine (2003) with linoleic acid as the substrate for LOX. 5-LOX has the ability to catalyze the oxidation of unsaturated fatty acids with 1-4 pentadiene structures with arachidonic acid as the biological substrate converting them into conjugated dienes, which could result in the continuous increase in the absorption at 234 nm. A reference or standard was prepared, and that was made up of with 10 μ L of DMSO in tween 20, alongwith 2.95 mL of phosphate buffer (pH 6.3), which was pre-warmed in a water bath at 25 $^{\circ}$ C, 50 μ L of linoleic acid solution (100 μ M final concentration), 12 μ L of enzyme, and 12 μ L of phosphate buffer. The extracts were prepared in concentrations ranging from 125 to 2000 ppm. Briefly, the extracts were

aliquoted in 10 μL followed by the addition of 2.95 mL of phosphate buffer (pH 6.3), which was pre-warmed in a water bath at 25 $^{\circ}\text{C}$, 50 μL of linoleic acid solution (100 μM final concentration), 12 μL of enzyme, and 12 μL of phosphate buffer. The absorbance was measured at 234 nm over a period of 10 min. The absorbance was plotted against the different concentrations, and the percentage activity was calculated by the slope of the straight line portions of the sample and that of the control curves, from the graph obtained. The percentage inhibition was calculated using the following formula, $(A_0 - A_1)/A_0 \times 100$, where, A_0 = absorbance of control, $A_1 = \{(\text{absorbance of sample} + \text{reagent}) - \text{absorbance of sample alone}\}$. A graph was plotted with the concentrations in X axis and the percentage inhibition in Y axis. The IC_{50} value (the concentration at which the sample would inhibit 50% of its original activity) was calculated from the equation obtained from the graph, wherein the IC_{50} values were calculated by recording the 'x' value in the straight line equation, $y = mx + c$ obtained from the graph.

3.2.9 Antibacterial disc diffusion assay

The agar well diffusion method was used to test the susceptibility of pathogenic bacteria to the bacterial extracts (Chakraborty *et al.*, 2014). Pathogen cultures of bacteria *V. parahemolyticus*, *E. coli*, methicillin resistant *S. aureus*, *A. caviae* were used as the test pathogens that were inoculated in 10 mL of sterilized nutrient broth before being incubated at 34 $^{\circ}\text{C}$ for 18 h. The extracts were prepared in 30 μg , 60 μg and 100 μg on the sterile discs. The pathogens were swabbed in Mueller Hinton agar (MHA) with sterile cotton buds and the extracts prepared in discs were placed on the medium, whereas chloramphenicol and methanol were used as the positive and negative controls, respectively.

3.2.10 2,2'-Azino-bis-3-ethylbenzothiozoline-6-sulfonic acid diammonium salt (ABTS⁺) radical scavenging assay

The radical scavenging potentials of EtOAc:MeOH extracts of *Bacillus amyloliquefaciens* were determined by ABTS⁺ decolourization assay (Re *et al.*, 1999). In

brief, ABTS⁺ (7 mM) and potassium persulfate (2.45 mM) were mixed and kept for 16 h in dark at room temperature. The intensely coloured resultant ABTS⁺ stock solution was diluted with MeOH to get ~0.70 absorbance at 734 nm. The diluted ABTS⁺ (5 mL) was mixed with 0.1 mL of extracts (0.25 to 2.0 mg/mL; in MeOH) and their corresponding absorbance were recorded at 734 nm against blank solution (MeOH) using UV-VIS spectrophotometer. An equal volume of test samples with different concentrations (0.25-2.00 mg/mL) were analyzed to determine the percentage inhibition and the IC₅₀ values, the concentration of samples at which it inhibits/scavenge 50 % of radical activities and were expressed in mg/mL.

3.2.11 Determination of minimum inhibitory concentration of the extract to pathogenic bacteria

The minimum inhibitory concentration of the bacterial extract was assessed by broth microdilution method in consonance with the National Committee for Clinical Laboratory Standards (CLSI, 2009) with some refinements. The crude extract was serially diluted to different concentrations, such as 6.25 µg, 12.5 µg, 25 µg, 50 µg and 100 µg. About 100 µL of 18 h old pathogenic cultures of bacteria *Aeromonas caviae*, *Escherichia coli* and methicillin resistant *Staphylococcus aureus* were aliquoted into the microtitre well plate along with 100 µL of the crude extract. The absorbance was measured at 660 nm against nutrient broth blank.

3.2.12 Statistical analysis

One-way analysis of variance (ANOVA) was carried out to assess the significant differences between the means of bioactivities. The significant differences were represented as $p < 0.05$, and the values were presented as the means of triplicates \pm standard deviation (Girden, 1992).

3.2.13 High pressure liquid chromatography (HPLC)

The purification was carried out using the preparatory high pressure liquid chromatography (PHPLC) system (Shimadzu Corporation, Nakagyo-ku, Japan) connected

with a bonded reverse phase C18 (RP C18) column (Shimadzu; Luna 250 mm X 14.0 mm, 5 μ m) fitted with binary gradient pump (Shimadzu LC-20AP), column oven (CTO-20AC, Shimadzu), a controller (CBM-20A, Shimadzu) and photodiode array detector (SPD-M20A, Kyoto, Japan). About 2 mL of the diluted extract with methanol was injected and the column temperature was maintained at 40°C. Methanol and acetonitrile were the mobile phases used with a flow rate of 6-8 mL/min. The absorbances were recorded at the wavelengths ranging from 200-800 nm.

The purity of the isolated compounds were analyzed by an analytical HPLC system (Shimadzu Corporation, Nakagyo-ku, Japan) attached with reverse phase C18 (RP C18) column (Phenomenex, Torrance, California, USA; Luna 250 mm X 4.6 mm, 5 μ m) fitted to column oven (CTO-20A, Shimadzu), binary gradient pump (Shimadzu LC-20AD), controller (CBM-20A, Shimadzu) and a controller (CBM-20A, Shimadzu). About 20 μ L of the diluted sample in methanol was injected and the column temperature was retained at 40 °C. Methanol and acetonitrile were the mobile phase used in various percentages, and the sample was run at a flow rate of 1 mL/min. The absorbances were recorded at wavelengths ranging from 200-800 nm.

The samples were allowed to pass through solid phase extraction (SPE) cartridges (Strata C18-E; 55 Mm, 70 Å; Phenomenex, Torrance, California, USA) and they were filtered with a syringe filter (0.20 μ m, PTFE, Minisart syringe filter, Sartorius, Goettingen, Germany) before being injected into reversed phase HPLC instruments.

3.2.14 Spectrophotometric analysis

The UV-VIS absorption spectra of the purified chromatographic fractions were acquired on ultraviolet-visible (UV-VIS) spectrophotometer (Varian Cary 50, Walnut Creek, California, USA). The quartz cuvettes (1 cm X 1 cm X 4.5 cm) were used in the UV-VIS spectrophotometer.

3.2.15 Nuclear magnetic resonance (NMR) spectroscopy

The two dimensional NMR analyses, such as ^1H - ^1H correlation spectroscopy (^1H - ^1H COSY), heteronuclear multiple-bond correlation spectroscopy (^1H - ^{13}C HMBC), heteronuclear single-quantum coherence spectroscopy (^1H - ^{13}C HSQC), and nuclear overhauser effect spectroscopy (NOESY) along with the one dimensional NMR analyses, such as carbon (^{13}C NMR; 125 MHz), proton (^1H NMR; 500 MHz) and distortionless enhancement by polarization transfer ($^{135}\text{DEPT}$) were analyzed with a Bruker AVANCE III 500MHz (AV 500) spectrometer (Bruker, Karlsruhe, Germany) in CDCl_3 as aprotic solvent at an ambient temperature with internal standard (TMS; δ 0 ppm) fitted to 5 mm probes. The types of hydrogen nuclei in a molecule are obtained by the corresponding ^1H NMR signals and the proton integral values provide the numbers of characteristic protons. Different types of carbons in a molecule are analyzed by the ^{13}C NMR signals. $^{135}\text{DEPT}$ spectra differentiated the multiplicities of carbons, differentiating the number or possibilities of methines ($-\text{CH}$; signals appeared in the upward direction with higher chemical shift values in the range δ 45-160), methyls ($-\text{CH}_3$; signals appeared in the upward direction with lower chemical shift values in the range δ 10-40), and methylenes ($-\text{CH}_2$; signals appeared in the downward direction). The occurrence of quaternary carbons were denoted by analyzing the signal which was absent in the $^{135}\text{DEPT}$ spectra and apparent in the ^{13}C NMR spectra. The ^1H - ^1H COSY spectra determined the signals, which were correlated with the neighbouring protons by J couplings through-bond and the spectra were obtained by diagonal peaks and cross peaks. ^1H - ^{13}C correlations were determined by the resonances in HSQC spectra, which determined the unique proton directly attached to unique carbon heteronucleus. The correlations between protons and carbons were determined by the HMBC spectra, which were separated by bond distances, two, three and four. The NOESY spectra were attained with diagonal peaks and cross peaks, which were similar to ^1H - ^1H COSY. The cross peaks represented the resonances from the nucleus, and were spatially nearby to each other than the direct bond couplings. In brief, NOESY spectra determined the special conformations and adjacent proximities of adjacent spin systems. The NMR spectral interpretations were performed with the software

MestReNova ver. 7.1.1-9649 © 2012 (Mestrelab Research, S.L. Feliciano Barrera, Santiago de Compostela, Spain).

3.2.16 Chromatographic purification of pure compounds from *Bacillus amyloliquefaciens*

The organic fraction of the crude bacterial extract was purified by reverse phase octadecylsilane-C₁₈ (RP-C₁₈) stationary phase using 80% acetonitrile (MeCN): 20 % methanol (MeOH) (v/v) to yield four fractions (BA-1 to BA-4). The crude extract of *B. amyloliquefaciens* was initially eluted through C-18 column (of 55 μ particle size and 70 Å pore size) to remove lesser polar compounds in the mixture. The eluted fraction was further purified by preparative HPLC (reverse phase C18 PHPLC) using MeCN: MeOH (80:20, v/v; 10 mL/min) to yield four fractions (BA1-BA4). Among these fractions BA4 was obtained with greater yield, which was further purified by reverse-phase preparative high-pressure liquid chromatography (RP-HPLC, C₁₈-1.4 cm × 25 cm, 5 μm) using MeCN:MeOH (80:20, v/v; 10 mL/min) to yield compounds 1 and 2, which were found to be homogeneous in TLC (CHCl₃/MeOH, 4:1 v/v) and RP-HPLC (MeOH:MeCN, 80:20 v/v).

3.2.17 *In vitro* antioxidant and anti-inflammatory activities of pure compounds

The antioxidant (DPPH and ABTS⁺ scavenging) and anti-inflammatory (5-LOX inhibitory) activities were determined according to the procedures described under the sections 3.2.7 through 3.3.10.

RESULTS

4. RESULTS

The results of the study entitled 'Identification and characterization of bioactive leads from mangrove sediment associated bacteria and assessment of their therapeutic potential' carried out at the ICAR-Central Marine Fisheries Research Institute, Kochi, Ernakulam during 2018-2019 were depicted in this chapter.

4.1 ISOLATION AND CHARACTERIZATION OF MANGROVE SEDIMENT ASSOCIATED BACTERIA

4.1.1 Sample collection and isolation of microbes

A total of 10 sediment samples associated with the mangrove species *A. ilicifolius* and *A. officinalis* were collected from the Mangalavanam mangrove ecosystem of Kochi, Kerala. The spread plate cultures of serially diluted sample S3 from 10^{-1} to 10^{-7} was presented in Figure 4.1 (Lemos *et al.*, 1985; Behera *et al.*, 2014). The serial dilutions of 10 sediment samples were performed. The growth was visible from 24 hours and the plates were observed for almost 1 week. A total of four well-grown isolates from each sample were sub-cultured into the nutrient agar plates supplied with 0.5 % NaCl, and the sub-cultures were preserved in 50 % glycerol stock for long term storage at -80°C , whereas short term storage was carried out in nutrient agar slants and stab cultures along with glycerol at 20°C (Pelczar *et al.*, 1977).

4.1.2 Antimicrobial screening by spot-over-lawn assay

A total of 40 bacterial isolates selected from the nutrient agar plates were tested against both gram positive and gram negative pathogenic bacteria, such as *V. parahemolyticus*, methicillin resistant *S. aureus*, *A. caviae* and *E. coli* (Chakraborty *et al.*, 2014). Among the total of 40 isolates, 25 isolates, i.e., 62.5 % of the isolates were active against at least one of the test pathogen with an inhibition zone diameter ≥ 10 mm, whereas 15 isolates i.e., 37.5 % showed an activity of ≥ 15 mm. A total of 6 of the isolates were active against at least one

pathogen with an inhibition zone diameter ≥ 20 mm. About 16 of the isolates showed activity against methicillin resistant *S. aureus* with an inhibition zone ≥ 10 mm, whereas 4 of them exhibited the inhibition zone of ≥ 15 mm against the pathogen. About 18 of the isolates displayed anti-infective properties against *V. parahemolyticus* with an inhibition zone ≥ 10 mm, whereas 12 of them displayed the inhibition zone of ≥ 15 mm against the pathogen. Notably, 5 of the isolates showed significant activity against *E. coli*, whereas only 1 exhibited significant antibacterial activities with ≥ 15 mm inhibitory zone diameter. About 8 of the isolates showed activity against *A. caviae* with an inhibition zone ≥ 10 mm, whereas 4 of them exhibited the inhibition zone of greater than 20 mm against the pathogen.

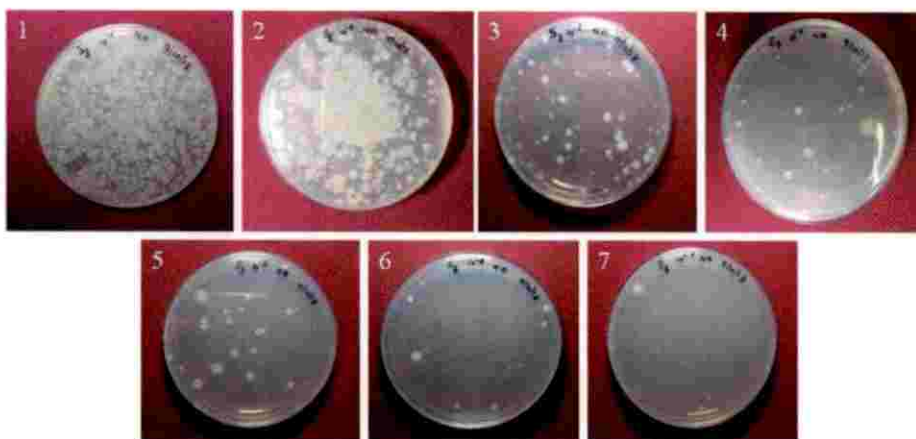


Figure 4.1. Serially diluted and spread plated nutrient agar plates from dilutions ranging from 10^{-1} and 10^{-7} from 1 to 7, respectively.

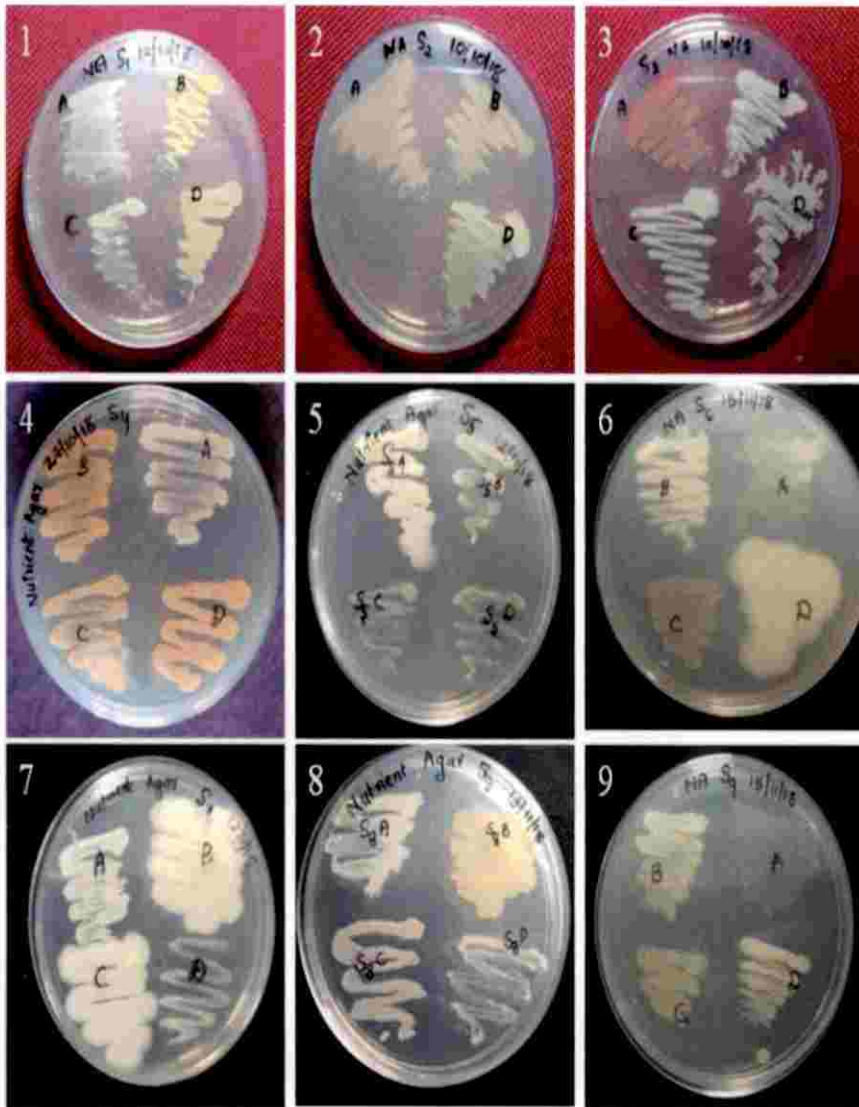


Figure 4.2. The streak cultures of bacteria from S1 to S9 in nutrient agar plates from 1 to 9, respectively.

Table 4.1. Antimicrobial activity* of isolates from samples S1 through S10

| Bacterial Strains | Inhibition zone diameter (mm) | | | |
|-------------------|-------------------------------|----------------|-------------|---------------------------|
| | <i>A. cavie</i> | <i>E. coli</i> | <i>MRSA</i> | <i>V. parahemolyticus</i> |
| S1A | 14 | 14 | - | 16 |
| S1C | - | 15 | 15 | 15 |
| S1D | - | - | 14 | - |
| S2A | 13 | - | 12 | 20 |
| S2B | - | - | 12 | - |
| S2C | - | - | 14 | - |
| S2D | - | 13 | - | 14 |
| S3A | - | - | 12 | - |
| S3B | - | - | - | 15 |
| S3C | - | - | 12 | - |
| S3D | - | - | - | 13 |
| S4A | - | - | 16 | 16 |
| S4B | - | 12 | - | 17 |
| S4C | - | - | 13 | - |
| S4D | - | - | 14 | 13 |
| S5A | - | - | - | 18 |
| S5D | 14 | 14 | - | 16 |
| S6D | - | - | 15 | 16 |
| S7B | 13 | - | 20 | 13 |
| S7C | - | - | 12 | 13 |
| S8A | 26 | - | - | 37 |
| S8C | 25 | - | - | - |
| S8D | - | - | - | 20 |
| S10A | - | - | - | 17 |
| S10B | - | - | - | 20 |
| S10C | - | - | 13 | - |

*Antimicrobial activity was recorded as the diameter of inhibition zones determined as a distance of ≥ 1 mm between the circular area (= lawn of the isolate) and the end of the clear zone bounded by the lawn of the test strain. The strains with ≥ 15 mm inhibition zone diameter from spot-over-lawn assay are mentioned (inhibition zone diameter ≤ 10 mm was ignored).

4.1.3 Biochemical and morphological characterization of the bacterial isolates

Biochemical characterization and motility tests were performed for the selected 23 isolates (Krieg and Holt, 1984). Gram staining was performed for all the 40 isolates, whereas 25 were gram positive and 15 were found to be gram negative. A total of 47.5 % of the isolates were gram positive rods, wherein 10 % were gram positive cocci, and 1 of the isolate was a gram negative cocci. The biochemical characterization was carried out for 23 isolates using HiBacillus identification kit (Sigma Aldrich).

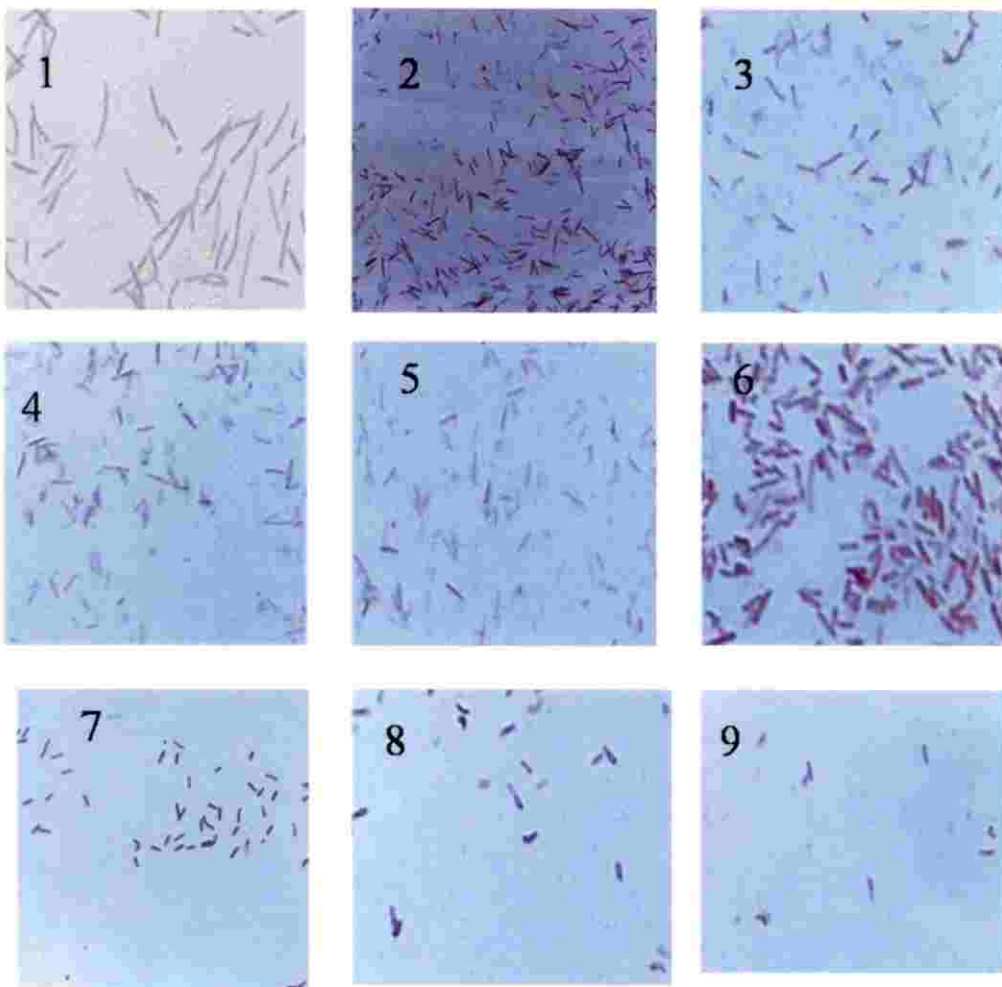


Fig. 4.3. Gram stained *Bacillus* strains, S1A, S1C, S2A, S2B , S2C, S2D, S4A, S10B and S10C (denoted as 1-9)..

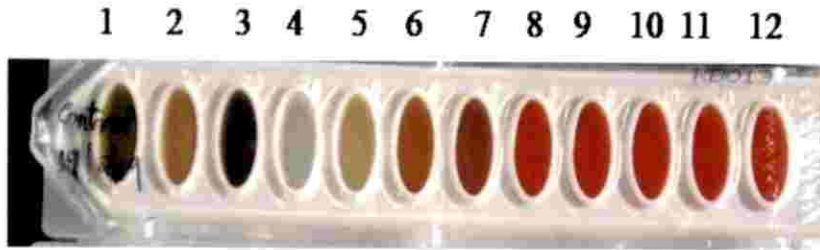


Figure 4.4. Control of biochemical characterization

It represents 12 different wells from 1 to 12, containing the medium required for detecting the utilization of malonate, voges proskauer, citrate utilisation, ONPG, nitrate reduction, catalase, arginine utilization and utilization of sugars, such as sucrose, mannitol, glucose, arabinose and trehalose, respectively.

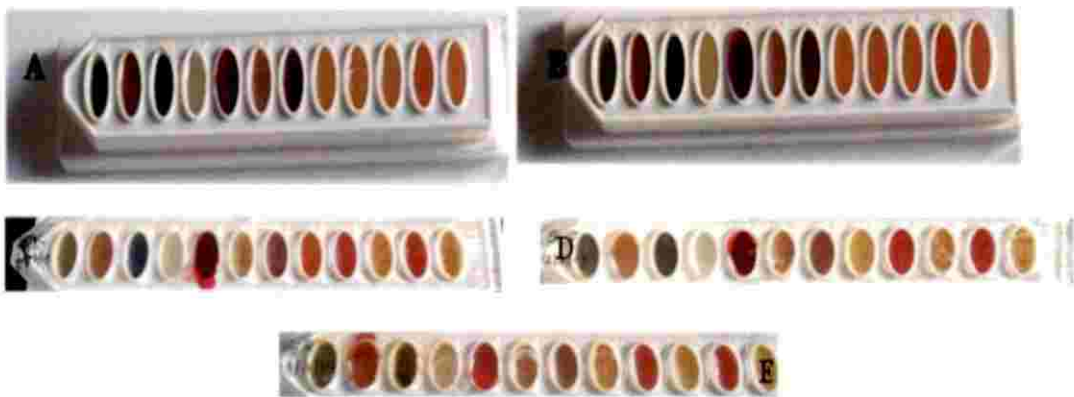


Figure. 4.5. Biochemical characterization of S2A (A), S4A (B), S10C (C), S1C (D) and S2D (E).

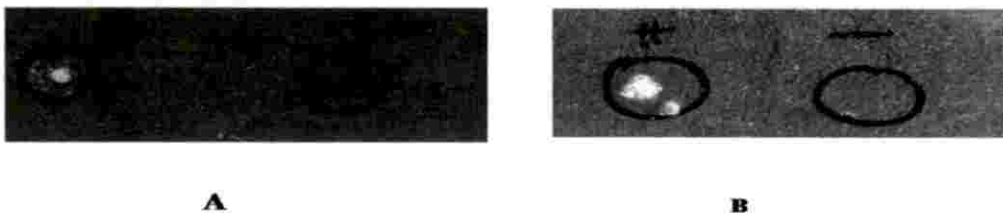


Figure 4.6. Catalase test for S2A (A) and catalase test of S10B (B).

**Table 4.2.** Biochemical characteristics of the selected isolates

| Characteristics | 1 | 2 | 3 | 4 | 5 | 6 | 7 | 8 | 9 | 10 |
|-------------------|---|---|---|---|---|---|---|---|---|----|
| Malonate | - | - | - | - | - | - | - | + | - | - |
| Citrate | + | - | - | - | - | - | + | + | + | - |
| ONPG | - | - | - | - | - | - | - | - | - | - |
| Catalase | + | + | + | + | + | + | + | + | + | + |
| Arginine | + | + | + | + | - | + | - | - | + | + |
| Sucrose | + | + | + | + | + | + | + | + | + | - |
| Mannitol | - | - | + | - | - | - | + | + | - | - |
| Glucose | + | + | + | + | + | + | + | + | + | + |
| Arabinose | - | - | + | - | - | - | + | - | - | - |
| Trehalose | + | + | + | + | + | + | + | - | + | + |
| Motility | + | + | + | + | + | - | + | + | + | + |
| Voges Proskauer | - | - | + | - | - | - | - | - | - | - |
| Nitrate Reduction | + | + | + | + | + | + | + | - | + | + |

(+) Signified the positive reaction of the bacterial isolate towards the specific biochemical test, and (-) signified no reaction. S1A, S1C, S2A, S2B, S2C, S2D, S4A, S5D, S10B and S10C (1-10) were represented.

Table 4.2. Biochemical characteristics of the selected isolates (Cont'd)

| Characteristic | 1 | 2 | 3 | 4 | 5 | 6 | 7 | 8 | 9 | 10 | 11 | 12 | 13 |
|----------------------|---|---|---|---|---|---|---|---|---|----|----|----|----|
| Malonate | - | - | - | - | + | - | + | + | - | - | + | + | + |
| Citrate | - | - | - | - | + | + | + | + | + | + | + | + | + |
| ONPG | - | - | - | - | - | - | - | - | - | - | - | - | - |
| Catalase | + | + | + | + | - | + | + | + | + | + | + | + | + |
| Arginine | + | + | - | + | - | + | + | + | + | - | - | - | - |
| Sucrose | + | + | + | + | + | + | - | - | + | + | - | - | - |
| Mannitol | + | - | - | - | + | - | - | - | - | - | - | + | + |
| Glucose | + | + | + | + | + | + | - | - | + | + | + | - | - |
| Arabinose | - | - | - | - | - | - | - | - | - | - | - | - | - |
| Trehalose | + | + | + | + | - | + | - | - | + | + | - | - | - |
| Voges Proskauer | + | + | - | - | - | - | - | - | - | - | - | - | - |
| Nitrate reduction | + | + | + | + | + | + | + | - | + | + | + | - | + |

(+) Signified the positive reaction of the bacterial isolate towards the specific biochemical test, and (-) signified no reaction. S1B, S3B, S3C, S4D, S5B, S5C, S6B, S6C, S7A, S7D, S8B, S9C and S9D (1-13) were the selected strains represented.

Table 4.3. Morphological characters of the selected isolates

| Tests | S1A | S1C | S2A | S2B | S2C |
|--------------------------|--------------------|-----------------|-----------|-----------------|--------------------|
| Colony morphology | | | | | |
| Configuration | Round | Round | Wrinkled | Round | Round |
| Margin | Undulate to curled | Wavy | Rhizoidal | Wavy | Undulate to curled |
| Elevation | Convex | Slightly convex | Flat | Slightly convex | Convex |
| Pigment | Offwhite | Offwhite | Offwhite | Offwhite | Offwhite |
| Surface | Mucosal | Waxy | Rough | Waxy | Mucosal |
| Opacity | Opaque | Opaque | Opaque | Opaque | Opaque |
| Gram's reaction | + | + | + | + | + |
| Cell shape | Rod | Rod | Rod | Rod | Rod |
| Motility | + | - | + | - | + |
| Arrangement | Short chained | Chains | Chains | Chains | Short chained |

(+) Signified the positive reactions of the bacterial isolate towards Gram reaction and motility, and (-) signified the negative.

Table 4.3 Morphological characters of the selected isolates (cont'd)

| Tests | S2D | S10B | S4A | S10C |
|--------------------------|----------------------|-----------------|-----------|--------------------|
| Colony morphology | | | | |
| Configuration | Comma shaped | Round | Wrinkled | Round |
| Margin | Curled and irregular | Wavy | Rhizoidal | Undulate to curled |
| Elevation | Slightly convex | Slightly convex | Flat | Convex |
| Pigment | Offwhite | Offwhite | Offwhite | Offwhite |
| Surface | Sticky | Waxy | Rough | Mucosal |
| Opacity | Opaque | Opaque | Opaque | Opaque |
| Gram's reaction | + | + | + | + |
| Cell shape | Rod | Rod | Rod | Rod |
| Motility | - | - | + | + |
| Arrangement | Short chains | Chains | Chains | Round |

(+) Signified the positive reactions of the bacterial isolate towards Gram reaction and motility, and (-) signified the negative.

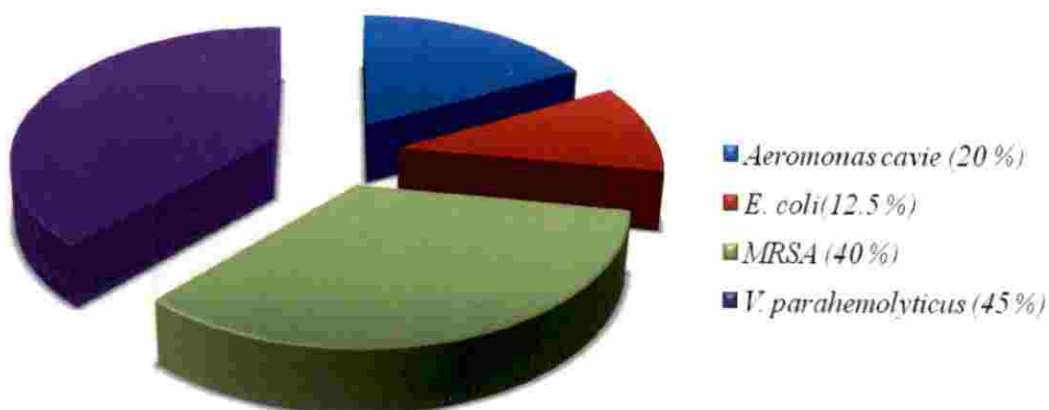


Fig. 4.7. Pie diagram representing the percentage of isolates which exhibited an inhibition zone ≥ 10 mm against various pathogens

4.1.4 Preliminary screening of antioxidant activities

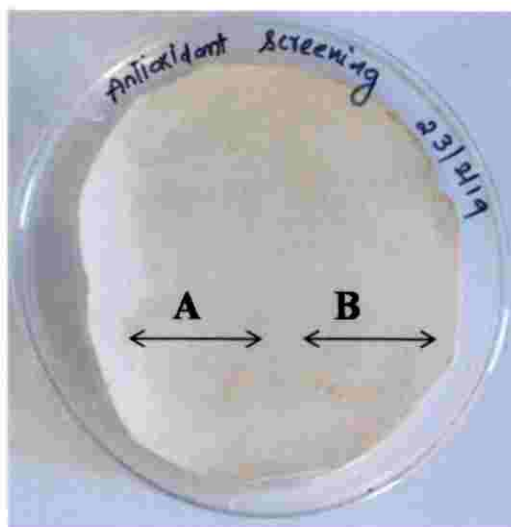


Figure 4.8. Zone of clearance produced by S2A (A) and S10B (B) in DPPH sprayed filter papers incubated with bacteria

The preliminary screening of the anti-oxidant activities of the isolated strains were carried out by using DPPH and the filter paper incubated along with the strains (Velho-Pereira *et al.*, 2005). The inhibition zone diameter obtained after spraying of DPPH into the filter paper was analyzed. Among the isolated strains, those designated as S2B, S10B and S10C exhibited potentially greater inhibition zones ranging from 18-20 mm, against the studied pathogens, whereas

S2C and S2A were found to display inhibition zones of 25 mm and 40 mm, respectively, representing potential anti-oxidant properties against the target free radical.

4.1.5 Molecular characterization of the selected isolates

Genomic DNAs of a total of 10 strains were isolated and performed agarose gel electrophoresis for the detection of DNA. The quality and quantity of the DNA samples were checked, and the ratios of absorbances at $\lambda_{260/280}$ nm were distributed from 1.7 to 2, attributing the superior qualities of DNA. The 16S rRNA amplification was further performed, and the PCR product was obtained in the size range of 1200-1517 bp. The similarities of sequences to the existing nucleotide sequences were checked by NCBI-Blast. A higher similarity of $\geq 99\%$ was obtained for the isolates of *B. amyloliquefaciens*, *B. cereus*, *B. paramycoides* and *B. anthracis*. The forward trimmed sequences of 9 strains were submitted in the GenBank and the accession numbers obtained were represented in the Table 4.5. The bacterial isolates designated as S2A and S4A were identified as *B. amyloliquefaciens*, while S1A, S2C, S10B and S10C were found to be *B. cereus*. The strains designated as, S1C and S2B were recognized as *B. paramycoides*, whereas S2D was found to be *B. anthracis*.

PKS and NRPS are biosynthetic gene clusters, which were involved in the synthesis of many secondary metabolites, and were found to be the biologically active compounds in microorganisms (Thilakan *et al.*, 2016). The occurrences of these gene systems in the microorganisms could be found out by targeting specific primers to the PKS and NRPS gene sequence (Ayuso-sacido *et al.*, 2005). The bacterial isolate S2A, found out to be *B. amyloliquefaciens* was recorded for the presence of PKS gene using the primers *gcf* and *gcr*, wherein the 700 bp fragment obtained was sequenced and submitted in EMBOSS software before being submitted in GenBank. The GenBank accession number obtained for the *pkS* sequence was MN 165388.

Table 4.4. Quality of DNA at absorbance 260/ 280 nm and quantity of DNA

| Strain | Quality of DNA at Abs 260/280 | Quantity of DNA at (ng/ μ l) |
|--------|-------------------------------|----------------------------------|
| S1A | 1.72 | 87.49 |
| S1C | 1.77 | 152.2 |
| S2A | 1.79 | 115.87 |
| S2B | 1.63 | 149.4 |
| S2C | 1.76 | 114.7 |
| S2D | 1.9 | 145.6 |
| S4A | 1.75 | 60.6 |
| S5D | 2.1 | 197.3 |
| S10B | 1.83 | 109.6 |
| S10C | 1.89 | 114 |

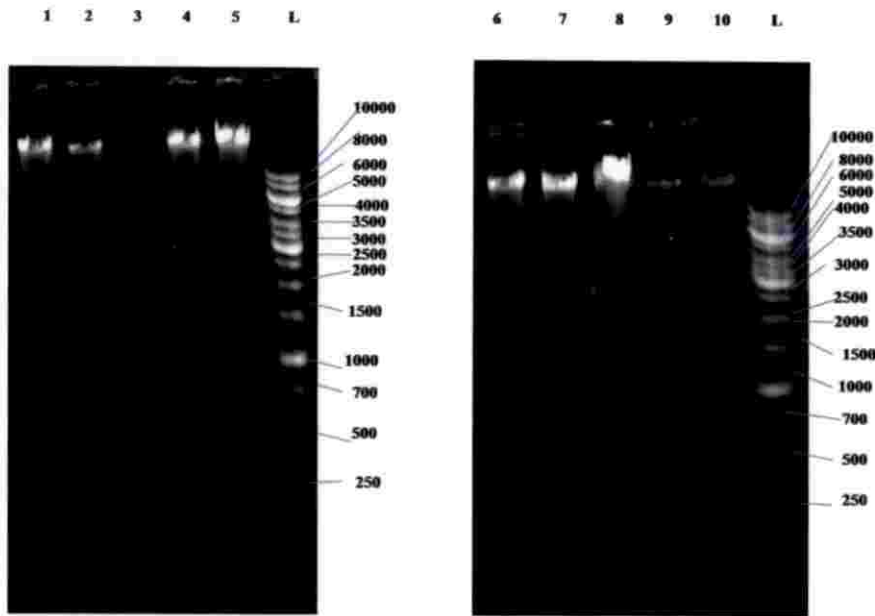


Figure 4.9. Gel profiles of the isolated DNA samples

Gel profiles of the isolated DNA samples along with 1 kb DNA ladder, L (Gene Ruler™, Thermo Scientific). The lanes from 1 to 10 represents the DNA isolated from the bacterial isolates, S2C, S2B, S2A, S1C, S1A, S10C, S10B, S5D, S4A and S2D, respectively. The molecular marker used was Gene Ruler™ 1 kb DNA Ladder (Thermo Scientific, 250–10,000 bp).

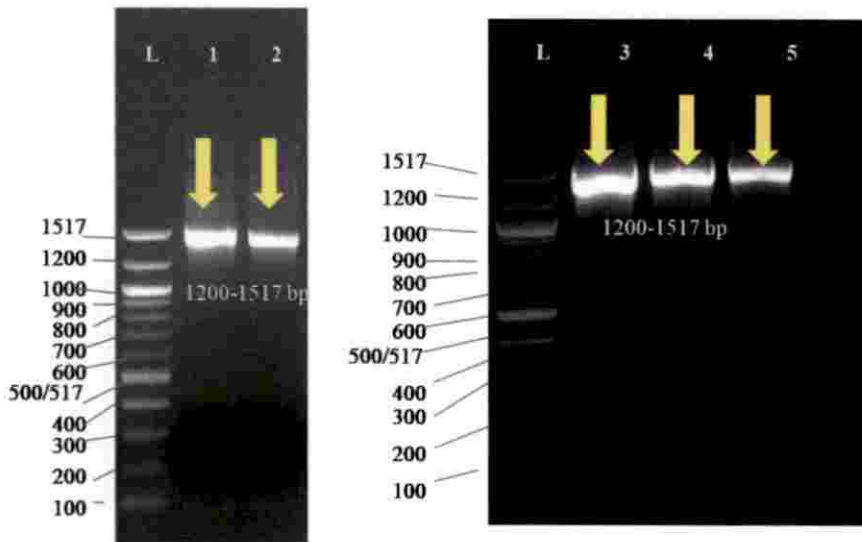


Figure 4.10. Gel profile of the amplified, 16S rRNA gene of bacteria

Gel profile of the amplified, 16S rRNA gene of bacterial isolates, S2A, S10C, S1A, S4A and S10B (from lanes 1 to 5, respectively), with ladder, L (100 bp DNA ladder, NEB).

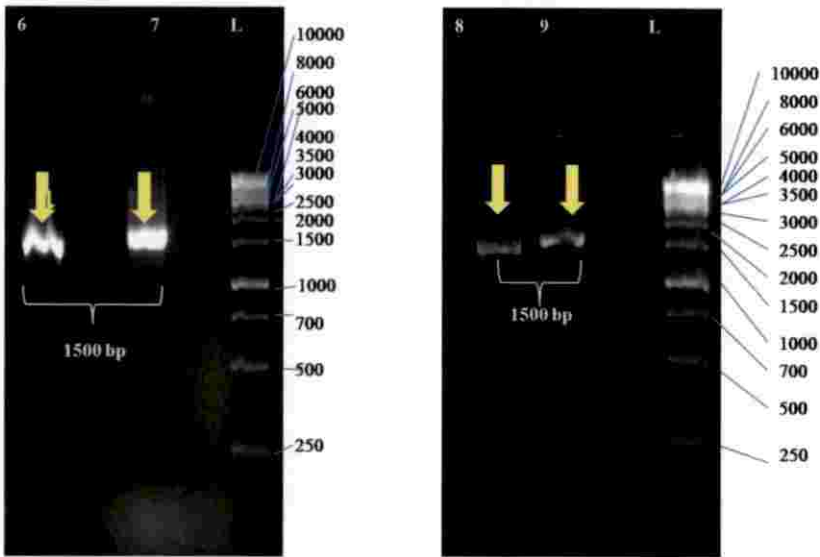


Figure 4.10. Gel profile of the amplified, 16 S rRNA gene of isolates (Cont'd) Gel profile of the amplified, 16 S rRNA gene of strains, Lane 1: S1C, Lane 2: S2B, Lane 3: S2C and Lane 4: S2D. (L) The molecular marker used is Gene Ruler™ 1 kb DNA Ladder (Thermo Scientific, 250–10, 000 bp).

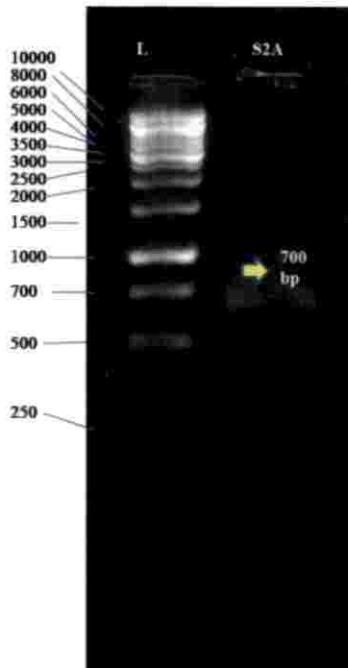


Figure 4.11. Polyketide synthase product of *B. amyloliquefaciens* MK765025 Polyketide synthase (*pks*) product (~700 bp) of the bacterium (S2A) *B. amyloliquefaciens* MK765025 associated with mangrove sediment. (L) Gene Ruler™ 1 kb DNA ladder, Thermo Scientific (250- 10, 000 bp).

Table 4.5. GenBank accession numbers of the strains identified by NCBI-BLAST

| Strains | GenBank Accession No. | Bacteria |
|---------|-----------------------|-----------------------------|
| S1A | MN204214 | <i>B. cereus</i> |
| S1C | MN204219 | <i>B. paramycoides</i> |
| S2A | MK765025 | <i>B. amyloliquefaciens</i> |
| S2B | MN204220 | <i>B. paramycoides</i> |
| S2C | MN204215 | <i>B. cereus</i> |
| S2D | MN204226 | <i>B. anthracis</i> |
| S4A | MN165386 | <i>B. amyloliquefaciens</i> |
| S10B | MN240446 | <i>B. cereus</i> |
| S10C | MN165387 | <i>B. cereus</i> |

The phylogenetic analysis of the 9 isolates were carried out after aligning the sequences together with bacterial sequences of different species in the genus *Bacillus*, such as *B. subtilis*, *B. methylotrophicus*, *B. thuringiensis*, *B. vallismortis*, *B. megaterium*, *B. clausii* and *B.s atropheaus* along with different sequences of *B. amyloliquefaciens* obtained from the NCBI database. The phylogenetic tree, showing the relationship among the different species was constructed with the MEGA6 software by neighbor-joining method.

The isolated *B. amyloliquefaciens* strains, S2A and S4A fell under the clade including several other *B. amyloliquefaciens* strains, *B. vallismortis*, *B. subtilis* and *B. methylotrophicus*. The *B. cereus* strains S1A, S10B and S10C fell under the same clade with an isolated *B. paramycoides* strain (S1C), along with *B. thuringiensis*. The reason for this exclusion from a similar clade was due to the insufficient divergence in the 16S rRNA sequence region (Maughen and Van der Auwera, 2011). Hence, an essential housekeeping gene, which evolve more rapidly than the 16S rRNA gene, could be used for taxonomic classification (Palys *et al.*, 2000).

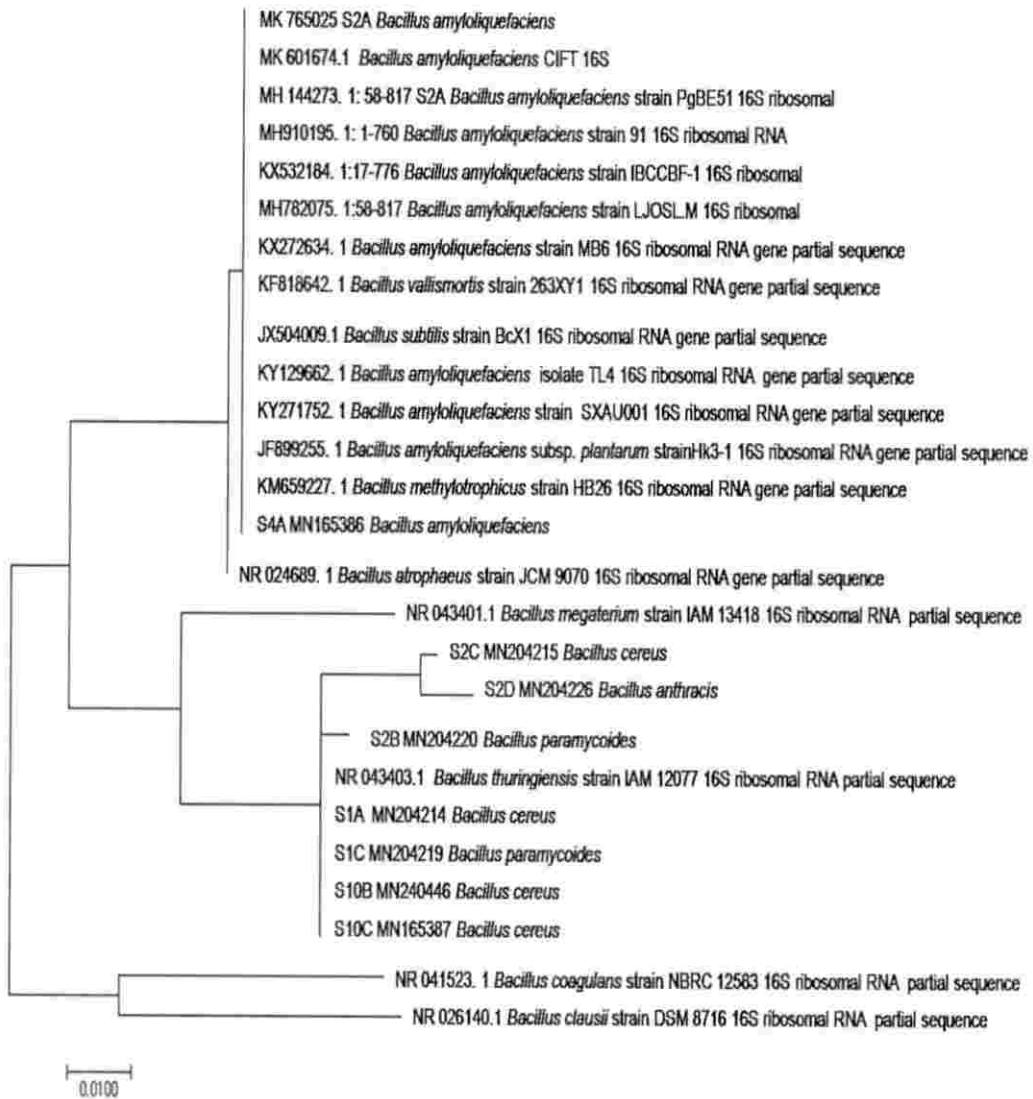


Figure 4.12. Phylogenetic analysis of the selected isolates

Phylogenetic analysis of isolates, S2A, S1A, S1C, S2B, S2C, S2D, S4A, S10B and S10C along with related strains by neighbor joining method in MEGA 6 software.

4.1.6 Bacterial growth curve of *B. amyloliquefaciens* (S2A)

The bacteria produce most of the secondary metabolites in the stationary phase of growth, whereas the exponential growth was stationary. Hence, the bacterial growth curve has been crucial for finding the phase of the production of secondary metabolites or bioactive compounds in the bacteria. Previous reports of literature suggest that the secondary metabolite production in *B. amyloliquefaciens* occurs after 72 hours of incubation (Boottanun *et al.*, 2017). The bacterial curve plotted with time at 660 nm also appropriately inferred that the stationary phase was at 68-72 h, thus supporting the existing reports and the growth began to decline after 72 h, before being attained its death phase. The findings helped to find the stationary phase to extract the extracellular and intracellular metabolites released by the bacteria.

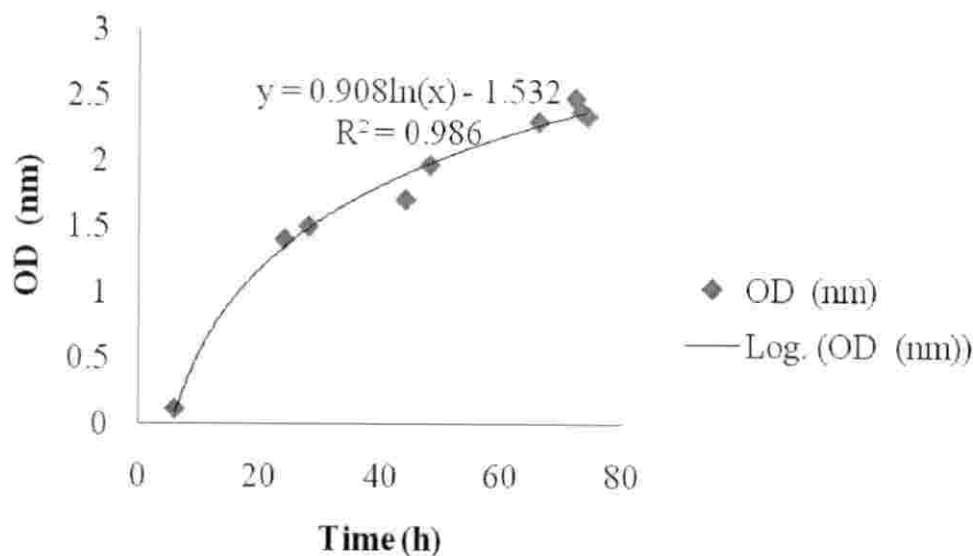


Fig 4.13. Bacterial growth curve of *B. amyloliquefaciens* MK765025 at 660 nm.

4.2 BIOASSAY GUIDED ISOLATION AND CHARACTERIZATION OF BIOACTIVE COMPOUNDS FROM *B. amyloliquefaciens*

4.2.1 Extraction of bioactive compounds from *B. amyloliquefaciens*

The shortlisted bacteria *B. amyloliquefaciens* (S2A), with greater bioactivities, was grown in nutrient broth supplied with 0.5 % NaCl and the culture was swabbed in nutrient agar plates supplied with 0.5 % NaCl. The bioactive compounds from the selected bacterial isolate were extracted in solvent ethyl acetate by refluxing in a heating mantle for 72 h of incubation at 34 °C. The intracellular compounds from the bacteria were released by sonicating at amplitude of 37 % with a 10 sec on and off pulse mode for 20 minutes. Intracellular and extracellular compounds were extracted separately in the round bottom flasks, before being concentrated in rotary vacuum evaporator, and the presence of compounds were recorded by TLC experiments.

4.2.2 Thin layer chromatographic documentation of intracellular and extracellular extracts

The individual components (compounds) of the intracellular and extracellular extracts showed good separation in the solvent system containing 5 % methanol and 95 % DCM, whereas the TLC documentation was carried out at the wavelengths of 254 nm and 365 nm. Spots were observed at various intervals from the day of first extraction till the process of extraction. The UV spots were visualized at the wavelengths of 254 nm and 365 nm.

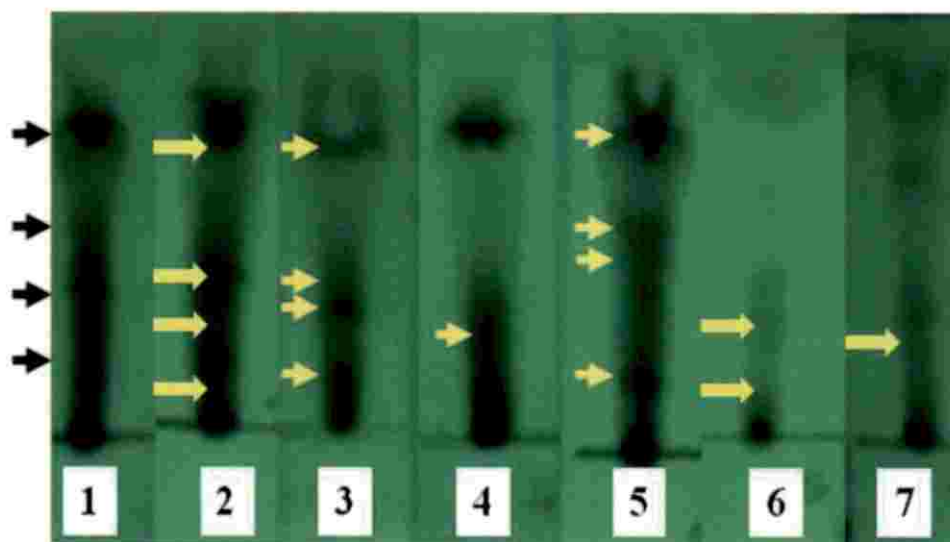


Figure 4.14. TLC chromatogram of the extracellular compounds from *B. amyloliquefaciens* MK765025

TLC chromatogram of the extracellular compounds from *B. amyloliquefaciens* (S2A) at 254 nm, where lanes 1 to 7 represented extraction days in an ascending order. The arrows indicated the possible presence of individual compounds in the extract.

The organic compounds were colourless on the white surface of the TLC plate, and therefore, the visualizing agents, such as iodine, DPPH and vanillin-sulphuric acid were commonly used. Iodine could strongly react with aromatics and vanillin along with sulphuric acid could detect the presence of aldehydes, ketones and alcohols. A total of 6-7 spots were visible in the TLC plate visualized with iodine, indicating the presence of aromatics, 4-5 spots were visible on TLC plates visualized with vanillin-sulphuric acid indicating the presence of either aldehydes, ketones or alcohols, and the presence of anti-oxidant compounds were indicated by the decolourization of spots in the TLC plates visualized with DPPH. An immediate decolourization of the spots from purple to white, was observed in the TLC plates indicating that they could scavenge the free radical, DPPH.

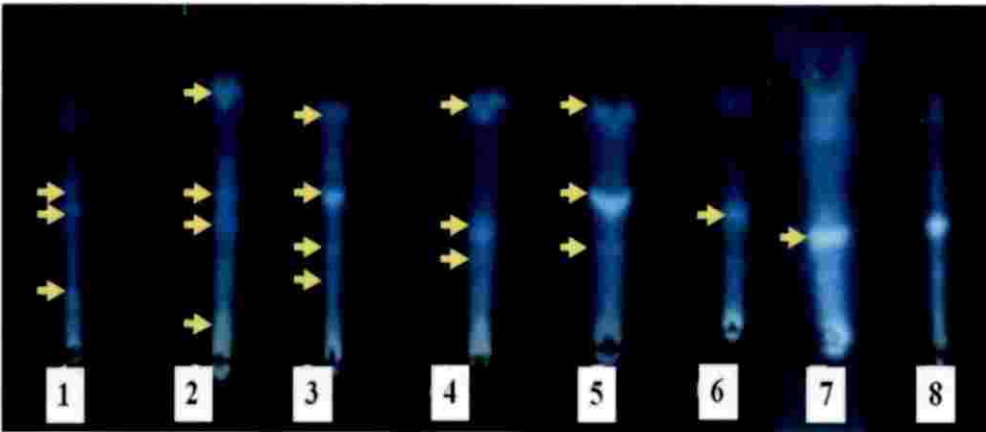


Figure 4.15. TLC chromatogram of the extracellular compounds from *B. amyloliquefaciens* (S2A) at 365 nm, where lanes 1 to 8 represented extraction days in an ascending order. The arrows indicated the possible presence of individual compounds in the extract.

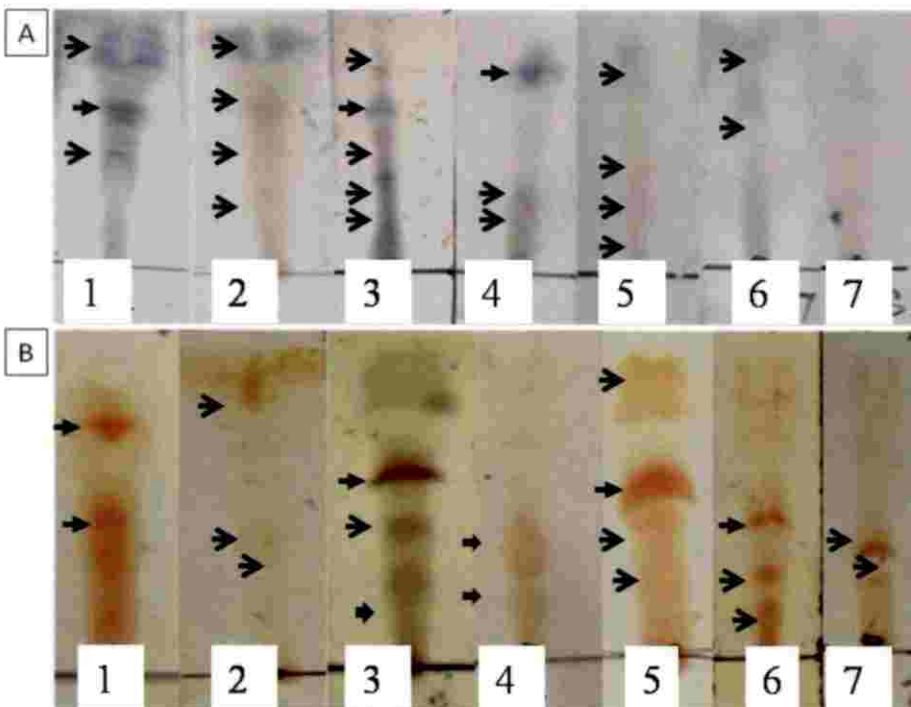


Figure 4.16. (A) TLC chromatogram of the extracellular compounds from *B. amyloliquefaciens* (S2A) stained with vanillin-sulphuric acid, where lanes 1 to 7 represented days of extraction in an ascending order. (B) TLC chromatogram of the extracellular compounds from *B. amyloliquefaciens* (S2A) stained with iodine, where lanes 1 to 7 represented days of extraction in an ascending order. The arrows indicated the possible presence of individual compounds in the extract.



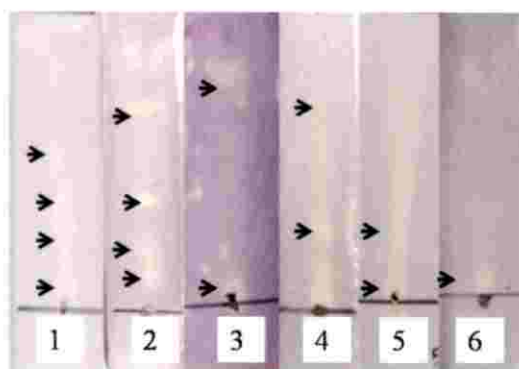


Fig 4.17. TLC chromatogram of the extracellular compounds from *B. amyloliquefaciens* (S2A) stained with DPPH, where 1 to 6 represented days of extraction in ascending order, and the decolorized spots were recorded.

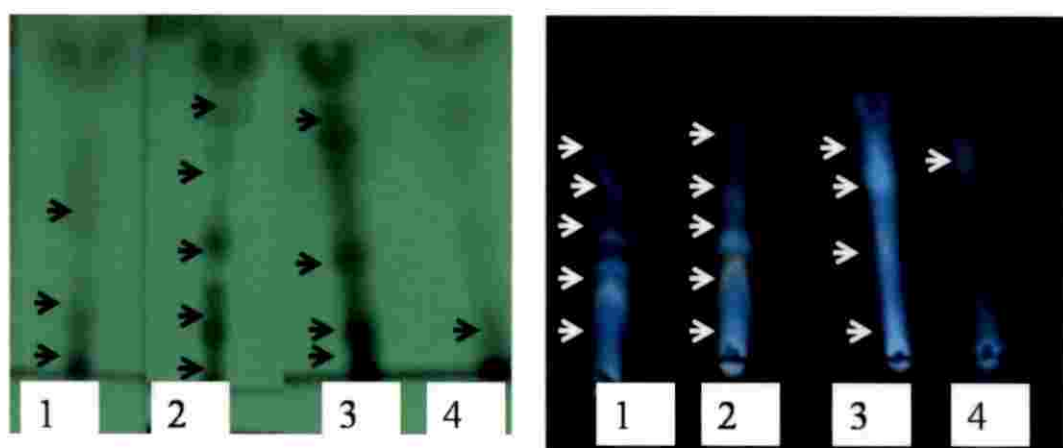


Fig 4.18. TLC chromatogram of the intracellular compounds from *B. amyloliquefaciens* (S2A) visualized at 254 nm and at 365 nm, respectively where 1 to 4 represented days of extraction, in an ascending order.

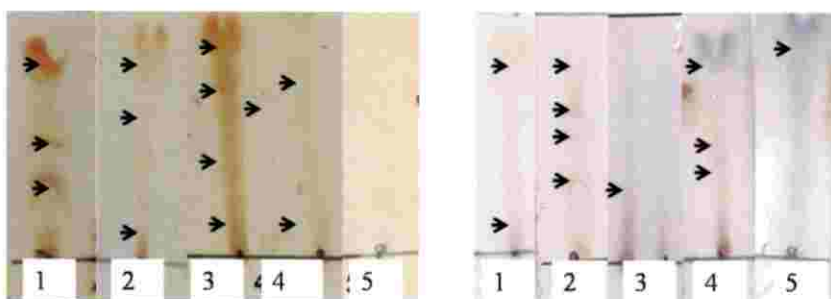


Fig 4.19. TLC chromatogram of the intracellular compounds from *B. amyloliquefaciens* (S2A) stained with (A) iodine and (B) vanillin-sulphuric acid, whereas the lanes designated as 1 to 5 represented days of extraction, in an ascending order.

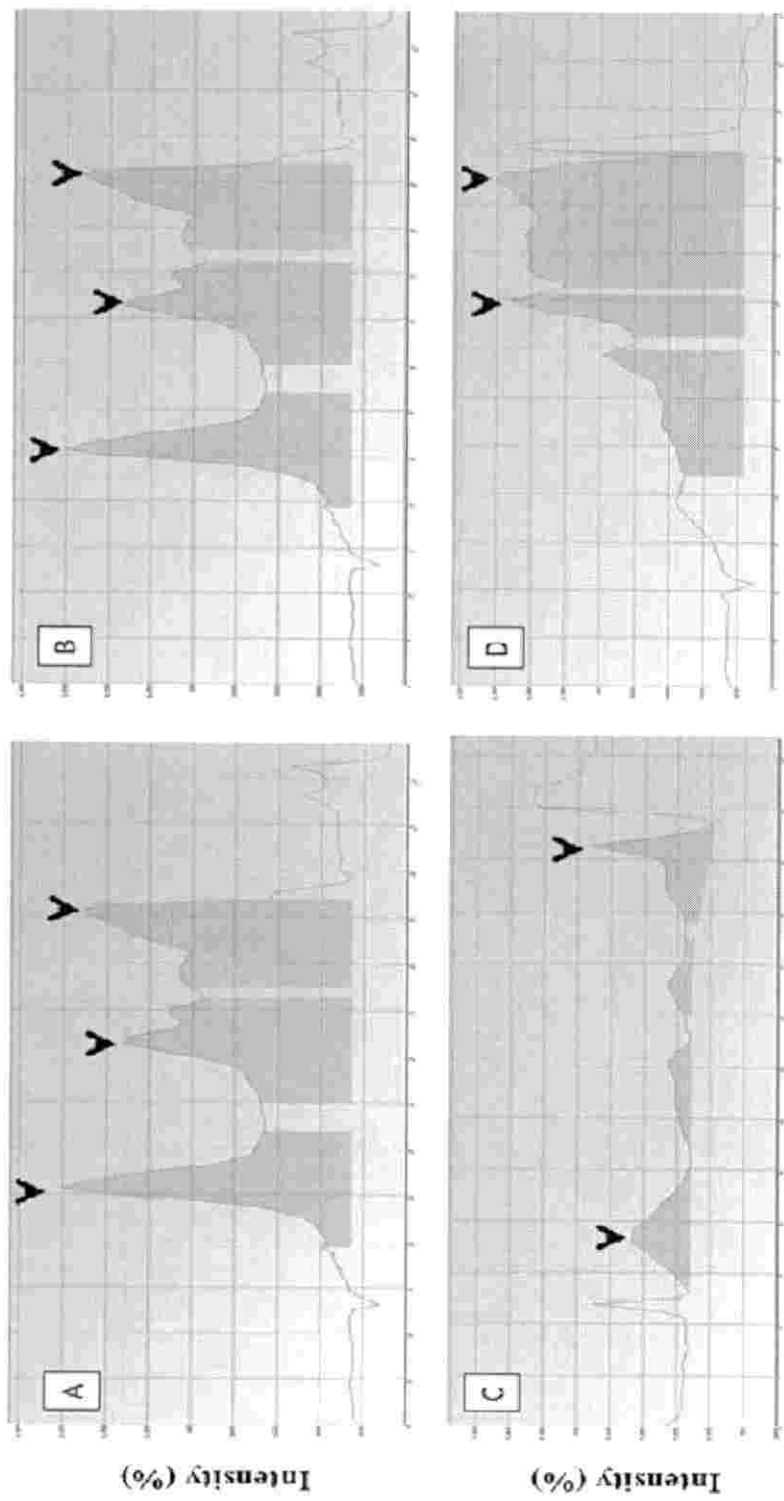


Fig 4.20. HPTLC chromatogram of the extracellular compounds from *B. amyololiuefaciens*

4.2.3 Antioxidant and anti-inflammatory activities of the crude organic extracts of *B. amyloliquefaciens* (S2A)

The ethyl acetate extracts of *B. amyloliquefaciens* exhibited potential antioxidant activity with IC_{50} 3.5 $\mu\text{g/mL}$ to quench DPPH radical and IC_{50} 3.9 $\mu\text{g/mL}$ to scavenge ABTS radical cation. Notably, the antioxidant activities were significantly greater than those displayed by the commercially available antioxidant α -tocopherol. The inhibitory activities of the organic extract of *B. amyloliquefaciens* against inducible pro-inflammatory enzyme 5-LOX was significantly higher (IC_{50} 6 $\mu\text{g/mL}$) than that exhibited by commercially available synthetic anti-inflammatory drug ibuprofen.

Table 4.6. Antioxidant and anti-inflammatory activities of the crude bacterial extract

| Bioactivities (IC_{50} $\mu\text{g/mL}$) | Crude extract of <i>B. amyloliquefaciens</i> | Control |
|----------------------------------------------|-------------------------------------------------|-----------------------------|
| DPPH radical scavenging activity | 3.5 | 660 (α -tocopherol) |
| ABTS scavenging activity | 3.9 | 760 (α -tocopherol) |
| 5-LOX inhibitory activity | 6.0 | 920 (ibuprofen) |

4.2.4 Antimicrobial activity of the organic extract of *B. amyloliquefaciens* (S2A) by disc diffusion assay

The antimicrobial activities of both intracellular and extracellular crude extracts of *B. amyloliquefaciens* were tested against various pathogens, such as *V. parahemolyticus*, MRSA, *E. coli* and *A. caviae*. The crude extracts possessed a higher activity when compared to the spot-over lawn assay and the positive control, chloramphenicol (30 μg).

Table 4.7. Inhibition zone diameter* exhibited by the intracellular organic extract

| Test pathogens | Inhibition zone diameter (mm) at various loading of the organic extract of S2A | | | | |
|-------------------------------|--------------------------------------------------------------------------------|-------|--------|--------------------------|------------------|
| | 30 µg | 60 µg | 100 µg | Positive control (30 µg) | Negative control |
| <i>Aeromonas caviae</i> | 10 | 14 | 18 | 10 | 0 |
| <i>MRSA</i> | 10 | 12 | 14 | 10 | 10 |
| <i>E. coli</i> | 10 | 16 | 18 | 0 | 0 |
| <i>Vibrio parahemolyticus</i> | 10 | 12 | 14 | 12 | 10 |

Inhibition zone diameter* exhibited by the intracellular organic extract of *B. amyloliquefaciens* (S2A) by disc diffusion assay against various pathogens and the positive control, chloramphenicol (30 µg) and negative control, methanol

*Antimicrobial activity was recorded as the diameter of inhibition zones determined as a distance of ≥ 1 mm between the circular area (= lawn of the isolate) and the end of the clear zone bounded by the lawn of the test strain.

The extracellular extracts of the bacterium possessed antibacterial activity against pathogenic *E. coli* with an inhibition zone diameter of 15 mm for 30 µg and 16 mm for 100 µg, whereas the intracellular extracts exhibited 18 mm inhibition zone for 100 µg of the organic extract. The extracellular extracts showed significantly higher activity against *V. parahemolyticus* with an inhibition zone diameter of 20 mm for 100 µg, whereas the intracellular extracts exhibited 12 mm inhibition zone for 100 µg of the extract. The intracellular extract containing 100 µg of the crude exhibited 20 mm inhibition zone against the test pathogen *A. caviae*, and was not significantly different than the activity exhibited by the extracellular extract (~ 18 mm). The extracellular extracts of the studied bacterium displayed higher activity towards the test pathogen *MRSA* with an inhibition zone of 22 mm for 100 of the extract, whereas the intracellular extract exhibited 16 mm.

Table 4.8. Inhibition zone diameter* exhibited by the extracellular organic extract

| Test pathogens | Inhibition zone diameter (mm) | | | | |
|---------------------------|-------------------------------|------------|-------------|-------------------------------|------------------|
| | 30 μ g | 60 μ g | 100 μ g | Positive control (30 μ g) | Negative control |
| <i>A. caviae</i> | 13 | 14 | 20 | 10 | 0 |
| <i>MRSA</i> | 13 | 14 | 16 | 10 | 0 |
| <i>E. coli</i> | 15 | 15 | 16 | 0 | 10 |
| <i>V. parahemolyticus</i> | 10 | 12 | 20 | 13 | 10 |

Inhibition zone diameter* exhibited by the extracellular extract of *B. amyloliquefaciens* (S2A) by disc diffusion assay against various pathogens, *vis-à-vis* the positive control, chloramphenicol and negative control (methanol)

*Antimicrobial activity was recorded as the diameter of inhibition zones determined as a distance of ≥ 1 mm between the circular area (= lawn of the isolate) and the end of the clear zone bounded by the lawn of the test strain.

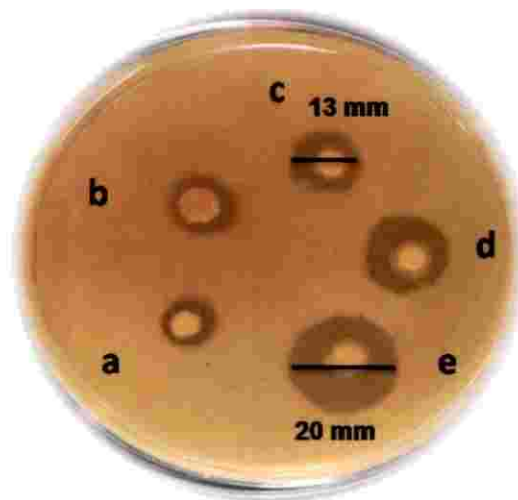


Figure 4.21. The antimicrobial activity of the crude extract of *B. amyloliquefaciens* against *A. caviae* by disc diffusion assay

4.2.5. Determination of the minimum inhibitory concentration (MIC)

The minimum inhibitory concentration was determined by broth dilution method. The pathogenic bacteria, such as *A. caviae*, *V. parahemolyticus* and *E. coli* were inoculated in nutrient broth and incubated at 34 °C for 16 h till the turbidity attained at about 1×10^5 CFU/mL. The extracellular crude extracts were prepared in concentrations, such as 6.25 µg, 12.5 µg, 25 µg, 50 µg and 100 µg in methanol. The test inoculum (100 µL) was added into the micro-titre well plates along with 100 µL of the test organism, whereas solvent methanol (100 µL) was used as blank. The absorbance was measured at 650 nm. The MIC was determined at the concentration where the absorbance was less than 0. The MIC was found to be lesser than 12.5 µg for all the test organisms.

4.3 PURIFICATION AND CHARACTERIZATION OF THE SECONDARY METABOLITES FROM *B. amyloliquefaciens*

4.3.1 Chromatographic purification of secondary metabolites from *B. amyloliquefaciens*

The crude extract of *B. amyloliquefaciens* was initially eluted through C-18 E strata to remove less polar compounds in the mixture. The eluted fraction was further purified by over reverse octadecylsilane-C₁₈ stationary phase using acetonitrile (MeCN): methanol (MeOH) (80:20, v/v; 10 mL/min) to yield four fractions (BA1-BA4). Among these fractions BA4 was obtained with greater yield, which was further purified by reverse-phase preparative high-pressure liquid chromatography (RP-HPLC, C₁₈-1.4 cm × 25 cm, 5 µm) using MeCN:MeOH (80:20, v/v; 10 mL/min) to yield compounds 1 and 2, which were found to be homogeneous in TLC (CHCl₃/MeOH, 4:1 v/v) and RP-HPLC (MeOH:MeCN, 80:20 v/v).

4.3.2. Spectroscopic analysis of bioactive secondary metabolites isolated from EtOAc extract of *B. amyloliquefaciens*

Repetitive chromatographic fractionations of EtOAc extract of *B. amyloliquefaciens* yielded two pure compounds. The structures of identified

metabolites were assigned by extensive one-dimensional (1D) nuclear magnetic resonance (NMR) spectroscopy including proton (^1H)-500 MHz, carbon (^{13}C)-125 MHz, $^{135}\text{DEPT}$ -distortionless enhancement by polarization transfer and two-dimensional (2D) NMR analyses including ^1H - ^1H COSY-correlation spectroscopy, HSQC-heteronuclear single quantum coherence, HMBC-heteronuclear multiple bond correlation, NOESY-nuclear overhauser effect spectroscopic experimentations combined with mass and fourier-transform-infrared (FTIR) experiments. The characterized bioactive secondary metabolites from *B. amyloliquifaciens* was classified as polyketide class of compounds characterized as 1-(8-hydroxy-1-oxoisochroman-3-yl)propyl 4'-(6'-hydroxy-8'-oxotetrahydrofuran-5'-yl)acetate (1) and 6'a-(3'-(1'-(8-hydroxy-1-oxoisochroman-3-yl)propoxy)-3'-oxoethyl)-8'-oxotetrahydrofuran-6'-yl butyrate (2).

Table 4.9. Structural characterization of polyketide compound (1)

| 1-(8-Hydroxy-1-oxoisochroman-3-yl)propyl-4'-(6'-hydroxy-8'-oxotetrahydrofuran-5'-yl)acetate (1) | |
|-------------------------------------------------------------------------------------------------|----------------------------------------|
| | |
| Yield | 45.23 mg |
| Physical description | brown oily |
| Molecular formula | $\text{C}_{18}\text{H}_{20}\text{O}_8$ |
| Molecular mass | 364.1158 |

The polyketide class of compound designated as 1-(8-hydroxy-1-oxoisochroman-3-yl)propyl 4'-(6'-hydroxy-8'-oxotetrahydrofuran-5'-yl)acetate (1) was isolated as a brown oily compound. It displayed UV absorbance (in MeOH) at λ_{max} (log ϵ 4.093) 207 nm. The purity of the compound was supported by RP C_{18} HPLC {using 80:20 MeCN:MeOH, v/v (R_t 2.77)} experiment.

| Wavelength (λ) | Absorbance (nm) |
|--------------------------|-----------------|
| 77.1 | 1.072 |
| 270.9 | 1.108 |
| 266.1 | 1.119 |
| 261 | 1.134 |
| 255 | 1.182 |
| 241.1 | 1.507 |
| 236 | 2.144 |
| 234 | 1.924 |
| 220 | 3.19 |
| 214.1 | 3.617 |
| 207.9 | 4.093 |
| 206 | 3.396 |
| 203.1 | 3.392 |

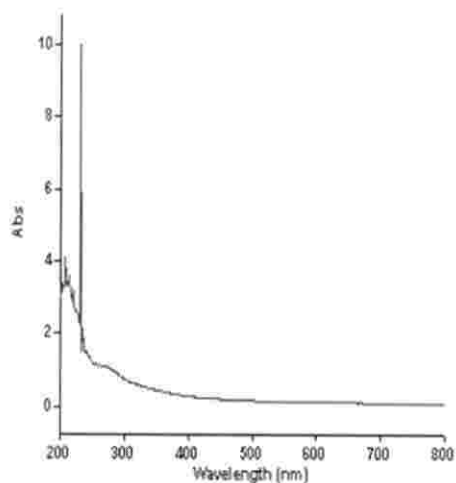


Figure 4.22. Absorption maximum of polyketide (1)

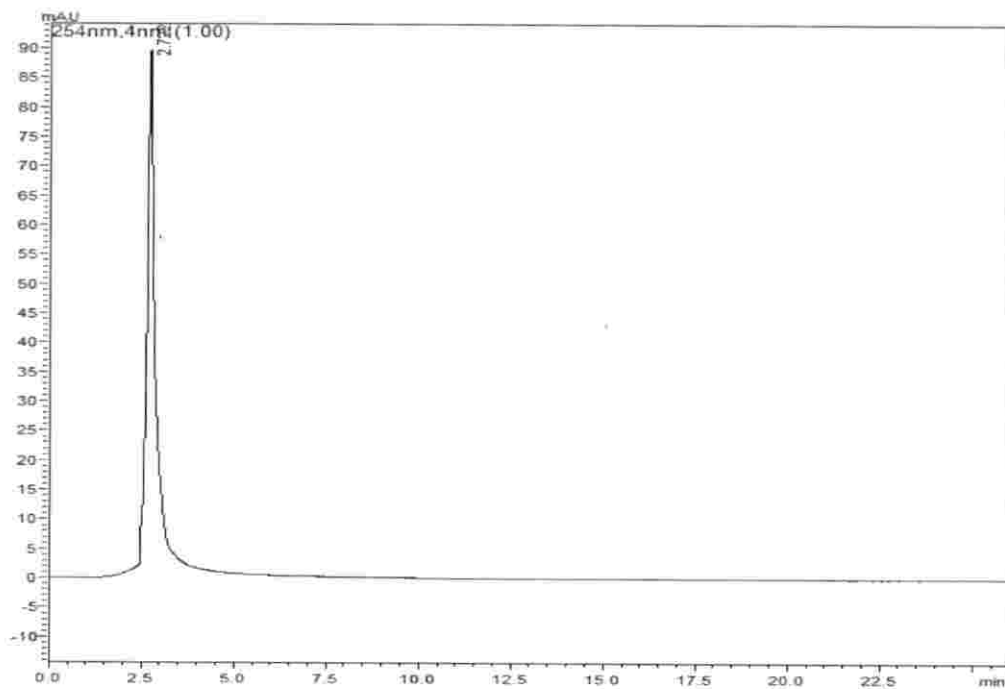


Figure 4.23. HPLC chromatogram of polyketide (1)

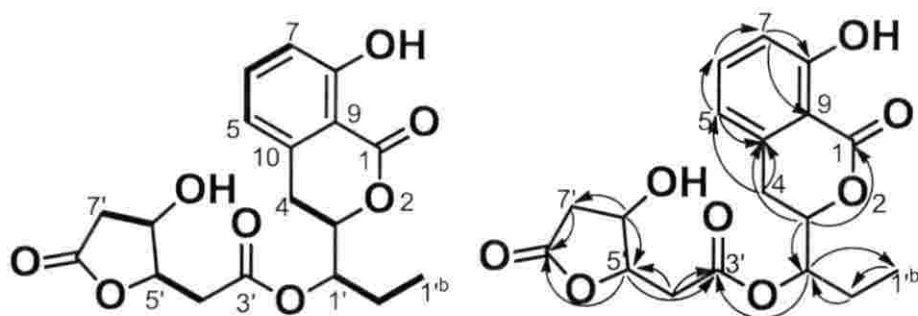


Figure 4.24. ^1H - ^1H COSY (bold-face red-bonds), selected HMBC (double-barbed arrows) correlations of compound 1

Table 4.10. NMR spectroscopic data of polyketide(1) in MeOD^a

| C. No. | ^{13}C | ^1H (int., mult., J in Hz) ^b | ^1H - ^1H COSY | HMBC |
|-----------------|-----------------|----------------------------------------------------|----------------------------------|----------------------|
| 1 | 168.42 | | | |
| 3 | 83.54 | 4.64 (1H α , q, 7.29) | H-4 | C-1, 10, 1' |
| 4 | 36.87 | 3.18 (2H, d, 6.28) | | C-5, 10 |
| 5 | 130.61 | 7.09 (1H, d, 6.02) | H-6 | C-6, 10 |
| 6 | 141.95 | 7.47 (1H, dd, 8.31) | H-7 | C-7 |
| 7 | 115.55 | 6.85 (1H, d, 6.13) | | C-8, 9 |
| 8 | 161.57 | | | |
| 9 | 117.93 | | | |
| 10 | 139.26 | | | |
| 1' | 76.69 | 4.43 (1H β , m) | H-1 ^{na} | C-3, 1' ^b |
| 3' | 172.92 | | | |
| 4' | 34.23 | 2.67 (2H, d, 5.62) | H-5' | C-3', 5' |
| 5' | 87.36 | 5.28 (1H α , m) | | C-8', 3' |
| 6' | 72.22 | 3.69 (1H α , m) | H-7' | C-5', 7' |
| 7' | 36.39 | 2.42 (2H, d, 8.94) | | C-8' |
| 8' | 177.68 | | | |
| 1 ^{na} | 29.63 | 1.31 (2H, m) | H-1 ^{nb} | C-1' |
| 1 ^{nb} | 18.29 | 0.97 (3H, t, 7.15) | | C-1 ^{na} |

^aNMR spectra recorded using Bruker AVANCE III 500 MHz (AV 500) spectrometers.

^bValues in ppm, multiplicity and coupling constants ($J = \text{Hz}$) are indicated in parentheses.

Assignments were made with the aid of the ¹H-¹H COSY, HSQC, HMBC and NOESY experiments.

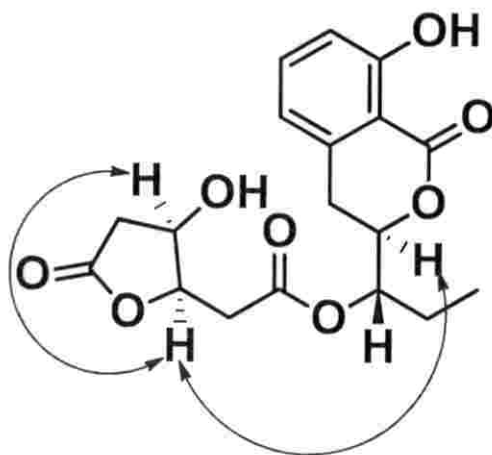


Figure 4.25. NOESY (coloured arrows) cross-peaks of the polyketide (1). NOESY correlations were represented by two-sided double barbed arrows.

4.3.3. Spectroscopic characterization of 1-(8-hydroxy-1-oxoisochroman-3-yl)propyl 4'-(6'-hydroxy-8'-oxotetrahydrofuran-5'-yl)acetate (1)

1-(8-hydroxy-1-oxoisochroman-3-yl) propyl-4'-(6'-hydroxy-8'-oxotetrahydrofuran-5'-yl)acetate (1), a previously undescribed polyketide was isolated as a brown oily liquid upon repeated chromatographic purification of the EtOAc extract of *B. amyloliquefaciens*. Its mass spectrum demonstrated a molecular ion peak at m/z 364 (m/z : 364.1162 [M]⁺, cal. for 364.1158), which in combination with its one and two dimensional NMR data (Table 4.9) suggested the elemental composition of the compound as C₁₈H₂₀O₈.

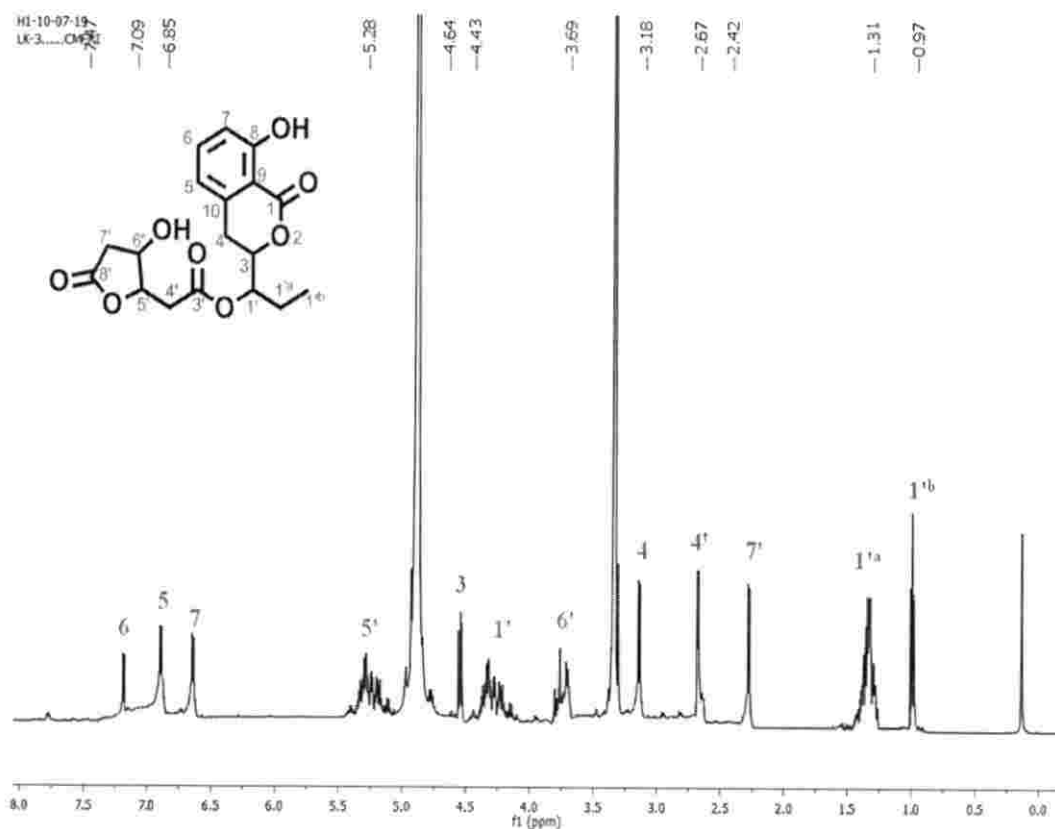


Figure 4.26. ¹H NMR spectrum of polyketide (1)

The ¹³C-NMR spectrum of the compound 1, exhibited 18 carbon signals, which were assigned to four sp³ methylenes, four sp³ methines, one sp³ methyl, three sp² methines, and six quaternary carbons based on ¹³C NMR and DEPT₁₃₅ NMR data of the titled compound 1.

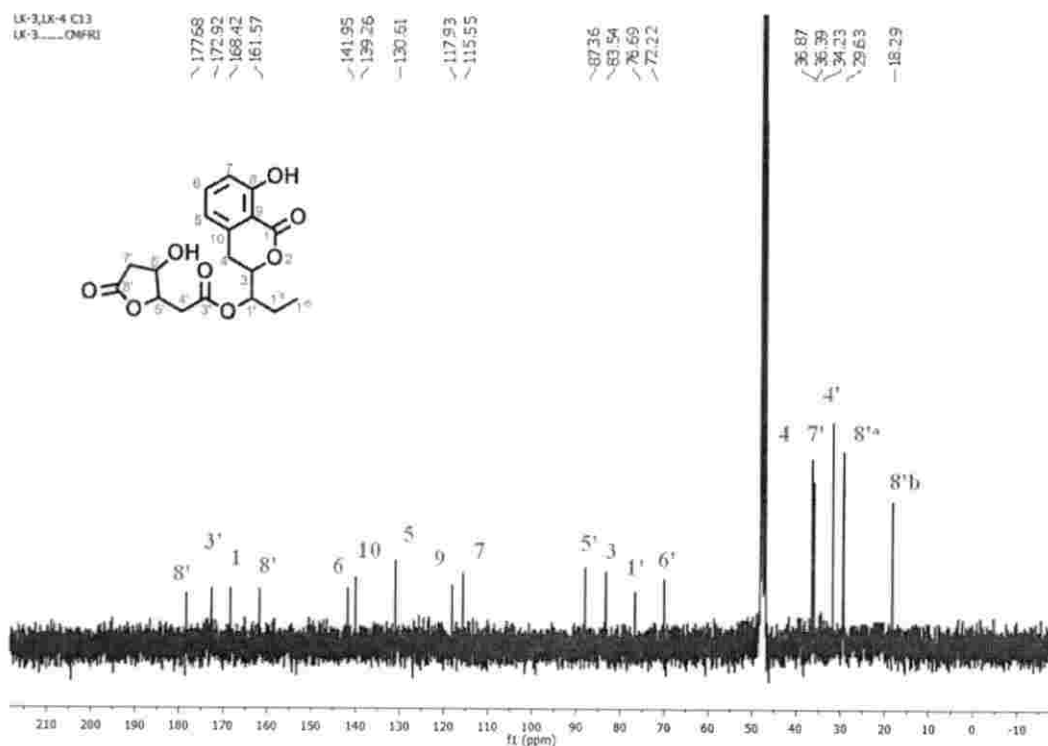


Figure 4.27. ¹³C NMR spectrum of polyketide (1)

The ¹H and ¹³C NMR spectra demonstrated characteristic signals for three ester carbonyls (δ C 168.42, 172.92 and 177.68), hydroxylated quaternary carbon (δ C 161.57), oxygenated methines (δ H 4.64/ δ C 83.54; δ H 4.43/ δ C 76.69; δ H 3.69/ δ C 72.22), carbonyl methylenes (δ H 2.42/ δ C 36.39; δ H 2.67/ δ C 34.23) and hydroxylated methine (δ H 3.69/ δ C 72.22). The carbon signal at δ C 76.69 (HSQC with δ H 4.43), δ C 87.36 (HSQC with δ H 5.28) and δ C 83.54 (HSQC with δ H 4.64) supported the occurrence of ester groups in the studied compound 1.

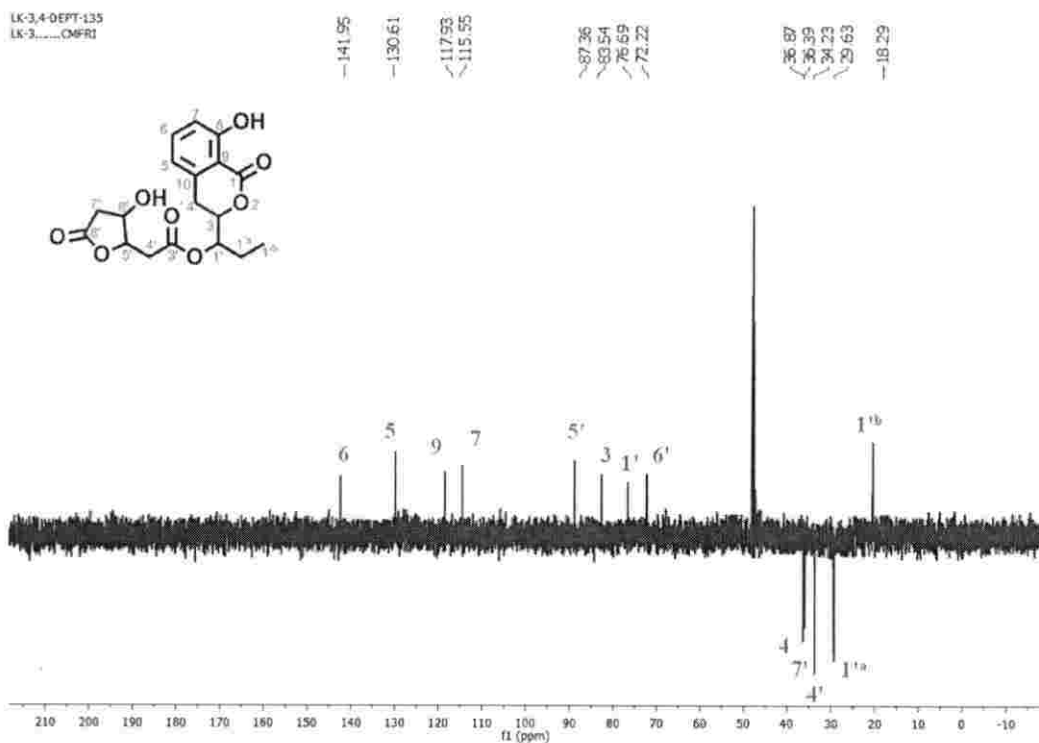


Figure 4.28. $^{135}\text{DEPT}$ NMR spectrum of polyketide(1)

The ^1H -NMR signals at δH 7.09 (HSQC with δC 130.61), 7.47 (HSQC with δC 141.95), 6.85 (HSQC with δC 115.15) appropriately suggested the presence of benzene ring in the compound. The ^1H - ^1H COSY correlations, such as H-5 to H-7: δH 7.09 (designated as H-5)/ 7.47 (H-6)/ 6.82 (H-7) along with the HMBC correlations from δH 7.09 (H-5) to δC 141.95 (C-6), 139.26 (C-10); δH 7.47 (H-6) to δC 115.55 (C-7) and δH 6.85 (H-7) to δC 161.57 (C-8) further substantiated the existence of the benzene ring in compound 1.

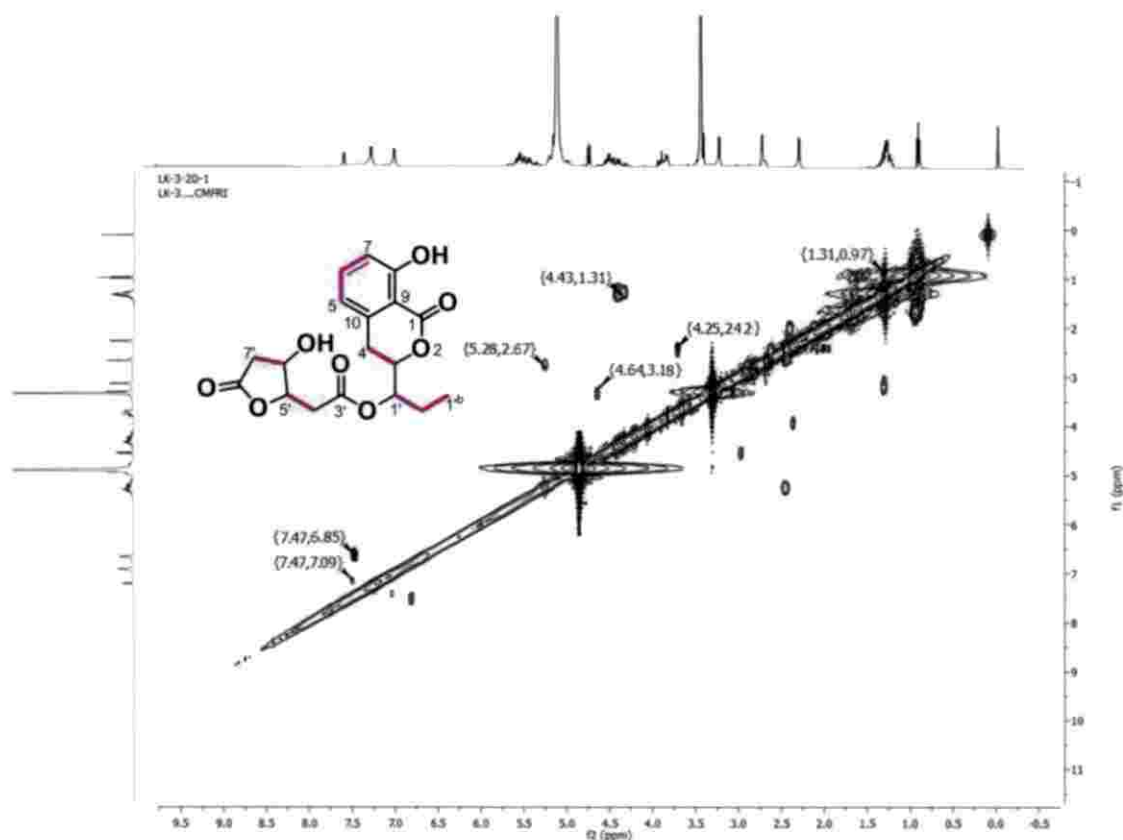


Figure 4.29. ^1H - ^1H COSY NMR spectrum of polyketide (1)

Similarly, the COSY correlations, such as δH 4.64 (H-3)/ δH 3.18 (H-4) together with the HMBC correlations from δH 4.64 (H-3) to δC 168.42 (C-1), 139.26 (C-10) and δH 3.18 (H-4) to δC 139.26 (C-10) appropriately supported the pyranone ring in the compound. The carbon signals at δC 117.93 (C-9) and δC 139.26 (C-10) did not exhibit HSQC correlation with any of the proton, thus, these could be quaternary carbons. The highly deshielded carbon signal at δC 161.57 did not exhibit any HSQC correlations, and therefore, it could be a quaternary carbon, and its remarkably downfield value might owe to the attachment of hydroxyl group.

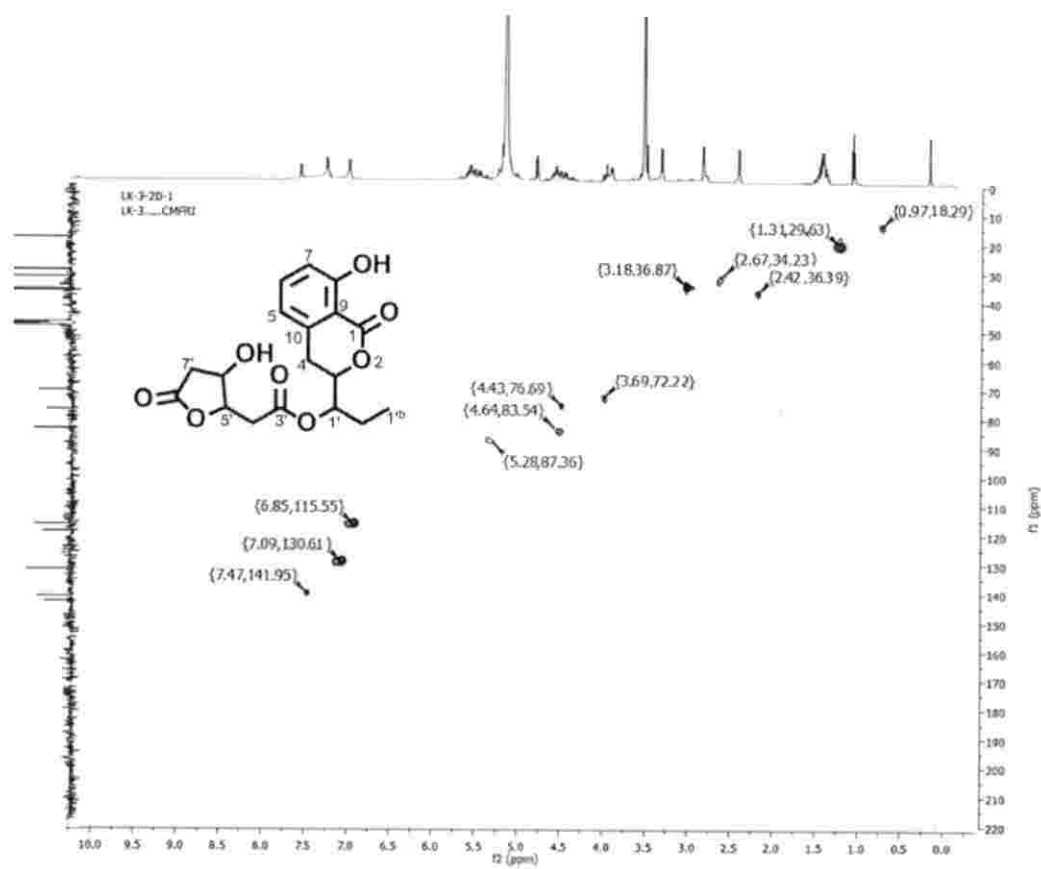


Figure 4.30. HSQC NMR spectrum of polyketide (1)

The HMBC cross peaks from δ H 3.18 (H-4) to δ C 130.61 (C-5), 139.26 (C-10); δ H 7.09 (H-5) to δ C 139.26 (C-10) and δ H 6.85 (H-7) to δ C 117.93 (C-9) suggested that the benzene ring was fused with the pyranone ring, and thus it supported the presence of 8-hydroxyisochromanone as the basic skeleton in the compound 1 (Park *et al.*, 2016). The ester carbonyl in the isochromanone was designated as C-1 and other carbon atoms were numbered according to the previous literature (Li *et al.*, 2012). The HMBCs from δ H 4.43 (H-1') to δ C 172.92 (C-3'); δ H 2.67 (H-4') to δ C 172.92 (C-3'), 87.36 (C-5') and δ H 5.28 (H-5') to δ C 172.92 (C-3') suggested an isopropyl propionate chain, and its position of attachment to 8-hydroxyisochromanone at C-3 position was further supported by the HMBC correlations from δ H 4.65 (H-3) to δ C 76.69 (C-1'). The ^1H - ^1H COSY correlations from H-1' to H-1'^b {4.43 (H-1')/ 1.31 (H-1'^a)/ 0.97 (H-1'^b)} accounted for an ethane chain, which was attached to C-1' position of the

isopropyl propionate moiety. These assignments were further confirmed by the HMBC correlations, such as δH 0.97 (H-1^b) to δC 29.63 (C-1^{ab}); δH 4.43 (H-1') to 18.29 (C-1^b), 172.92 (C-3').

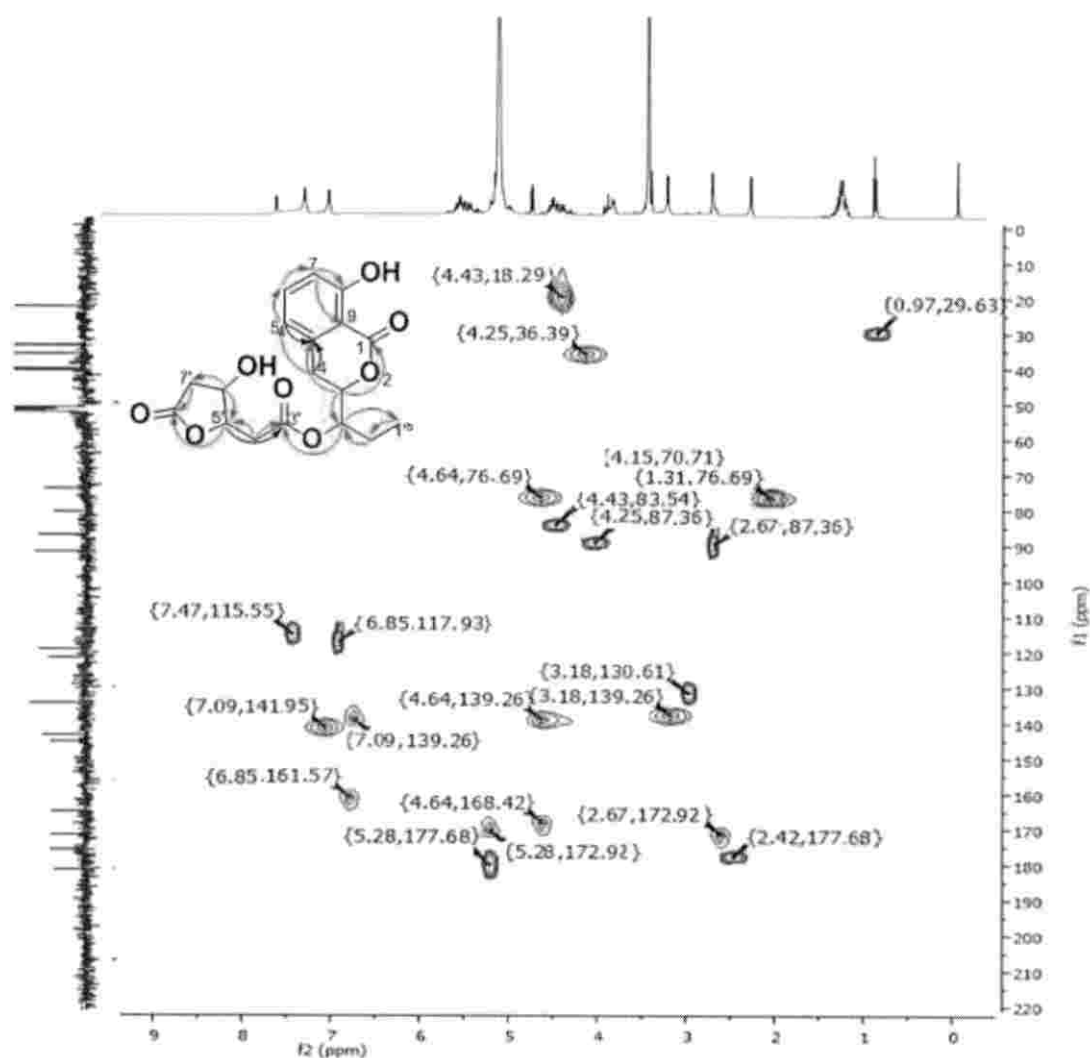


Figure 4.31. HMBC NMR spectrum of polyketide (1)

The ^1H - ^1H COSY correlations from H-6' to H-7' (δH 3.69 (H-6')/ 2.42 (H-7')) together with the HMBC correlations, such as δH 5.28 (H-5') to δC 177.68 (C-8'), δH 3.69 (H-6') to δC 36.39 (C-7'), 87.36 (C-5') and δH 2.42 (H-7') to δC 177.68 (C-8') proposed a dihydrofuranone ring in the compound 1. In addition, HMBCs

from δH 5.28 (H-5') to δC 172.92 (C-3') and δH 2.67 (H-4') to δC 87.36 (C-5') attributed the attachment of this dihydrofuranone moiety with the isopropyl propionate at C-5' position. Thus, the 8-hydroxyisochromanone attached with the butyl 2-(5-oxotetrahydrofuran-2-yl)acetate chain could yield 1-(8-hydroxy-1-oxoisochroman-3-yl)propyl 2-(5-oxotetrahydrofuran-2-yl)acetate. The latter was found to be similar to amicoumacins isolated from a marine-derived bacterium *B. subtilis* (Li *et al.*, 2012)

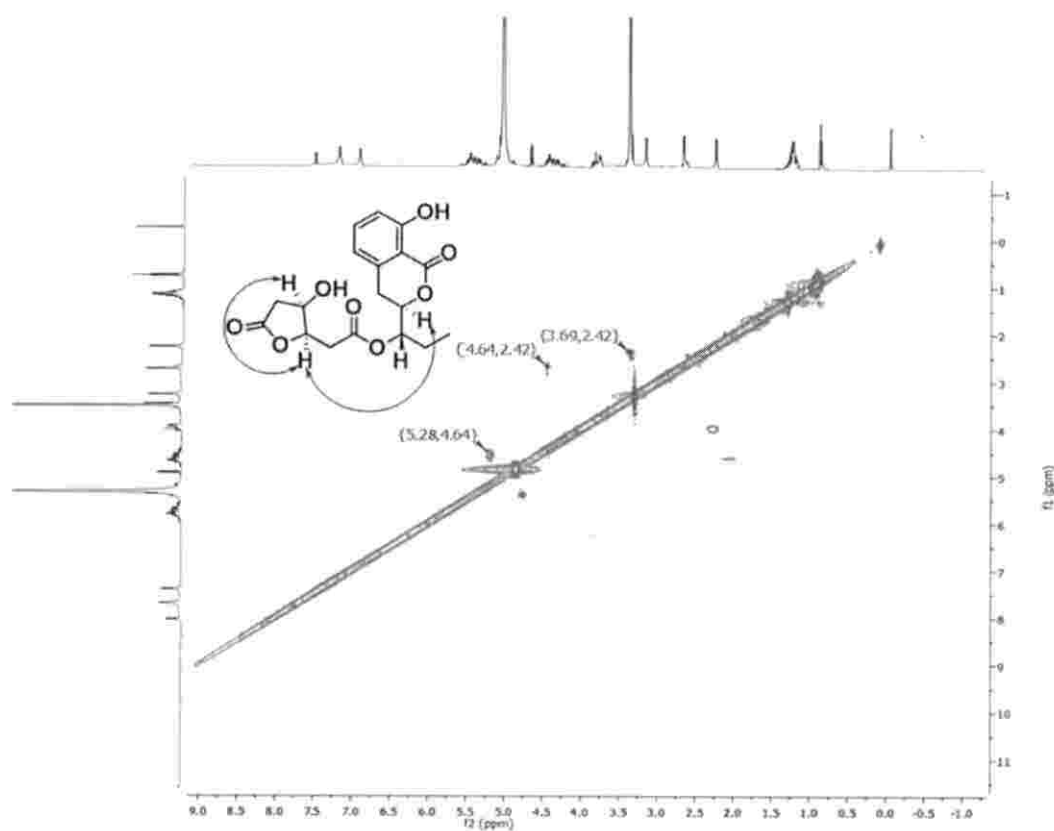


Figure 4.32. NOESY spectrum of polyketide (1)

The NOE correlations, such as δH 4.64 (H-3)/ 5.28 (H-5')/ 2.42 (H-7')/ 3.69 (H-6') suggested the close proximity of these protons, and were assigned to be α -oriented (Park *et al.*, 2016). Thus the isopropyl propionate C-5' could be β -oriented. Notably, the proton signal at δH 4.43 (H-1') did not exhibit NOE correlation with the α -oriented protons, which showed that it was β -oriented, and the ethane side chain attached to it was assigned as β -oriented (Park *et al.*, 2016).

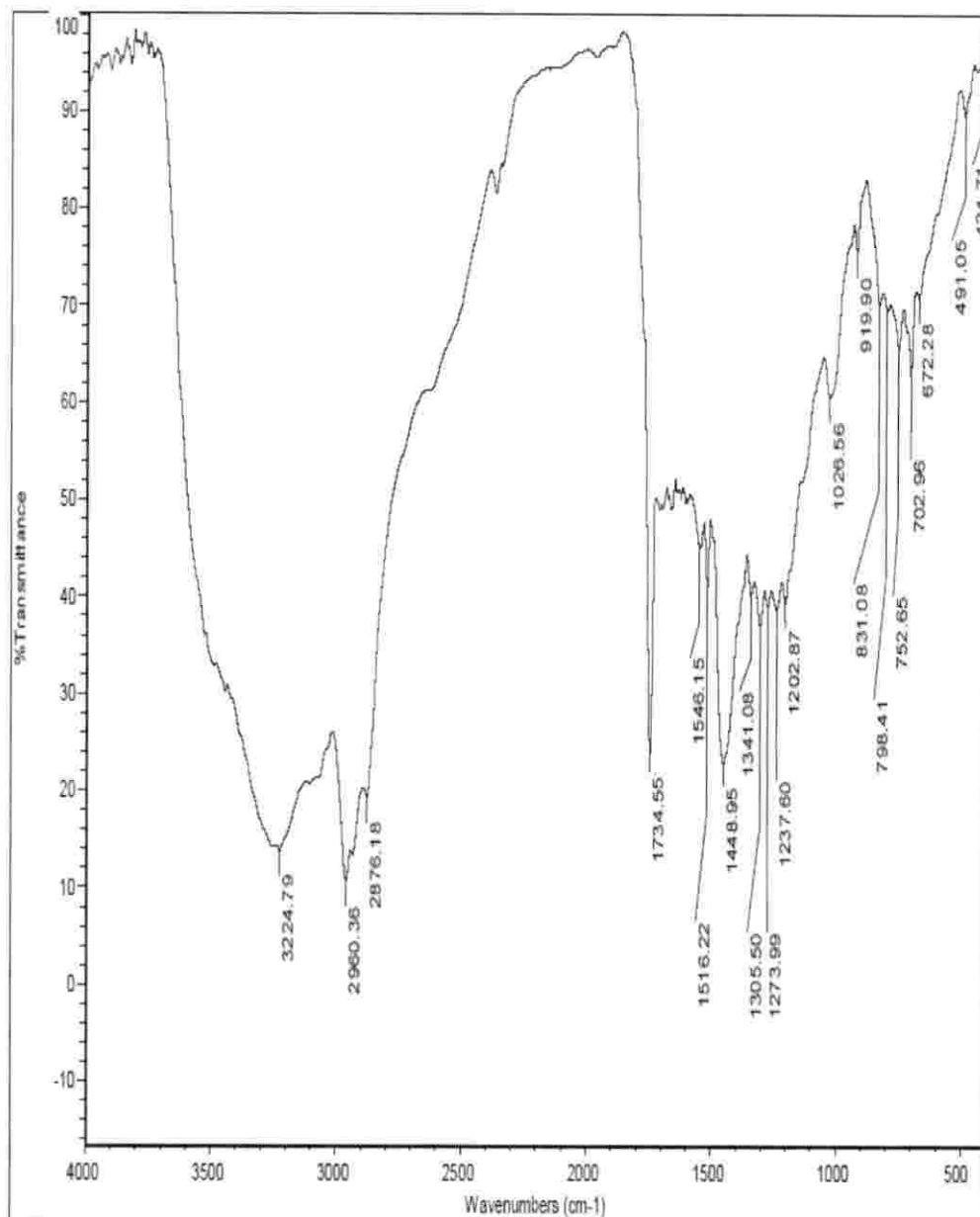


Figure 4.33. FT-IR spectrum of polyketide (1)

The FTIR spectrum of the compound 1, exhibited absorption bands at 3224 cm^{-1} thus confirming the presence of hydroxyl group in the compound. Similarly, the absorption bands at 1735 cm^{-1} could correspond to the C=O stretching, and that at 1546 cm^{-1} was attributed to the aromatic C=C stretching vibrations.

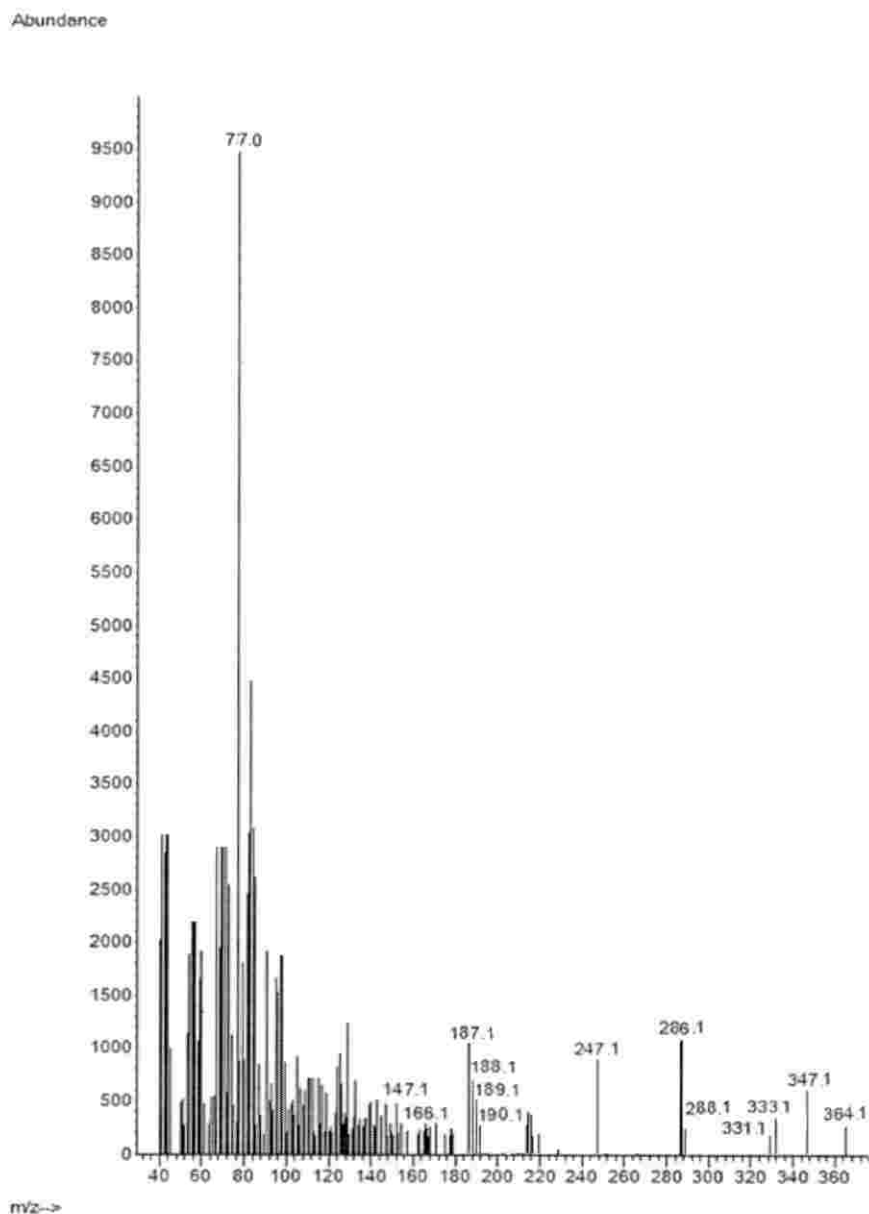


Figure 4.34. GCMS spectrum of polyketide (1)

The mass spectrum of the titled compound exhibited molecular ion peak at m/z 364.1, which on elimination of the hydroxyl group yielded 1-(1-oxoisochroman-3-yl)propyl 2-(3-hydroxy-5-oxotetrahydrofuran-2-yl)acetate (B) with m/z 347.1. The latter underwent elimination of hydroxyl group from C-6', to yield 1-(1-oxoisochroman-3-yl)propyl 2-(5-oxotetrahydrofuran-2-yl)acetate (C) with m/z 333.1.

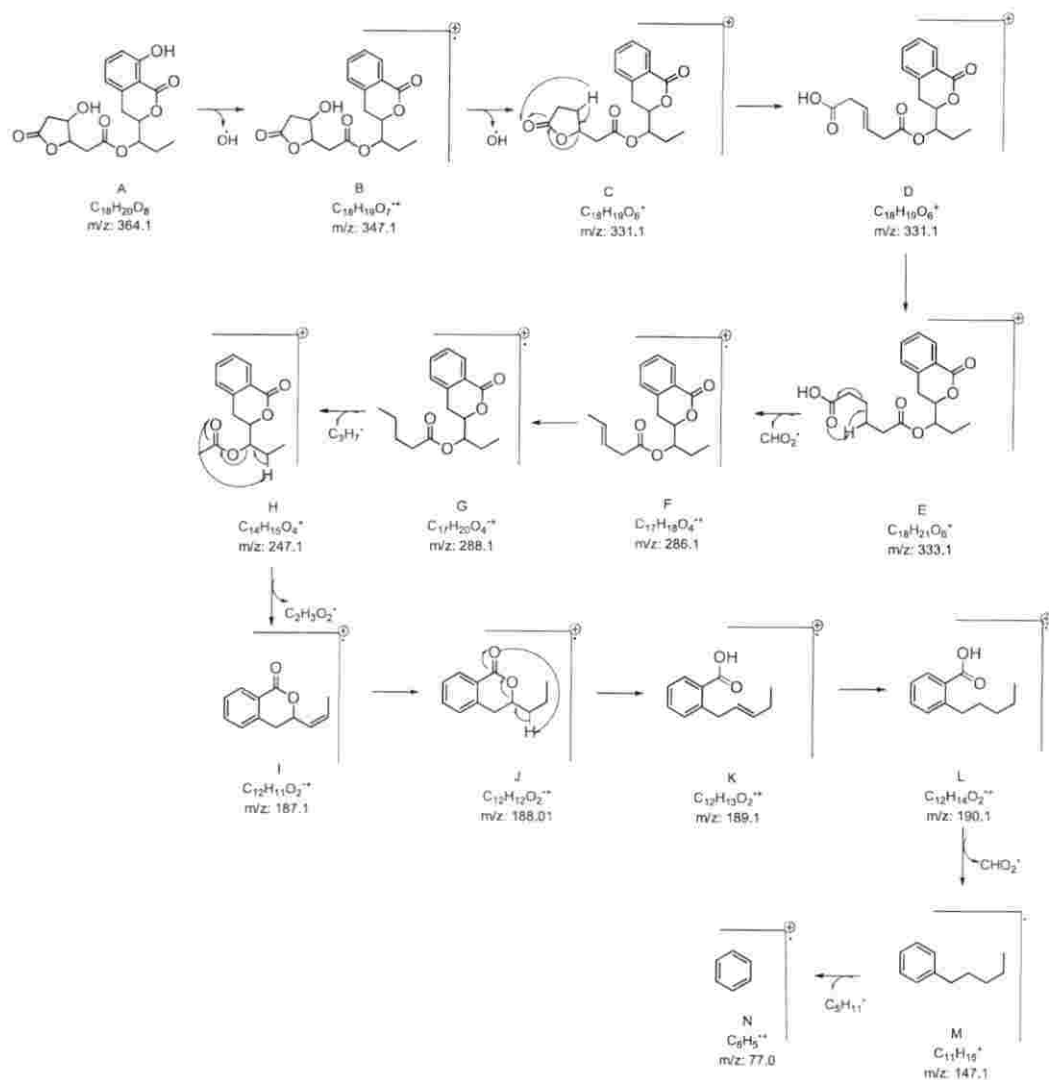


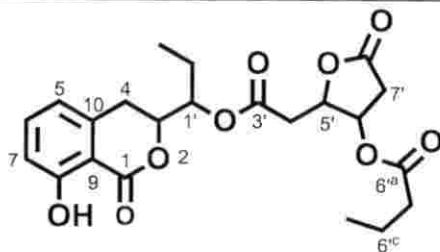
Figure 4.35. Mass fragmentation pattern of polyketide (1)

The fragment ion further underwent McLafferty rearrangements to afford a fragment ion at m/z 331.1 {6-oxo-6-(1-(1-oxoisochroman-3-yl)propoxy)hex-3-enoic acid (D)}, which on hydrogenation of the double bond and McLafferty rearrangement yielded a fragmented ion at m/z 286.1 {1-(1-oxoisochroman-3-yl)propyl-pent-3-enoate (F)}. The latter underwent hydrogenation and McLafferty rearrangements to obtain a fragment ion at m/z 247.1 (H). This fragment ion appeared to undergo subsequent hydrogenation and McLafferty rearrangement to yield 3-(prop-1-en-1-yl)isochroman-1-one (I, m/z 187.1). This radical cation repeatedly underwent McLafferty rearrangement and hydrogenation to yield 2-

(pent-2-en-1-yl)benzoic acid (**L**) with m/z 190.1. This fragmented ion further eliminated CHO_2^\bullet , followed by removal of $\text{C}_5\text{H}_{11}^\bullet$ to yield phenyl radical cation with m/z 77.0 (**N**) as the base peak.

Table 4.11. Structural characterization of polyketide compound (2)

6'a-(3'-(1'-(8-Hydroxy-1-oxoisochroman-3-yl)propoxy)-3'-oxoethyl)-8'-oxotetrahydrofuran-6'-yl butyrate (2)



| | |
|----------------------|----------------------------------------|
| Yield | 38.52 mg |
| Physical description | brown oily |
| Molecular formula | $\text{C}_{22}\text{H}_{26}\text{O}_9$ |
| Molecular mass | 434.1577 |

Structural characterization of polyketide compound (2) bearing 3'-oxoethyl-8'-oxotetrahydrofuran-6'-yl butyrate moiety

The polyketide-type of compound characterized as 6'a-(3'-(1'-(8-hydroxy-1-oxoisochroman-3-yl)propoxy)-3'-oxoethyl)-8'-oxotetrahydrofuran-6'-yl butyrate (2), was isolated as a brown oily compound. It displayed UV absorbance (in MeOH) at λ_{max} ($\log \epsilon$ 3.849) 274 nm. The homogeneity of the compound was supported by RP C18 HPLC { 80:20 MeCN:MeOH, v/v (R_t 2.75)} experiments.

| Wavelength (λ) | Absorbance (nm) |
|--------------------------|-----------------|
| 323 | 1.018 |
| 310 | 1.177 |
| 289 | 2.007 |
| 284 | 2.527 |
| 274.1 | 3.849 |
| 267 | 2.67 |
| 260.1 | 2.569 |
| 256.9 | 3 |
| 255 | 2.457 |
| 249.1 | 2.959 |
| 244 | 2.757 |
| 239 | 2.292 |
| 233.1 | 2.204 |
| 207.9 | 3.419 |

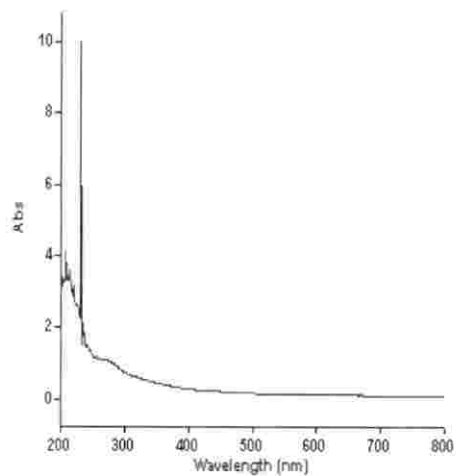


Figure 4.36. Absorption maximum of polyketide (2)

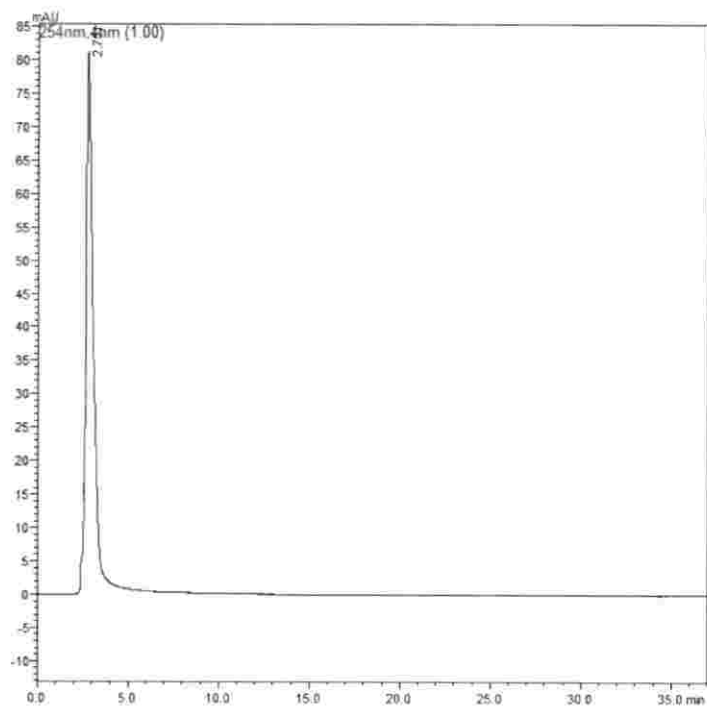
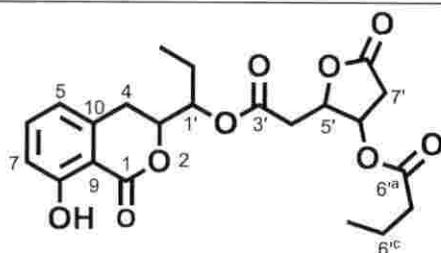


Figure 4.37. HPLC chromatogram of polyketide (2)

Table 4.12. NMR spectroscopic data of polyketide (2) in MeOD^a

| C. No. | ¹³ C | ¹ H (int., mult., <i>J</i> in Hz) | ¹ H- ¹ H COSY | HMBC |
|----------------|-----------------|----------------------------------------------|-------------------------------------|-----------------------------------|
| 1 | 169.85 | | | |
| 3 | 82.58 | 4.65 (1H α , q, 7.11) | H-4 | C-1, 10, 1' |
| 4 | 36.49 | 3.18 (2H, d, 6.23) | | C-5, 10 |
| 5 | 130.61 | 7.07 (1H, d, 6.11) | H-6 | C-6, 10 |
| 6 | 141.95 | 7.42 (1H, dd, 8.02) | H-7 | |
| 7 | 115.17 | 6.75 (1H, d, 6.13) | | C-6, 8, 9 |
| 8 | 165.37 | | | |
| 9 | 118.31 | | | |
| 10 | 139.56 | | | |
| 1' | 77.73 | 4.41 (1H β , m) | H-1 ^a | C-3, 1 ^b |
| 3' | 175.28 | | | |
| 4' | 34.30 | 2.68 (2H, d, 5.78) | | C-3', 5' |
| 5' | 92.20 | 5.62 (1H α , m) | | C-8' |
| 6' | 68.11 | 4.25 (1H α , m) | H-7' | C-5', 7', 6 ^a |
| 7' | 36.84 | 2.46 (2H, d, 8.54) | | C-8', 3' |
| 8' | 178.88 | | | |
| 1 ^a | 28.27 | 1.31 (2H, m) | H-1 ^b | C-1' |
| 1 ^b | 21.41 | 0.97 (3H, t, 7.19) | | C-1 ^a |
| 6 ^a | 172.9 | | | |
| 6 ^b | 38.94 | 2.33 (2H, t, 6.18) | 6 ^c | C-6 ^a , 6 ^c |
| 6 ^c | 20.00 | 1.70 (2H, q, 7.54) | | |
| 6 ^d | 18.29 | 0.94 (3H, t, 5.09) | | C-6 ^c , 6 ^b |

NMR spectroscopic data of 6'a-(3'-(1'-(8-hydroxy-1-oxoisochroman-3-yl)propoxy)-3'-oxoethyl)-8'-oxotetrahydrofuran-6'-yl butyrate (2) in MeOD^a

^aNMR spectra recorded using Bruker AVANCE III 500 MHz (AV 500) spectrometers.

^bValues in ppm, multiplicity and coupling constants (*J* = Hz) are indicated in parentheses.

Assignments were made with the aid of the ¹H-¹H COSY, HSQC, HMBC and NOESY experiments.

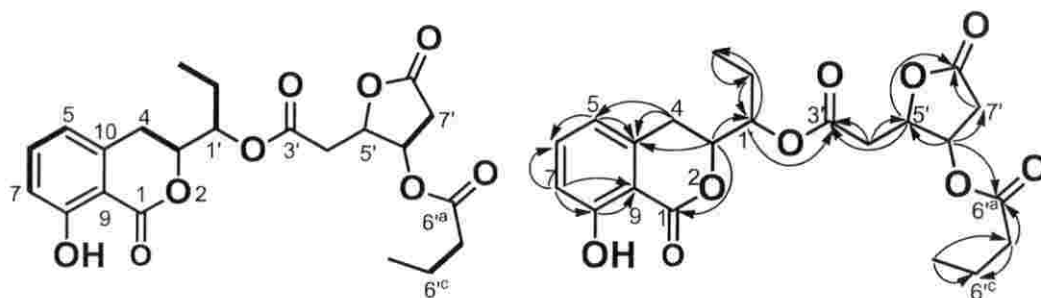


Figure 4.38. ^1H - ^1H COSY (bold-face red-bonds), selected HMBC (double-barbed arrows) correlations of compound 2

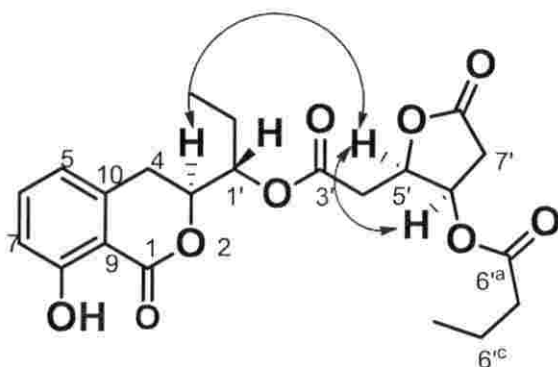


Figure 4.39. NOESY (coloured arrows) cross-peaks of the polyketide compound (2). NOESY correlations were represented by two-sided double barbed arrows.

4.3.4 Spectroscopic characterization of compound 6'a-(3'-(1'-(8-hydroxy-1-oxoisochroman-3-yl)propoxy)-3'-oxoethyl)-8'-oxotetrahydrofuran-6'-yl butyrate (2)

The polyketide compound (2), characterized as 6'a-(3'-(1'-(8-hydroxy-1-oxoisochroman-3-yl)propoxy)-3'-oxoethyl)-8'-oxotetrahydrofuran-6'-yl butyrate (2) was obtained as a brown oily liquid after repeated chromatographic purification of EtOAc extract of *B. amyloliquefaciens*. The molecular formula of the compound was obtained as $\text{C}_{22}\text{H}_{26}\text{O}_9$ that was further supported by the molecular ion peak at m/z 434 (m/z : 434.1577 $[\text{M}]^+$, cal. for 434.1573).

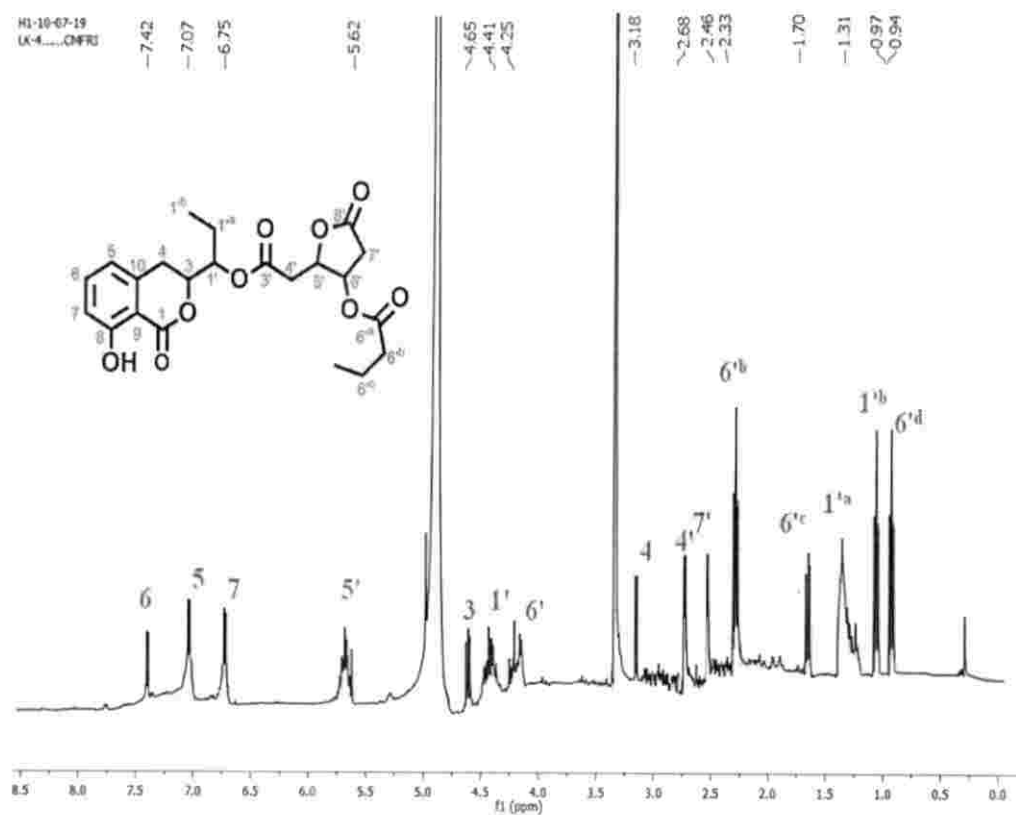


Figure 4.40. ^1H NMR spectrum of polyketide (2)

The ^{13}C -NMR spectrum of the compound 2, showed 22 carbon signals, which were assigned to six sp^3 methylenes, four sp^3 methines, two sp^3 methyls, three sp^2 methines, seven quaternary carbons based on combined ^{13}C NMR and DEPT_{135} experiments.

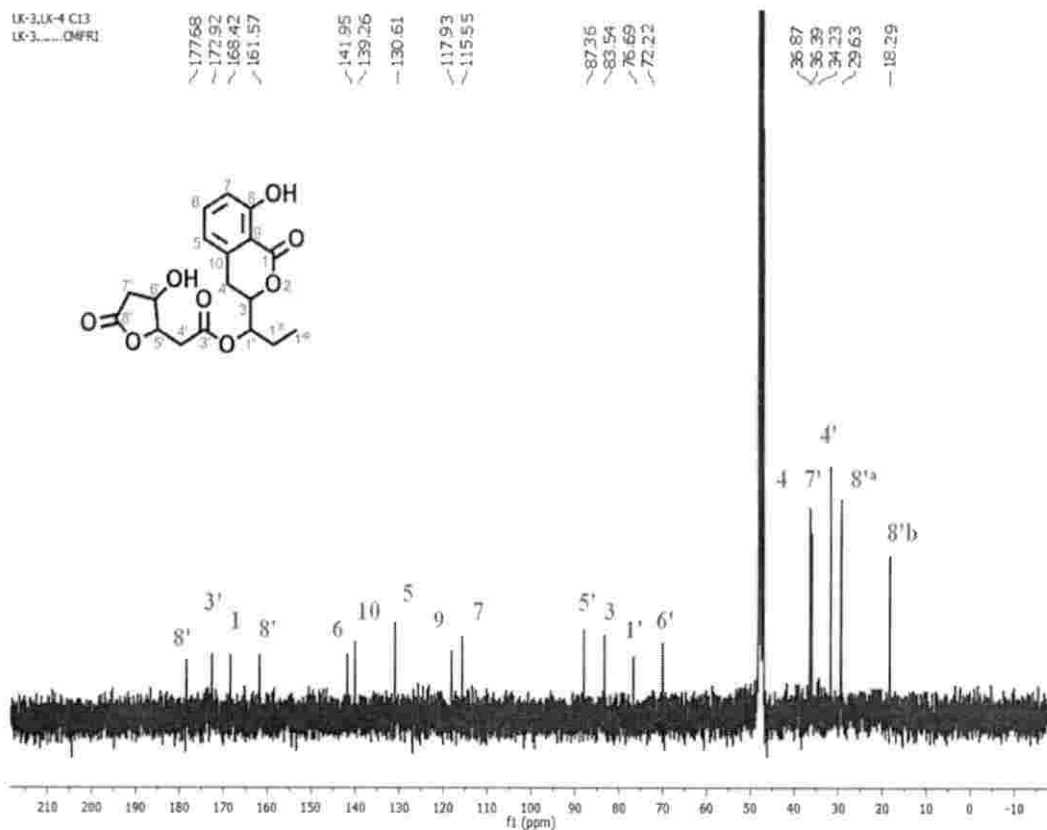


Figure 4.41. ¹³C NMR spectrum of polyketide (2)

The ¹H and ¹³C NMR spectra demonstrated characteristic signals for four ester carbonyls (δ C 169.85, 175.28, 178.88 and 172.90), hydroxylated quaternary carbon (δ C 165.37), oxygenated methines (δ H 4.65/ δ C 82.58; δ H 4.41 / δ C 77.73; δ H 4.25/ δ C 68.11; δ H 5.62/ δ C 92.20) and carbonyl methylenes (δ H 2.68/ δ C 34.30; δ H 2.46/ δ C 36.84; δ H 2.33/ δ C 38.94). The carbon signal at δ C 82.58 (HSQC with δ H 4.65), δ C 77.73 (HSQC with δ H 4.41), δ C 92.20 (HSQC with δ H 5.62) and δ C 68.11 (HSQC with δ H 4.25) appropriately supported the presence of ester groups in the titled compound. The proton signals at δ H 7.07 (HSQC with δ C 130.61), 7.42 (HSQC with δ C 141.95), 6.75 (HSQC with δ C 115.17) supported the presence of benzene ring in the studied compound.

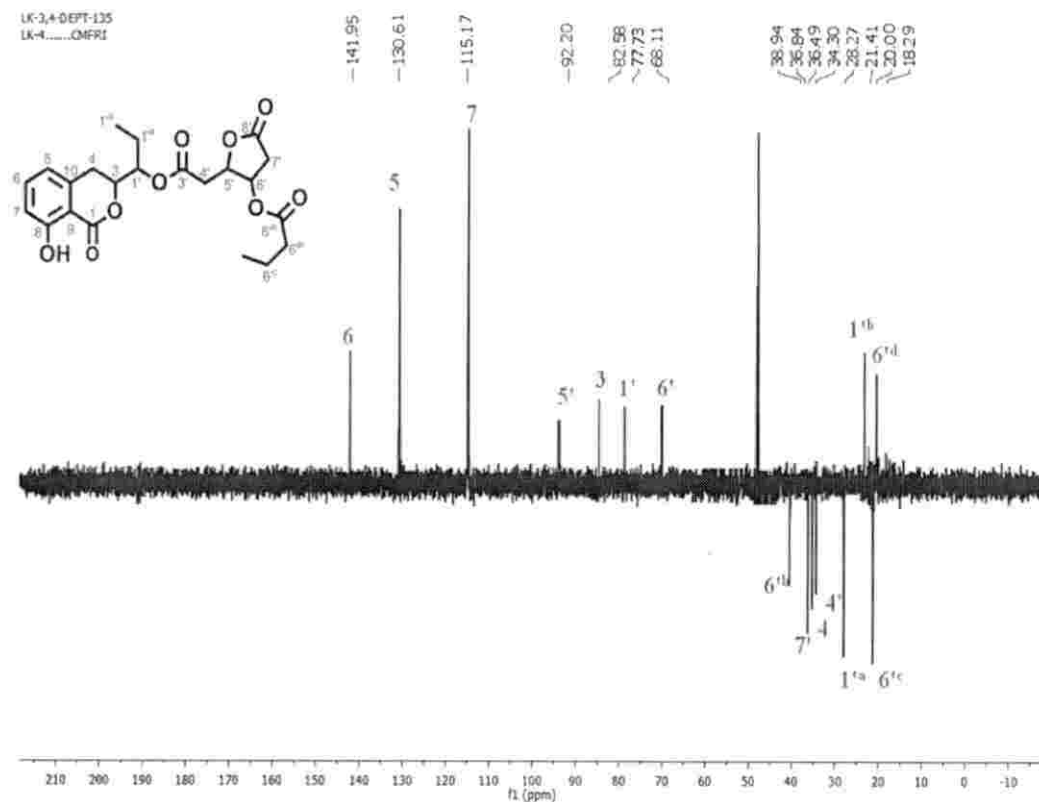


Figure 4.42. $^{135}\text{DEPT}$ NMR spectrum of polyketide (2)

The ^1H - ^1H COSY spin system such as, H-5 to H-7: δH 7.07 (designated as H-5)/ 7.42 (H-6)/ 6.75 (H-7) along with the HMBC correlations from δH 7.07 (H-5), 6.75 (H-7) to δC 141.95 (C-6) and δH 6.75 (H-7) to δC 165.37 (C-8) further confirmed the presence of benzene ring in the compound. Subsequently the COSY correlations such as, δH 4.65 (H-3)/ δH 3.18 (H-4) combined with the HMBC correlations from δH 4.65 (H-3) to δC 169.82 (C-1), 139.86 (C-10) suitably supported the pyranone ring in the studied compound. The carbon signals at δC 118.31 (C-9) and δC 139.56 (C-10) does not exhibit HSQC correlation with any of the proton thus these must be quaternary carbons. The highly downfield carbon signal at δC 165.37 does not exhibit any HSQC correlations, thus it must be a quaternary carbon and its highly downfield value might be due to the attachment of hydroxyl group.



Figure 4.43. ^1H - ^1H COSY NMR spectrum of polyketide (2)

The HMBC cross peaks from δH 6.75 (H-7) to δC 118.31 (C-9); δH 7.07 (H-5) to δC 139.65 (C-10) and δH 3.18 (H-4) to δC 139.56 (C-10), 130.61 (C-5) suggested the attachment of benzene ring with pyranone ring and thus it supported 8-hydroxyisochromanone as the basic skeleton in the compound 2 (Park *et al.*, 2016). The ester carbonyl in the isochromanone was designated as C-1 and other carbon atoms are numbered according to the previous literature (Li *et al.*, 2012). The HMBCs from δH 4.41 (H-1') to δC 175.28 (C-3'); δH 2.68 (H-4') to δC 175.28 (C-3'), 92.20 (C-5') and δH 5.62 (H-5') to δC 175.28 (C-3') suggested an isopropyl propionate chain and its attachment to 8-hydroxyisochromanone at C-3 position was further supported by the HMBC correlations from δH 4.65 (H-3) to δC 77.73 (C-1'), 169.82 (C-1).

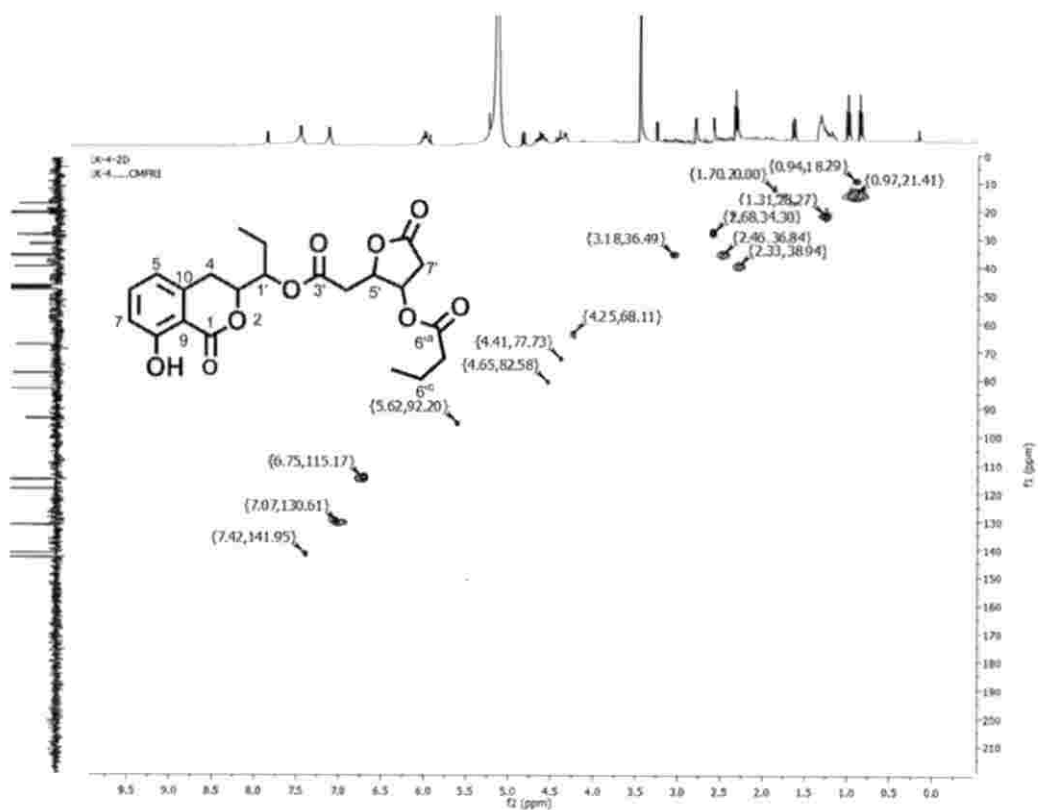


Figure 4.44. HSQC NMR spectrum of polyketide (2)

The ^1H - ^1H COSY correlation from H-1' to H-1^{ib} {4.41 (H-1')/ 1.31 (H-1^a)/ 0.97 (H-1^b)} accounts for ethane chain. The attachment of this ethane side chain at C-1' of the isopropyl propionate was confirmed by the HMBC correlations such as; δH 0.97 (H-1^b) to δC 28.27 (C-1^a); δH 4.41 (H-1') to 21.41 (C-1^b), 175.28 (C-3'). Consequently ^1H - ^1H COSY correlations from H-6' to H-7' { δH 4.25 (H-6')/ 2.46 (H-7')} together with the HMBC correlations such as, δH 5.62 (H-5') to δC 178.88 (C-8'), δH 4.25 (H-6') to δC 36.84 (C-7'), 92.20 (C-5') and δH 2.46 (H-7') to δC 178.88 (C-8') suggested dihydrofuranone ring in the compound 2.

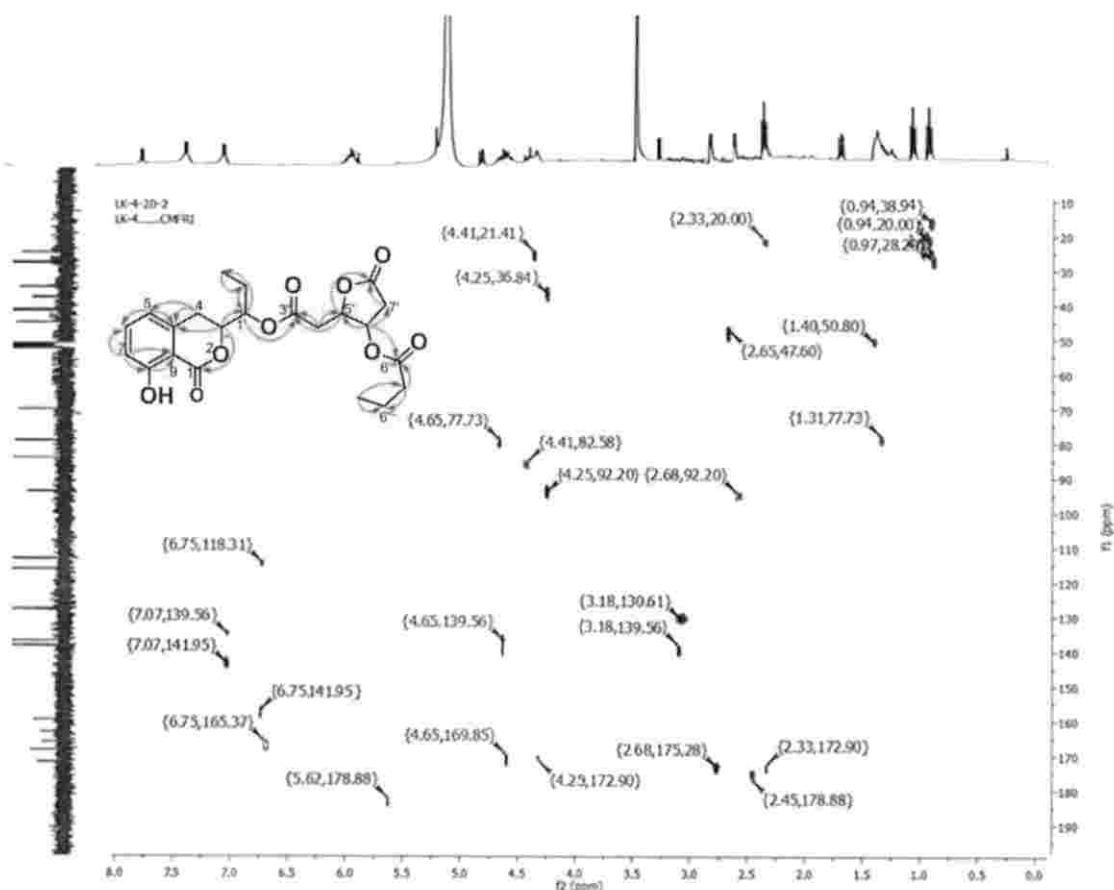


Figure 4.45. HMBC NMR spectrum polyketide (2)

The attachment of this dihydrofuranone moiety with the isopropyl propionate at C-5' was supported by the HMBCs from δ H 5.62 (H-5') to δ C 175.28 (C-3') and δ H 2.68 (H-4') to δ C 92.20 (C-5'). Thus, the 8-hydroxyisochromanone attached with the butyl 2-(5-oxotetrahydrofuran-2-yl)acetate chain to obtain 1-(8-hydroxy-1-oxoisochroman-3-yl)propyl 2-(5-oxotetrahydrofuran-2-yl)acetate and which was found to be similar to amicoumacins Isolated from a marine-derived bacterium *B. subtilis* (Li *et al.*, 2012). The COSY spin system from H-^b to H-6^c { δ H 2.33 (H-6^b)/ δ H 1.70 (H-6^c) along with the HMBC correlations from δ H 2.33 (H-6^b) to δ C 172.9 (C-6^a), 20.00 (C-6^c) and δ H 0.94 (H-6^d) to δ C 20.00 (C-6^c), δ C 38.94 (C-6^b) confirmed butyrate side chain. The attachment of this

butyrate chain at C-6' of the dihydrofuranone ring was confirmed by the HMBC correlations from δ H 4.25 (H-6') to δ C 172.90 (C-6'^a), 92.20 (C-5'), 36.84 (C-7').

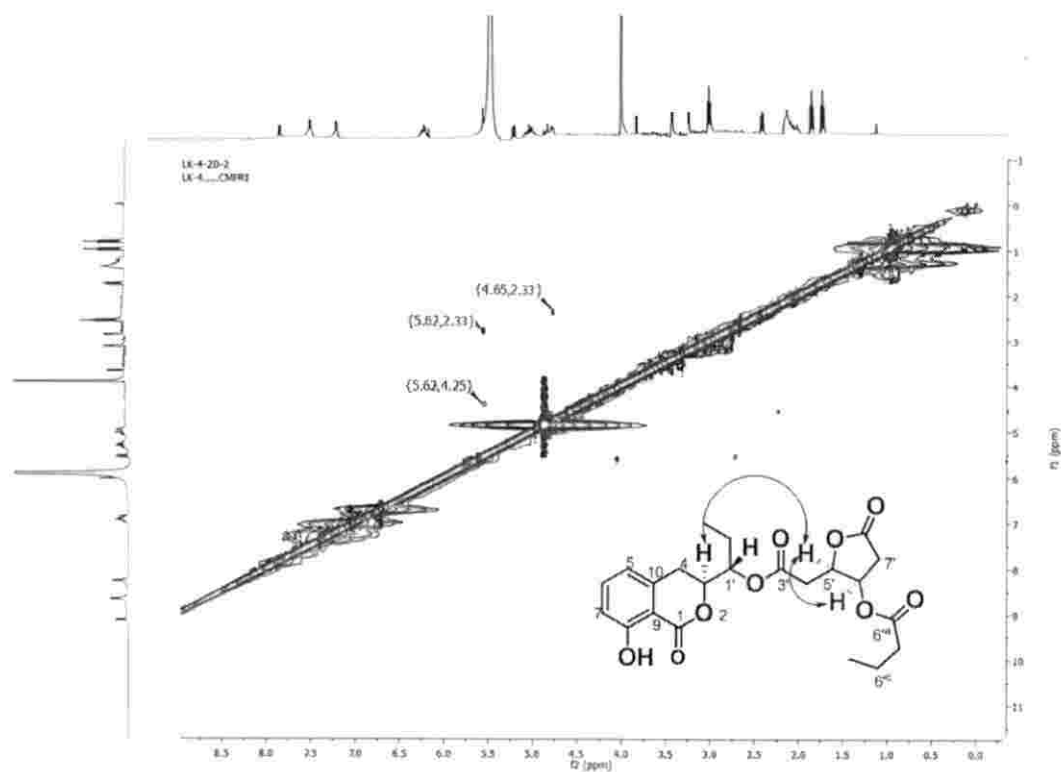


Figure 4.46. NOSEY spectrum of polyketide (2)

The NOE correlations such as, δ H 4.65 (H-3)/ 5.62 (H-5')/ 2.33 (H-6'^b)/ 4.25 (H-6') suggested the close proximity of these protons and these protons were arbitrarily assigned to α -oriented (Park *et al.*, 2016). Thus the butyrate chain at C-6' must be β - oriented. Whereas, the proton signal at δ H 4.41 (H-1') does not exhibit NOE correlation with α -oriented protons, which showed that it was β -oriented and the ethane side chain attached to it was assigned as β - oriented (Park *et al.*, 2016).

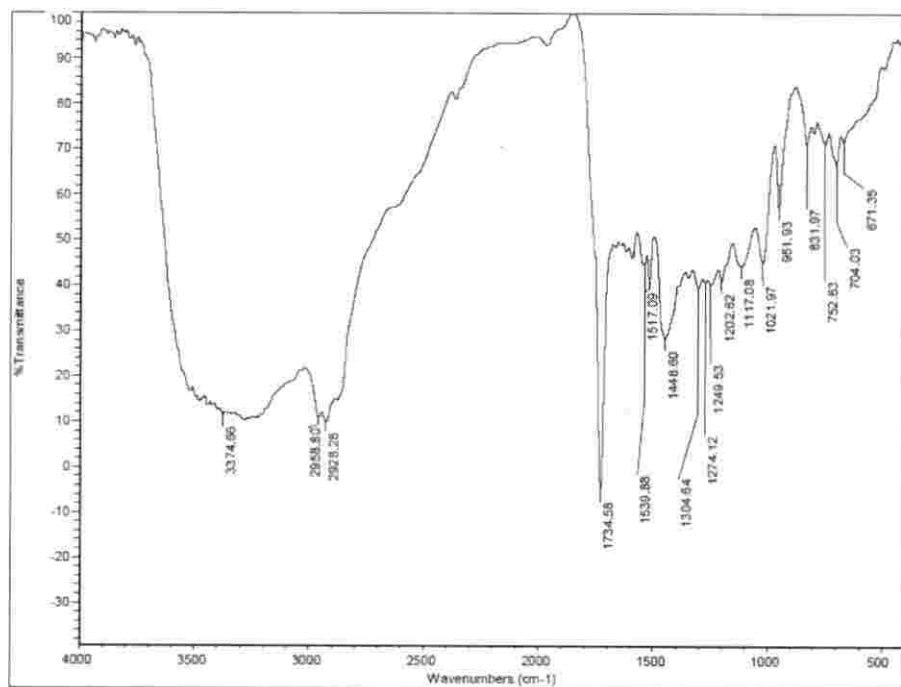


Figure 4.47. FT-IR spectrum of compound of polyketide (2)

The FTIR spectrum of the compound 2, exhibited absorption bands at 3374 cm^{-1} confirming the presence of hydroxyl group in the compound. Similarly the absorption bands at 1734 corresponds to C=O stretching and 1448 cm^{-1} corresponds to aromatic C=C stretching vibrations.

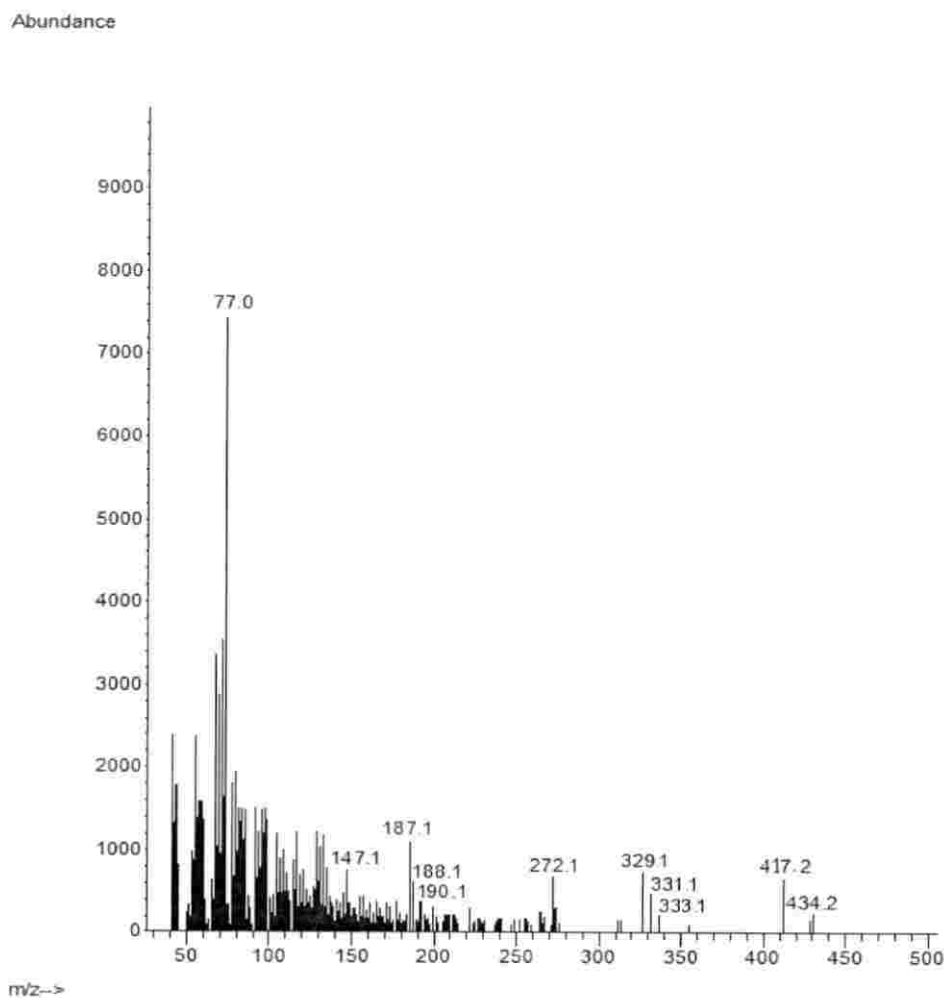


Figure 4.48. GCMS spectrum of polyketide (2)

The mass spectrum of the titled compound exhibited molecular ion peak at m/z 434.2, which on elimination of the hydroxyl group to yield 5-oxo-2-(2-oxo-2-(1-(1-oxoisochroman-3-yl)propoxy)ethyl)tetrahydrofuran-3-yl butyrate (B) with m/z 417.2. This ion further underwent subsequent McLafferty rearrangements to obtain radical cation at m/z 331.1 {6-oxo-6-(1-(1-oxoisochroman-3-yl)propoxy)hex-3-enoic acid (E)}, which on further McLafferty rearrangements to yield a fragmented ion at m/z 187.1 {3-(prop-1-en-1-yl)isochroman-1-one (H)}. This again underwent McLafferty rearrangements and subsequent hydrogenation of the double bond to obtain a fragment ion peak at m/z 190.1 (K). This further

eliminate CHO_2^\bullet and $\text{C}_5\text{H}_{11}^\bullet$ to yield phenyl radical cation with m/z 77.0 (M, base peak).

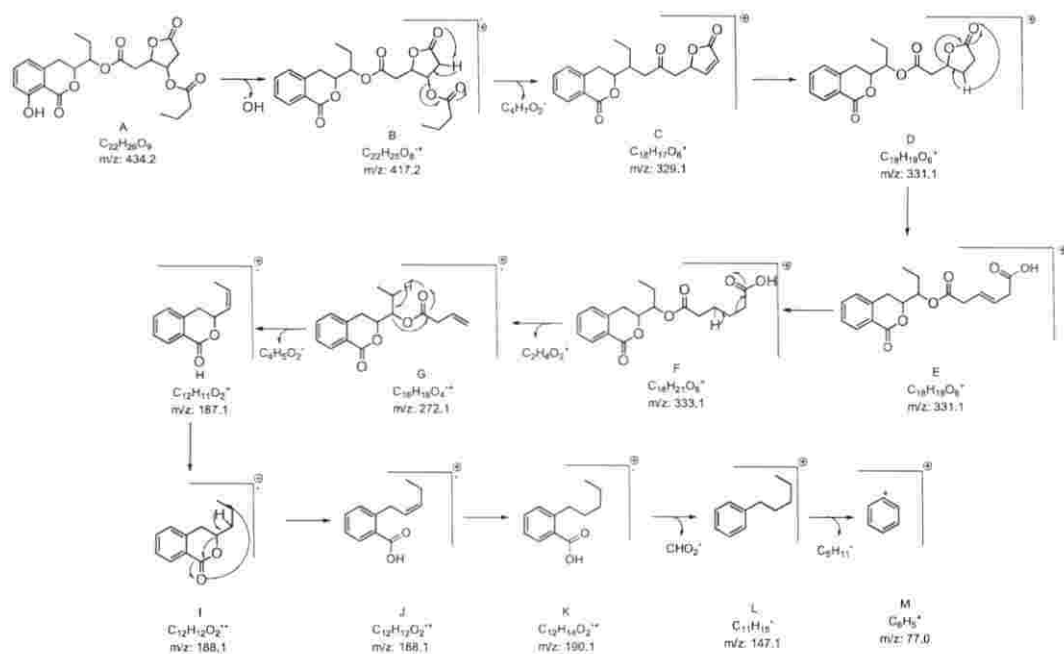


Figure 4.49. Mass fragmentation pattern of polyketide (2)

4.3.5 Bioactive (antioxidant and anti-inflammatory) potentials of secondary metabolite isolated from the organic extract of *B. amyloliquefaciens*

The free radical inhibiting activities of the polyketides 1 and 2, isolated from EtOAc extract of *B. amyloliquefaciens* were described in Table 4.13. The antioxidant activities of the isolated compounds were determined by the *in vitro* DPPH and ABTS⁺ scavenging experiments.

Table 4.13 *In vitro* bioactive potentials (antioxidant and anti-inflammatory) of polyketides (1-2)

| Antioxidant activity (IC₅₀; mg/mL) | 1 | 2 |
|------------------------------------------------------------|-------------------------|-------------------------|
| ^p DPPH scavenging activity | 0.35 ^a ±0.02 | 0.31 ^b ±0.03 |
| ^p ABTS ⁺ scavenging activity | 0.36 ^a ±0.02 | 0.32 ^b ±0.04 |
| Anti-inflammatory activity (IC₅₀; mg/mL) | 1 | 2 |
| ^p 5-LOX inhibition activity | 0.91 ^a ±0.01 | 0.90 ^b ±0.03 |

^pThe bioactivities were expressed as IC₅₀ values (mg/mL). The samples were analyzed in triplicate (n=3) and expressed as mean ± standard deviation. Means followed by different superscripts (a-b) within the same row indicated significant differences ($p < 0.05$).

The polyketide compound designated as 6'a-(3'-(1'-(8-hydroxy-1-oxoisochroman-3-yl)propoxy)-3'-oxoethyl)-8'-oxotetrahydrofuran-6'-yl butyrate (2) displayed significantly greater antioxidant activities against DPPH (IC₅₀ 0.31 mg/mL) (IC₅₀ 0.32 mg/mL) compared to 1-(8-hydroxy-1-oxoisochroman-3-yl)propyl 4'-(6'-hydroxy-8'-oxotetrahydrofuran-5'-yl)acetate (1) (DPPH IC₅₀ 0.35 mg/mL; ABTS⁺ IC₅₀ 0.36 mg/mL). Similarly, the compound also recorded with greater anti-inflammatory properties as determined by 5-LOX inhibitory assay (5-LOX, IC₅₀ 0.90 mg/mL) compared to that exhibited by compound 1 (5-LOX, IC₅₀ 0.98 mg/mL). Thus the antioxidant and anti-inflammatory activities were found to be greater for compound 2.

DISCUSSION

5. DISCUSSION

The natural products from coastal and marine ecosystems were continued to be a key source of previously undescribed compounds for developing novel pharmacophore leads (Cragg and Newman, 1997; Newman and Cragg, 2003; 2007; 2012; 2016). According to the recent reports, the natural product driven drugs attribute to more than 40 billion USD in the market apart from the non-pharmaceutical uses of bioactive compounds, such as terpenoids and polyketides in the field of aquaculture and agriculture (Demain, 2014). According to several reports, over the past 30 years, 75 % of novel antibiotics and 60 % of newer class of medicines for the treatment of cancer were originated from the natural products (Carrano and Marinelli, 2015, Pye *et al.*, 2017).

Microbial natural products have a broad spectrum of biological characteristics along with their structural diversities, which led into the treatment of several diseases including cancer, diabetics, hormonal and immune disorders, inflammatory diseases and microbial infections (Knight *et al.*, 2003). Mangrove sediment associated bacteria is a reservoir of metabolic diversity. In the last decades, the number of reported secondary metabolites from marine bacteria has progressively increased. Throughout the years, extensive screening programs were developed worldwide and great efforts have been devoted aiming of the isolation of new metabolites from mangrove associated microorganisms. In spite of great gains, several challenges exist in the field of microbial natural product discovery, such as the difficulties in the isolation and culturing of microbes under the laboratory conditions (Sun *et al.*, 2019). An approximate number of 107 bacteria, 102 fungal spores and 105 actinomycetes are present in 1 g of fertile soil, even though only 5% of those organisms were able to be cultivated under the laboratory conditions (Carrano and Marinelli, 2015). New methods are being investigated to increase the speed of isolation and characterization of bacteria and to develop plans to overcome these difficulties like OSMAC strategies, metagenomic sample sequencing from soil and water, metabolomic methods and genome mining (Handelsman *et al.*, 1998; Sekurova *et al.*, 2019).

The mangrove plants are specialized plants that grow in the intertidal coasts of tropical and subtropical regions of the world. The unique ecology and traditional medicinal uses of mangrove plants have attracted the attention of researchers over the years, and as a result, reports on biological activity of mangrove associates have increased significantly in recent years. Mangrove and mangrove associates were reported to contain biologically active compounds (Bandaranayake, 1995). They provide a rich source of small molecular bioactives including steroids, triterpenes, saponins, flavonoids, alkaloids and tannins (Bandaranayake, 1995). These adverse biochemical conditions also necessitate to enable these plants to generate various biologically active metabolites (Nebula *et al.*, 2013), which protect them from these destructive elements. These salt-resistant species are the richest natural sources of high value bioactive compounds, many of which belong to unprecedented chemical classes not found in other sources.

The explorations of previously unfathomed spaces for finding novel pharmacophore candidates were quite promising. Mangrove sediment associated bacteria have gained the attention many natural product drug discoverers apart from *Streptomyces* (Gao *et al.*, 2010; Sun *et al.*, 2019). Polyketide classes of compounds are structurally divergent molecules with potential pharmacological properties, and were reported to occur in microorganisms (Winter *et al.*, 2016). This group of compounds can potentially bind to the target enzymes required to exhibit the bioactivities, and were therefore, found potential applications in the discovery of more effective pharmacophores (Driggers *et al.*, 2008). Polyketide compounds, such as macrolactin have wide range of antibacterial activity against pathogenic bacteria such as *S. aureus* and *E. coli* (Gao *et al.*, 2010).

The present study titled 'Identification and characterization of bioactive leads from mangrove sediment associated bacteria and assessment of their therapeutic potential' was aimed to isolate, identify and characterize mangrove sediment associated bacteria and assessment of their therapeutic potential coupled

with the evaluation and characterization of the purified compounds from the bacteria.

A total of 10 sediment samples were collected from the Mangalavanam mangrove ecosystem, Kochi, India. The samples were serially diluted, spread plated in nutrient agar plates, supplied with 0.5 % NaCl and incubated at 34 °C for almost 1 week. The growth was visible after 24 h onwards. A total of 40 bacteria were selected from the nutrient agar plates were tested against both gram positive and gram negative pathogenic bacteria, such as *V. parahemolyticus*, *E. coli*, methicillin resistant *S. aureus* and *A. caviae* by spot-over-lawn-assay in Mueller Hinton Agar plates after a previous report of literature (Chakraborty *et al.*, 2014). The isolates were preserved as slant cultures and stab cultures at 20 °C and as glycerol stocks (50 %) at -80 °C.

Among the total number of 40 isolates, 25 isolates, i.e., 62.5 % of the isolates were active against at least one of the test pathogen with an inhibition zone diameter ≥ 10 mm, whereas 15 isolates i.e., 37.5 % showed an activity of ≥ 15 mm. A total of 15 % of the isolates were active against at least one pathogen with an inhibition zone diameter ≥ 20 mm, whereas 40 % and 10 % of the isolates displayed activities against methicillin resistant *S. aureus* with an inhibition zone ≥ 10 mm and ≥ 15 mm, respectively. A total of 45 % of the isolates were active against *V. parahemolyticus* with an activity of ≥ 10 mm, whereas 30 % of them showed activity with ≥ 15 mm inhibition zone. Among the total isolates, 12.5 % exhibited significant activity against *E. coli*, only 2.5 % of the isolates showed significant activity with ≥ 15 mm zone diameter. An inhibition zone of ≥ 10 mm was displayed by 20 % of the isolates against *A. caviae* but only 0.05 % showed activity greater than 20 mm.

Among the total 40 isolates, 25 were gram positive and 15 were gram negative. A total of 47.5 % of the isolates were gram positive rods, whereas 10 % were gram positive cocci, 40 % were gram positive rods, and one of the isolate was a gram negative coccus. Biochemical characterizations, such as malonate,

vogues proskauer, citrate, ONPG, nitrate reduction, catalase, arginine, coupled with sugar utilization tests for sucrose, mannitol, glucose, arabinose and trehalose were performed along with morphological characterization.

The bacterial isolates, which were found to exhibit negative reaction to catalase and nitrate reduction, were gram positive rods, and were found to ferment glucose, were grouped as *Clostridium* (Brown, 1939). The Gram positive rods, which were catalase positive were grouped as *Bacillus* species (Gordon *et al.*, 1973; PHE, 2018). *Bacillus* species was further differentiated based on the biochemical tests performed. Phenotypic differentiation has been difficult within the genus *Bacillus*, even though differences in motility, carbohydrate utilization, and hemolysis pattern were found to exist between the different species. The *Bacillus* group is divided mainly into two i.e. *B. cereus* group and *B. subtilis* group (PHE, 2018). The *B. cereus* group included species, such as *B. anthracis*, *B. mycoides*, *B. cereus*, *B. pseudomycoides*, *B. weihenstephanensis*, *B. thuringiensis*, *B. cytotoxicus* and *B. paramycoides* (Liu *et al.*, 2017; PHE, 2018). The characteristic feature of the *B. cereus* group were their presence of lecithinase and inability to produce acids from mannitol, motility and penicillin resistance was exhibited by all species belonging to *Bacillus*, except *B. anthracis*, which has been non-hemolytic in nature (PHE, 2018). Some strains of *B. cereus* were harmful for humans causing food borne illnesses, whereas there were reports of beneficial probiotics for feeding livestock (PHE, 2018).

The species in *B. subtilis* group, such as *B. subtilis* subsp. *subtilis*, *B. subtilis* subsp. *spizizenii*, *B. vallismortis*, *B. mojavensis*, *B. clausii*, *B. atrophaeus*, *B. amyloliquefaciens*, *B. licheniformis*, *B. atrophaeus*, *B. sonorensis*, *B. firmus*, *B. sporothermodurans* and *B. lentus* were difficult to differentiate since they have been closely related (PHE, 2018). Since *Bacillus* species were poorly stained, they could be confused with *Pseudomonas*. The cell of *B. subtilis* were lesser than 1 μm in width with ellipsoidal spores, and they were mesophilic, regarding temperature and neutrophilic with respect to pH but higher pH could be tolerated.

The isolates were screened for antioxidant activities by spraying DPPH into the filter paper with microbial extracellular metabolites in the medium (Velho-Pereira *et al.*, 2005). The isolates designated as S2A, S2C, S2B, S10B, S10C exhibited potentially greater zone of clearance than other bacterial isolates, indicating their antioxidant activities. The isolates S2A and S2B were later identified as *B. amyloliquefaciens* and *B. paramycoides*, whereas S2C, S10B and S10C were found out as *B. cereus*.

The molecular characterization of the selected isolates was carried out by extracting genomic DNA from the bacteria, amplification and 16S rRNA sequencing. The sequences were searched in NCBI-blast for similarity check and $\geq 99\%$ similarity was observed with the database. The bacterial sequences were submitted in the GenBank using BankIt software and the NCBI-GenBank accessions were obtained for the sequences. The isolates, S2A and S4A were identified as *B. amyloliquefaciens*, whereas S1A, S2C, S10B and S10C were found out as *B. cereus*. The isolates designated as, S1C and S2B were recognized as *B. paramycoides*, whereas S2D was found out as *B. anthracis*. The occurrence of functional gene systems, such as PKS and NRPS biosynthetic gene clusters which were involved in the synthesis of many secondary metabolites in the microorganisms could be found out by targeting specific primers to the PKS and NRPS gene sequence (Ayuso-sacido *et al.*, 2005). The presence of *pks* gene in the isolate S2A, *B. amyloliquefaciens* was attributed by using the primers *gcf* and *ger* and the 700 bp PKS gene sequence was submitted in EMBOSS software, and further submitted in GenBank. The GenBank accession number obtained for the PKS sequence was MN 165388.

The phylogenetic analysis of the 9 isolates were carried out after aligning the sequences together with bacterial sequences of different species in the *B.* genera, such as *B. subtilis*, *B. methylotrophicus*, *B. thuringiensis*, *B. vallismortis*, *B. megaterium*, *B. clausii* and *B. atropheaus* along with different sequences of *B. amyloliquefaciens* obtained from the NCBI database. The phylogenetic tree, showing the relationship among the different species was constructed with the

MEGA6 software by neighbor-joining method. The *B. amyloliquefaciens*, S2A and S4A fell under the clade including several other *B. amyloliquefaciens*, *B. vallismortis*, *B. subtilis* and *B. methylotrophicus*. The *B. cereus* designated as, S1A, S10B and S10C fell under the same clade with an isolated *B. paramycooides* (S1C), along with *B. thuringiensis*. The insufficient divergence in the 16S rRNA sequence region might be the reason for this exclusion from a similar clade (Maughen and Van der Auwera, 2011). Hence, an essential housekeeping gene, which could evolve more rapidly than the 16S rRNA gene, might be used for taxonomic classification (Palys *et al.*, 2000). Still, 16S rRNA sequencing is still considered as the gold standard for many identification projects due to the ease of amplification of the gene and its omnipresent nature (Palys *et al.*, 2000).

It is of note that most of the bioactive compounds or secondary metabolites were produced in the stationary phase of growth of the microorganism (Thilakan *et al.*, 2016). Hence, the bacterial growth curve is crucial for finding the phase of the production of secondary metabolites or bioactive compounds in the bacteria. The bacterial isolate designated as S2A, which was identified as *B. amyloliquefaciens* has exhibited potential antioxidant activity against the free radical, DPPH and antibacterial activity against pathogenic *V. parahemolyticus*. Hence, the isolate, S2A was selected for the extraction of intracellular and extracellular secondary metabolites. Earlier reports suggested that the secondary metabolite production in *B. amyloliquefaciens* (S2A) could occur after 72 hours of incubation. The stationary phase of S2A was found out to be in between 68-72 hours, thus supporting the existing reports, whereas the growth began to decline after 72 hours, reaching its death phase.

The selected bacteria *B. amyloliquefaciens* (S2A) was swabbed in nutrient agar plates supplied with 0.5 % NaCl. The bioactive compounds were extracted in solvent ethyl acetate by refluxing in a heating mantle after 72 hours of incubation at 34 °C. The extraction was continued for almost 1 week. The intracellular compounds from the bacteria were released by sonicating at amplitude of 37 % with a 10 s on-and-off pulse for 20 min. Intracellular and

extracellular compounds were extracted separately in the round bottom flasks before being concentrated in rotary vacuum evaporator, and the presence of compounds were checked by TLC at 254 nm and 365 nm. The spots in the TLC plate of extracellular extract were disappeared after 6 days of extraction, but that of intracellular extracts were disappeared earlier, i.e., after 3 or 4 days of extraction.

The individual components in the crude were separated on the TLC stationary phase with a solvent system containing 5 % methanol and 95 % dichloromethane. Visualizing agents, such as iodine, DPPH and vanillin-sulphuric acid were used for the detection of spots on the TLC plates. About 4-5 spots were detected on the TLC plates, visualized with vanillin-sulphuric acid indicating the presence of either aldehydes, ketones or alcohols, whereas a total of 6-7 spots were discerned on the TLC plate visualized with iodine, indicating the possible presence of aromatics. The presence of anti-oxidant compounds in the crude organic extract was attributed by the decolourization of spots from purple to white on the TLC plates, which were applied with DPPH reagent.

The extracellular crude extracts were further screened to check their antioxidant activities using the free radicals DPPH and ABTS, whereas the anti-inflammatory activities were attributed by their capacities to attenuate pro-inflammatory 5-LOX. The ethyl acetate extracts of the *B. amyloliquefaciens* exhibited potential antioxidant activities (i.e., IC_{50} 3.5 $\mu\text{g/mL}$ and 3.9 $\mu\text{g/mL}$ to quench DPPH and ABTS radical species) coupled with 5-LOX inhibitory activity (IC_{50} 6 $\mu\text{g/mL}$).

The antimicrobial activities of the organic extracts were analyzed by disc diffusion assay against pathogens, such as *V. parahemolyticus*, MRSA, *E. coli* and *A. caviae*. The crude extracts were found to possess higher activities when compared to the spot-over lawn assay and the positive control, chloramphenicol (30 μg). The extracellular extracts displayed significant higher activity against *V. parahemolyticus* with an inhibition zone diameter of 20 mm for 100 μg where, the

intracellular extracts exhibited 12 mm zone for 100 µg of the extract. No significant differences in the antibacterial activities between the intracellular and extracellular extracts were apparent against the pathogenic *A. caviae* with an inhibition zone of 18-20 mm by 100 µg of the test material. Notably, the extracellular extracts exhibited a higher activity towards the test pathogen MRSA (16 mm for 100 µg of the extract) than that of 16 mm displayed by the positive control. It is of note that no significant differences in the antibacterial activities between the intracellular and extracellular extracts were apparent against the pathogenic *E. coli* with an inhibition zone of 15-16 mm by 30 µg of the test material. The minimum inhibitory concentration was determined by broth dilution method against different pathogenic bacteria, such as *V. parahemolyticus* and *A. caviae*. The MIC was found to be lesser than 12.5 µg for all the test organisms. The minimum inhibitory concentration (MIC) was determined by broth dilution method against different pathogenic bacteria, such as *A. caviae*, *V. parahemolyticus* and *E. coli*. The MIC was found to be lesser than 12.5 µg for all the test organisms.

The crude extract of *B. amyloliquefaciens* exhibited significant antimicrobial, antioxidant (DPPH and ABTS free radical scavenging) and anti-inflammatory (5-LOX inhibitory) activities. Therefore, the organic (EtOAc) extract of *B. amyloliquefaciens* was selected for purification over reverse octadecylsilane stationary phase-C₁₈ to yield bioactive metabolites. The organic extract of *B. amyloliquefaciens* was purified by reverse octadecylsilane stationary phase-C₁₈ using 80:20 MeCN:MeOH (v/v) to yield four fractions (BA1-BA4). Among these fractions, BA4 was obtained with greater yield, which was further purified by reverse phase-C₁₈ column under high pressure (20 PSI) using MeCN:MeOH (80:20, v/v) to yield two homogenous compounds, characterized as 1-(8-hydroxy-1-oxoisochroman-3-yl)propyl 4'-(6'-hydroxy-8'-oxotetrahydrofuran-5'-yl)acetate (**1**) and 6'a-(3'-(1'-(8-hydroxy-1-oxoisochroman-3-yl)propoxy)-3'-oxoethyl)-8'-oxotetrahydrofuran-6'-yl butyrate (**2**). The structures of the compounds were assigned by extensive one (¹H, ¹³C and ¹³⁵DEPT NMR) and two

(^1H - ^1H COSY, HSQC, HMBC and NOESY) dimensional spectroscopic experiments combined with mass and FTIR analyses. The characterized bioactive secondary metabolite from *B. amyloliquefaciens* was classified as polyketides.

The polyketide compound 1, characterized as 1-(8-hydroxy-1-oxoisochroman-3-yl)propyl 4'-(6'-hydroxy-8'-oxotetrahydrofuran-5'-yl)acetate (1) was isolated as a brown oily compound. It displayed UV absorbance (in MeOH) at λ_{max} ($\log \epsilon$ 4.093) of 207 nm. The purity of the compound was supported by RP C₁₈ HPLC {using 80:20 MeCN:MeOH, v/v (R_t 2.77)} experiments. Its mass spectrum demonstrated a molecular ion peak at m/z 364, which in combination with its one and two dimensional NMR data suggested the elemental composition of the compound as C₁₈H₂₀O₈. The ^{13}C -NMR spectrum of the compound 1, exhibited 18 carbon signals, which were assigned to four each of sp^3 methylenes and sp^3 methines, along with one sp^3 methyl, three sp^2 methines, six quaternary carbons based on comprehensive ^{13}C NMR and DEPT₁₃₅ NMR data of the titled compound 1. The ^1H and ^{13}C NMR spectra demonstrated characteristic signals for three ester carbonyls (δC 168.42, 172.92 and 177.68), hydroxylated quaternary carbon (δC 161.57), oxygenated methines (δH 4.64/ δC 83.54; δH 4.43/ δC 76.69; δH 3.69/ δC 72.22), carbonyl methylenes (δH 2.42/ δC 36.39; δH 2.67/ δC 34.23) and hydroxylated methine (δH 3.69/ δC 72.22). The carbon signal at δC 76.69 (HSQC with δH 4.43), δC 87.36 (HSQC with δH 5.28) and δC 83.54 (HSQC with δH 4.64) appropriately supported the occurrence of ester groups in the studied compound 1. The ^1H -NMR signals at δH 7.09 (HSQC with δC 130.61), 7.47 (HSQC with δC 141.95), 6.85 (HSQC with δC 115.15) suggested the presence of benzene ring in the compound. The FTIR spectrum of the compound 1, exhibited absorption bands at 3224 cm^{-1} thus confirming the presence of hydroxyl group in the compound. Similarly the absorption bands at 1735 cm^{-1} corresponds to C=O stretching and 1546 cm^{-1} corresponds to aromatic C=C stretching vibrations. Thus based spectroscopic techniques including NMR, GCMS, FT-IR and UV, the structure of the compound was designated as 1-(8-hydroxy-1-oxoisochroman-3-

yl)propyl 4'-(6'-hydroxy-8'-oxotetrahydrofuran-5'-yl)acetate (1), and was classified under the class of polyketide compounds.

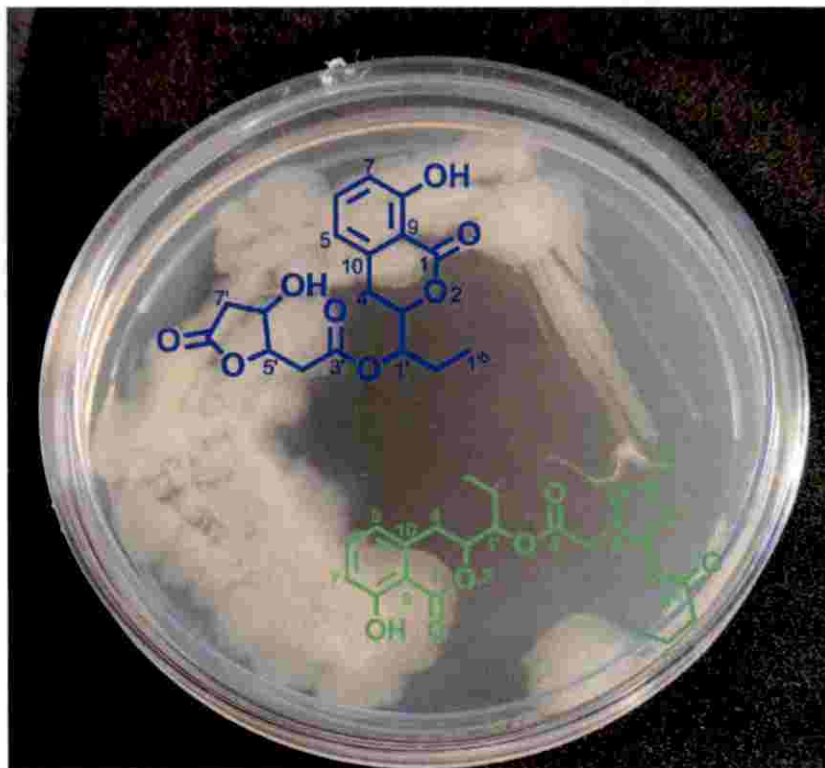


Figure 5.1 Polyketide compounds isolated from *B. amyloliquefaciens* (S2A)

The polyketide compound 2, characterized as 6'a-(3'-(1'-(8-hydroxy-1-oxoisochroman-3-yl)propoxy)-3'-oxoethyl)-8'-oxotetrahydrofuran-6'-yl butyrate (2) was isolated as a brown oily compound. It displayed UV absorbance (in MeOH) at λ_{max} ($\log \epsilon$ 3.849) 274 nm. The purity of compound was supported by RP C18 HPLC {using 80:20 MeCN:MeOH, v/v (Rt 2.75)} experiments. The molecular formula of the compound was obtained as $\text{C}_{22}\text{H}_{26}\text{O}_9$, and which was further supported by the molecular ion peak at m/z 434 (m/z : 434.1577 [M]⁺, cal. for 434.1573). The ^{13}C -NMR spectrum of the compound 2, showed 22 carbon signals, which were assigned to six sp^3 methylenes, four sp^3 methines, two sp^3 methyls, three sp^2 methines and seven quaternary carbons based on combined ^{13}C NMR and DEPT₁₃₅ experiments. The ^1H and ^{13}C NMR spectra demonstrated

characteristic signals for four ester carbonyls (δC 169.85, 175.28, 178.88 and 172.90), hydroxylated quaternary carbon (δC 165.37), oxygenated methines (δH 4.65/ δC 82.58; δH 4.41 / δC 77.73; δH 4.25/ δC 68.11; δH 5.62/ δC 92.20), and carbonyl methylenes (δH 2.68/ δC 34.30; δH 2.46/ δC 36.84; δH 2.33/ δC 38.94). The carbon signal at δC 82.58 (HSQC with δH 4.65), δC 77.73 (HSQC with δH 4.41), δC 92.20 (HSQC with δH 5.62) and δC 68.11 (HSQC with δH 4.25) supported the presence of ester groups in the titled compound. The proton signals at δH 7.07 (HSQC with δC 130.61), 7.42 (HSQC with δC 141.95), 6.75 (HSQC with δC 115.17) supported the presence of benzene ring in the compound. The FTIR spectrum of the compound 2, exhibited absorption bands at 3374 cm^{-1} confirming the presence of hydroxyl group in the compound. Similarly, the absorption bands at 1734 cm^{-1} was found to correspond to C=O stretching and that at 1448 cm^{-1} was due to the aromatic C=C stretching vibrations. Thus based spectroscopic techniques including NMR, GCMS, FT-IR and UV, the structure of the compound was designated as 6'a-(3'-(1'-(8-hydroxy-1-oxoisochroman-3-yl)propoxy)-3'-oxoethyl)-8'-oxotetrahydrofuran-6'-yl butyrate (2), and was classified under polyketide.

The purified polyketides were assessed for their antioxidant (DPPH and ABTS⁺ scavenging) and anti-inflammatory (5-LOX attenuation) activities. The 6'a-(3'-(1'-(8-hydroxy-1-oxoisochroman-3-yl)propoxy)-3'-oxoethyl)-8'-oxotetrahydrofuran-6'-yl butyrate (2) displayed significantly greater antioxidant activities against DPPH (IC₅₀ 0.31 mg/mL) and ABTS⁺ (IC₅₀ 0.32 mg/mL) compared to 1-(8-hydroxy-1-oxoisochroman-3-yl)propyl 4'-(6'-hydroxy-8'-oxotetrahydrofuran-5'-yl)acetate (1) (DPPH IC₅₀ 0.35 mg/mL; ABTS⁺ IC₅₀ 0.36 mg/mL). Similarly the compound 2 also recorded greater anti-inflammatory properties as determined by 5-LOX inhibitory assay (5-LOX IC₅₀ 0.90 mg/mL) compared to that displayed by compound 1 (5-LOX IC₅₀ 0.98 mg/mL). The antioxidant and anti-inflammatory properties were found to be greater for compound 2, and therefore, it could be used as valuable pharmacophore in pharmaceutical applications.

SUMMARY

6.SUMMARY

Mangroves are woody halophytes that occur in the tropical and sub-tropical latitudes (Kathiresan and Bingham, 2001; Alongi, 2002). These halophytic plants were found to exhibit a marked degree of tolerance to high salt concentrations and soil anoxia (Saenger, 2013). These extreme conditions prevailing in the mangrove ecosystem could be helpful for the microbes associated with the rhizospheric soil sediment in the production of secondary metabolites. Mangrove sediment associated bacteria is a reservoir of metabolic diversity. Mangroves and mangrove sediment associated microorganisms were widely known for their medicinal values against various human diseases from the ancient period, due to the occurrence of bioactive metabolites with intriguing carbon skeletons (Nebula et al., 2013; Joel and Bhimba, 2010). The secondary metabolites or bioactive compounds from mangrove sediment associated bacterial flora were reported to display potential antimicrobial, antiviral, antioxidant, anti-inflammatory and antidiabetic activities. Thus, those compounds could be used as therapeutic leads for curing diseases such as diabetes, microbial infections and inflammatory disorders, like arthritis.

In the present investigation, mangrove sediment associated bacteria exhibiting significant antioxidant and antimicrobial activities were isolated, identified and characterized by integrated biochemical, morphological, microbiological and 16S rRNA sequencing. Among the total 40 isolates, 25 isolates, i. e. 62.5 % of the isolates were active against at least one of the test pathogens with an inhibition zone diameter ≥ 10 mm; whereas 15 % of the total isolates were active against at least one pathogen with an inhibition zone diameter ≥ 20 mm. A total of 40% and 10% of the isolates showed activity against methicillin resistant *S. aureus* with an inhibition zone ≥ 10 mm and ≥ 15 mm, respectively, whereas 45% of the isolates were active against *V. parahemolyticus* with an activity of ≥ 10 mm and 30 % showed activity with ≥ 15 mm inhibition zone. A total of 12.5 % of the isolates showed significant activity against pathogenic *E. coli*, whereas only 2.5 % showed significant activity with ≥ 15 mm zone diameter. A total of 20 % of the isolates were active against *A. caviae* with an inhibition zone ≥ 10 mm but only 0.05 % showed activity greater than 20 mm. A total of 47.5 % of the isolates were gram positive

rods, 10 % were gram positive cocci, 40 % were gram positive rods, whereas 1 isolate was a gram negative coccus.

The bacteria were identified as *B. cereus*, *B. anthracis*, *B. paramycooides* and *B. amyloliquefaciens* by integrated biochemical, morphological, microbiological and 16S rRNA sequencing. *B. amyloliquefaciens* (S2A) was positive for PKS gene cluster, which has been a secondary metabolite biosynthetic gene cluster, involved in the synthesis of many secondary metabolites. The *B. amyloliquefaciens* (S2A) exhibiting significant antimicrobial activity against *V. parahemolyticus*, *A. caviae* and MRSA and antioxidant activity against the free radical, DPPH was selected for further purification of bioactive metabolites. The bacteria, S2A attained stationary phase in between 68-72 h. Therefore, the bioactive compound extraction was carried out after 72 h of incubation in nutrient agar plates. The extracellular and intracellular compounds from the bacteria were extracted in solvent ethyl acetate for 1-7 days. TLC was performed to detect the presence of compounds at 254 nm and 365 nm, and the extraction was continued till the spots got invisible.

The optimum separation of compounds was observed in 5 % methanol and 95 % dichloromethane. Spots were observed from the day of first extraction till it get faded and the extraction was stopped at a point where, the spots were not visible. Visualizing agents, such as iodine, DPPH and vanillin-sulphuric acid were also used for the detection of spots in the TLC plates. The presence of anti-oxidant compounds were indicated by the decolourization of spots from purple to white in the TLC plates visualized with DPPH. The extracellular crude extracts were further screened to check antioxidant activity using the oxidants DPPH and ABTS, whereas anti-inflammatory activity was reported by checking their capacities to attenuate pro-inflammatory 5-LOX. The ethyl acetate extracts of the *B. amyloliquefaciens* exhibited potential antioxidant activities (i.e., IC_{50} 3.5 $\mu\text{g/mL}$ and 3.9 $\mu\text{g/mL}$ to quench DPPH and ABTS radical species) coupled with 5-LOX inhibitory activity (IC_{50} 6 $\mu\text{g/mL}$).

The antimicrobial activities of the organic extracts were analyzed by disc diffusion assay against pathogens, such as *V. parahemolyticus*, MRSA, *E. coli* and *A. caviae*. The crude extracts were found to possess higher activities when compared to the spot-over

lawn assay and the positive control, chloramphenicol (30µg). The extracellular extracts displayed significant higher activity against *V. parahemolyticus* with an inhibition zone diameter of 20 mm for 100 µg where, the intracellular extracts exhibited 12 mm zone for 100 µg of the extract. No significant differences in the antibacterial activities between the intracellular and extracellular extracts were apparent against the pathogenic *A. caviae* with an inhibition zone of 18-20 mm by 100 µg of the test material. Likewise, no significant differences in the antibacterial activities between the intracellular and extracellular extracts were apparent against the pathogenic *E. coli* with an inhibition zone of 15-16 mm by 30 µg of the test material. Notably, the extracellular extracts exhibited a higher activity towards the test pathogen MRSA (16 mm for 100 µg of the extract) and *A. caviae* (20 mm for 100 µg of the extract). The inhibition zone diameter exhibited by the crude extracellular extracts against *A. caviae* and MRSA (13 mm 30 µg) was greater than that of the positive control chloramphenicol (10 mm 30 µg) for The minimum inhibitory concentration was determined by broth dilution method against different pathogenic bacteria, such as *A. caviae*, *V. parahemolyticus* and *A. caviae*. The MIC was found to be lesser than 12.5 µg for all the test organisms.

The crude extract of *B. amyloliquefaciens* exhibited significant antimicrobial, antioxidant (DPPH and ABTS free radical scavenging) and anti-inflammatory (5-LOX inhibitory) activities. Therefore, the organic (EtOAc) extract of *B. amyloliquefaciens* was selected for purification by preparatory HPLC to yield bioactive metabolites. The column chromatographic purification of the organic extract using preparative HPLC resulted in two new polyketide derivatives, characterized as 1-(8-hydroxy-1-oxoisochroman-3-yl)propyl 4'-(6'-hydroxy-8'-oxotetrahydrofuran-5'-yl)acetate (1) and 6'a-(3'-(1'-(8-hydroxy-1-oxoisochroman-3-yl)propoxy)-3'-oxoethyl)-8'-oxotetrahydrofuran-6'-yl butyrate (2). The structures of the compounds were assigned by extensive one (^1H , ^{13}C and $^{135}\text{DEPT}$ NMR) and two (^1H - ^1H COSY, HSQC, HMBC and NOESY) dimensional spectroscopic experiments combined with mass and FTIR analyses. The isolated compounds were further analyzed for antioxidant and anti-inflammatory activities. The compound 2, 6'a-(3'-(1'-(8-hydroxy-1-oxoisochroman-3-yl)propoxy)-3'-oxoethyl)-8'-oxotetrahydrofuran-6'-yl butyrate

exhibited significantly greater antioxidant activities against DPPH (IC_{50} 0.31 mg/mL) and $ABTS^+$ (IC_{50} 0.32 mg/mL) radicals compared to 1-(8-hydroxy-1-oxoisochroman-3-yl)propyl 4'-(6'-hydroxy-8'-oxotetrahydrofuran-5'-yl)acetate (1) (DPPH IC_{50} 0.35 mg/mL; $ABTS^+$ IC_{50} 0.36 mg/mL). Similarly the compound 2 also recorded greater anti-inflammatory properties as determined by 5-LOX inhibitory assay (5-LOX IC_{50} 0.90 mg/mL) compared to that displayed by compound 1 (5-LOX IC_{50} 0.98 mg/mL). Thus the antioxidant and anti-inflammatory properties were found to be greater for compound 2, and therefore, it could be used as valuable pharmacophore in medicinal applications. The research outcomes could able to identify the therapeutic potential of mangrove sediment associated bacteria as pool of bioactive pharmacophores of polyketide origin for use against oxidants and inflammatory pathophysiological conditions.

REFERENCES

7. REFERENCES

- Abada E., Al-Fifi Z., Osman M. 2019. Bioethanol production with carboxymethylcellulase of *Pseudomonas poae* using castor bean (*Ricinus communis* L.) cake. *Saudi J. Biol. Sci.* 26(4): 866-871
- Adams, M.W. and Kelly, R.M. 1998. Finding and using hyperthermophilic enzymes. *Trends in Biotechnol.* 16(8): 329-332.
- Ahimou, F., Jacques, P. and Deleu, M. 2000. Surfactin and iturin A effects on *Bacillus subtilis* surface hydrophobicity. *Enzyme Microb. Technol.* 27(10): 749-754.
- Ahmed, S. I., Hayat, M.Q., Tahir, M., Mansoor, Q., Ismail, M., Keck, K. and Bates, R.B. 2016. Pharmacologically active flavonoids from the anticancer, antioxidant and antimicrobial extracts of *Cassia angustifolia* Vahl. *BMC Complement. and Altern. Med.* 16(1): 460-462.
- Ali, A. I. B., El Bour, M., Ktari, L., Bolhuis, H., Ahmed, M., Boudabbous, A. and Stal, L.J. 2012. *Jania rubens*-associated bacteria: molecular identification and antimicrobial activity. *J. Appl. Phycol.* 24(3): 525-534.
- Alongi, D. M., 2002. Present state and future of the world's mangrove forests. *Environ. Conserv.* 29: 331-349.
- Ancheeva, E., Daletos, G. and Proksch, P. 2018. Lead compounds from mangrove-associated microorganisms. *Mar. drugs* 16(9): 319-320.
- Armstrong, E., Yan, L., Boyd, K. G., Wright, C. P. and Burgess, J. G. 2001. The symbiotic role of marine microbes on living surfaces. *Hydrobiologia.* 461: 37-40.
- Ashokkumar, S. and Irfan, Z. B. 2018. Current Status of Mangroves in India: Benefits, Rising Threats Policy and Suggestions for the Way Forward. Available : <http://www.mse.ac.in/wp-content/uploads/2018/08/Working-Paper-174.pdf> [July 2018]

- Ayuso-Sacido, A. and Genilloud, O. 2005. New PCR primers for the screening of NRPS and PKS-I systems in actinomycetes: detection and distribution of these biosynthetic gene sequences in major taxonomic groups. *Microbial ecol.* 49(1): 10-24.
- Bandaranayake, W. 1995. Survey of mangrove plants from Northern Australia for phytochemical constituents and UV-absorbing compounds. *Curr. Topics in Phytochem.* 14: 69-78.
- Bandaranayake, W. M. 2002. Bioactivities, bioactive compounds and chemical constituents of mangrove plants. *Wetlands Ecol. and Manag.* 10(6): 421-452.
- Basak, U.C., Singh, S. and Rout, P. 2016. Nutritional and antioxidant properties of some edible mangrove fruits used by rural communities. *J. Agric. Food Tech.* 6(1): 1-6.
- Baylac, S. and Racine, P. 2003. Inhibition of 5-lipoxygenase by essential oils and other natural fragrant extracts. *Int. J. Aromatherapy.* 13(2-3): 138-142.
- Behera, B.C., Parida, S., Dutta, S.K. and Thatoi, H.N. 2014. Isolation and identification of cellulose degrading bacteria from mangrove soil of Mahanadi River Delta and their cellulase production ability. *Am. J. Microbiol. Res.* 2(1): 41-46.
- Berdy, J., 2005. Bioactive microbial metabolites. *The J. Antibiot.* 58(1): 1-4.
- Besson, F., Peypoux, F., Michel, G. and Delcambe, L. 1976. Characterization of iturin A in antibiotics from various strains of *Bacillus subtilis*. *The J. antibiot.* 29(10): 1043-1049.
- Bhimba, B. V., Meenupriya, J., Joel, E. L., Naveena, D. E., Kumar, S. and Thangaraj, M., 2010. Antibacterial activity and characterization of secondary metabolites isolated from mangrove plant *Avicennia officinalis*. *Asian Pac J. Trop. Med.* 3(7): 544-546.

- Biswas, K., Choudhury, J. D., Mahansaria, R., Saha, M. and Mukherjee, J. 2017. *Streptomyces euryhalinus* sp. nov., a new actinomycete isolated from a mangrove forest. *The J. antibiot.* 70(6): 747-748.
- Blois, M. S. 1958. Antioxidant determinations by the use of a stable free radical. *Nat.* 181(4617): 1199-1200.
- Blumenthal, D., Brunton, L. L., Buxton, I. L. and Parker, K. L. 2008. Goodman & Gilman's manual of pharmacology and therapeutics (11th Edi) McGraw-Hill, Medical publishing division 1-2011.
- Blunt, J. W., Carroll, A. R., Copp, B. R., Davis, R. A., Keyzers, R. A. and Prinsep, M. R. 2018. Marine natural products. *Nat. Product Rep.* 35(1): 8-53.
- Boottanun, P., Potisap, C., Hurdle, J. G. and Sermswan, R.W. 2017. Secondary metabolites from *Bacillus amyloliquefaciens* isolated from soil can kill *Burkholderia pseudomallei*. *AMB express* 7(16): 6-11
- Brand-Williams, W., Cuvelier, M.E. and Berset, C.L.W.T., 1995. Use of a free radical method to evaluate antioxidant activity. *LWT-Food Sci. and Technol.* 28(1): 25-30.
- Brown, J. H. 1939. Bergey's manual of determinative bacteriology 29(4): 404-405.
- Cao, X. H., Liao, Z. Y., Wang, C. L., Yang, W. Y. and Lu, M. F. 2009. Evaluation of a lipopeptide biosurfactant from *Bacillus natto* TK-1 as a potential source of anti-adhesive, antimicrobial and antitumor activities. *Brazilian J. Microbiol.* 40(2): 373-379.
- Carrano, L. and Marinelli, F. 2015. The relevance of chemical dereplication in microbial natural product screening. *J. Appl. bioanalysis* 1(2): 55-67.
- Chakraborty, K., Thilakan, B. and Raola, V. K. 2014. Polyketide Family of Novel Antibacterial 7-O-Methyl-5'-hydroxy-3'-heptenoate-

- Macrolactin from Seaweed-Associated *Bacillus subtilis* MTCC 10403. *J. Agric. and food Chem.* 62(50): 12194-12208.
- Chakraborty, R. D., Chakraborty, K. and Thilakan, B. 2015. Isolation and characterization of antagonistic *Streptomyces* spp. from marine sediments along the southwest coast of India. 44(1): 1-5 Available : http://eprints.cmfri.org.in/10805/1/Indian%20Journal%20of%20Geomarine%20Sciences_2015_44_1_Isolation%20and%20characterization_Kajal.pdf
- Chakraborty, K., Thilakan, B., Raola, V. K. and Joy, M. 2017a. Antibacterial polyketides from *Bacillus amyloliquefaciens* associated with edible red seaweed *Laurenciae papillosa*. *Food chem.* 218:427-434.
- Chakraborty, K., Thilakan, B. and Raola, V. K. 2017b. Antimicrobial polyketide furanoterpenoids from seaweed-associated heterotrophic bacterium *Bacillus subtilis* MTCC 10403. *Phytochemistry* 142: 112-125.
- Chakraborty, K., Thilakan, B. and Kizhakkekalam, V. K. 2018a. Antibacterial aryl-crowned polyketide from *Bacillus subtilis* associated with seaweed *Anthophycus longifolius*. *J. Appl. Microbiol.* 124(1): 108-125.
- Chakraborty, K., Thilakan, B. and Raola, V. K., 2018b. Previously undescribed antibacterial polyketides from heterotrophic *Bacillus amyloliquefaciens* associated with seaweed *Padina gymnospora*. *Applied biochemistry and biotechnology* 184(2): 716-732.
- Chauhan, B., Kumar, G., Kalam, N. and Ansari, S. H. 2013. Current concepts and prospects of herbal nutraceutical: A review. *J. Adv. Pharma. Technol. & Res.* 4(1): 4.

- Chen, L., Chai, W., Wang, W., Song, T., Lian, X.Y. and Zhang, Z. 2017. Cytotoxic bagremycins from mangrove-derived *Streptomyces* sp. Q22. *J. Nat. products* 80(5): 1450-1456.
- Clinical and Laboratory Standards Institute, 2009. Performance standards for antimicrobial susceptibility testing of anaerobic bacteria: informational supplement. Clinical and Laboratory Standards Institute (CLSI). Available: <http://ljzx.cqrmhospital.com/upfiles/201601/20160112155335884.pdf>
- Colwell, R. R. 1997. Microbial diversity: the importance of exploration and conservation. *J. Ind. Microbiol. & Biotechnol.* 18(5): 302-307.
- Cosby, W. M., Vollenbroich, D., Lee, O. H. and Zuber, P. 1998. Altered srf Expression in *Bacillus subtilis* Resulting from Changes in Culture pH Is Dependent on the Spo0K Oligopeptide Permease and the ComQX System of Extracellular Control. *J. Bacteriol.* 180(6): 1438-1445.
- Cragg, G. M., Newman, D. J. and Snader, K. M. 1997. Natural products in drug discovery and development. *J. Nat. products* 60(1): 52-60.
- Cragg, G. M., Kingston, D. G. and Newman, D. J. 2011. *Anticancer agents from natural products*. CRC press.
- Dan, V.M. and Sanawar, R., 2017. Anti cancer agents from microbes. *Bioresources and Bioprocess in Biotechnol.* (pp. 171-184). Springer, Singapore.
- De Souza Sebastianes, F. L., Romao-Dumaresq, A. S., Lacava, P.T., Harakava, R., Azevedo, J. L., de Melo, I. S. and Pizzirani-Kleiner, A. A. 2013. Species diversity of culturable endophytic fungi from Brazilian mangrove forests. *Curr. Genet.* 59(3): 153-166.
- Demain, A. L., 2014. Importance of microbial natural products and the need to revitalize their discovery. *J. Ind. Microbiol. & Biotechnol.* 41(2): 185-201.

- Ding, L., Maier, A., Fiebig, H. H., Lin, W. H. and Hertweck, C., 2011. A family of multicyclic indolosesquiterpenes from a bacterial endophyte. *Org. & biomolecular Chem.* 9(11): 4029-4031.
- Ding, L., Maier, A., Fiebig, H. H., Lin, W. H., Peschel, G. and Hertweck, C., 2012. Kandenols A–E, eudesmenes from an endophytic *Streptomyces* sp. of the mangrove tree *Kandelia candel.* *J. Nat. products* 75(12): 2223-2227.
- Driggers, E. M., Hale, S. P., Lee, J. and Terrett, N. K. 2008. The exploration of macrocycles for drug discovery—an underexploited structural class. *Nat. Rev. Drug Discovery* 7(7): 608-609.
- El Bour, M., Ismail-Ben Ali, A. and Ktari, L. 2013. Seaweeds epibionts: Biodiversity and potential bioactivities. *Microbial pathogens and strategies for combating them: Science, technology and education. Spain: Formatex Research Center* 1298-306.
- El-Helow E. R. 2001. Identification and molecular characterization of a novel *Bacillus* strain capable of degrading Tween-80. *FEMS Microbiol. Lett.* 196(2):119-122
- Epifanio, R. D. A., Pinheiro, L. S. and Alves, N. C. 2005. Polyketides from the marine sponge *Plakortis angulospiculatus.* *J. Brazilian Chem. Soc.* 16(6B): 1367-1371.
- Falowo, A. B., Fayemi, P. O. and Muchenje, V. 2014. Natural antioxidants against lipid–protein oxidative deterioration in meat and meat products: A review. *Food Res. Int.* 64: 171-181.
- Farinati, F., Piciocchi, M., Lavezzo, E., Bortolami, M. and Cardin, R. 2010. Oxidative stress and inducible nitric oxide synthase induction in carcinogenesis. *Digestive Dis.* 28(4-5): 579-584.
- Federico, A., Morgillo, F., Tuccillo, C., Ciardiello, F. and Loguercio, C. 2007. Chronic inflammation and oxidative stress in human carcinogenesis. *Int. J. Cancer* 121(11): 2381-2386.

- Feling, R. H., Buchanan, G. O., Mincer, T. J., Kauffman, C. A., Jensen, P. R. and Fenical, W., 2003. Salinosporamide A: a highly cytotoxic proteasome inhibitor from a novel microbial source, a marine bacterium of the new genus *Salinospora*. *Angewandte Chemie Int. Edition* 42(3): 355-357.
- Feliu, J. X., Cubarsi, R. and Villaverde, A. 1998. Optimized release of recombinant proteins by ultrasonication of *E. coli* cells. *Biotechnol. and bioengineering* 58(5): 536-540.
- Fickers, P., 2012. Antibiotic compounds from *Bacillus*: why are they so amazing. *American Journal of Biochemistry and Biotechnol.* (8): 38-43.
- FSOI [Forest Survey of India]. 2015. *Biannual Report 2014- 2015*. Indian State of Forest Report, Dehradun.
- Fu, P., Yang, C., Wang, Y., Liu, P., Ma, Y., Xu, L., Su, M., Hong, K. and Zhu, W. 2012. Streptocarbazoles A and B, two novel indolocarbazoles from the marine-derived actinomycete strain *Streptomyces* sp. FMA. *Org. Lett.* 14(9): 2422-2425.
- Gao, C.H., Tian, X.P., Qi, S.H., Luo, X.M., Wang, P. and Zhang, S. 2010. Antibacterial and antilarval compounds from marine gorgonian-associated bacterium *Bacillus amyloliquefaciens* SCSIO 00856. *J. antibiotics* 63(4): 191-193.
- Gilbert, N. C., Bartlett, S. G., Waight, M. T., Neau, D. B., Boeglin, W. E., Brash, A.R. and Newcomer, M. E. 2011. The structure of human 5-lipoxygenase. *Sci.* 331(6014): 217-219.
- Girden, E.R. 1992. ANOVA: Repeated measures (No. 84). Sage.
- Goecke, F., Labes, A., Wiese, J. and Imhoff, J. F. 2010. Chemical interactions between marine macroalgae and bacteria. *Mar. Ecol. Progress Series* 409: 267-299.

- Gokhale, R. S., Tsuji, S. Y., Cane, D. E. and Khosla, C. 1999. Dissecting and exploiting intermodular communication in polyketide synthases. *Science* 284(5413): 482-485.
- Gomez, V.L.J., Soria-Mercado, I.E., Rivas, G.G., Ayala-Sanchez, N.E., 2010. Antibacterial and anticancer activity of seaweeds and bacteria associated with their surface. *Rev. Biol. Mar. Oceanogr.* 45, 267–275.
- Gordon, R. E., Haynes, W. C., Pang, C. H. N. and Smith, N. R. 1973. The genus *Bacillus*. *US Dep. of Agric. handbook* 427: 109-26.
- Gustafson, J. E. and Wilkinson, B. J. 1989. Lower autolytic activity in a homogeneous methicillin-resistant *Staphylococcus aureus* strain compared to derived heterogeneous-resistant and susceptible strains. *FEMS Microbiol. Lett.* 59(1-2): 107-111.
- Halliwell, B., Murcia, M. A., Chirico, S. and Aruoma, O. I. 1995. Free radicals and antioxidants in food and in vivo: what they do and how they work. *Crit. Rev. in Food Sci. & Nutr.* 35(1-2): 7-20.
- Han, Z., Xu, Y., McConnell, O., Liu, L., Li, Y., Qi, S., Huang, X. and Qian, P. 2012. Two antimycin A analogues from marine-derived actinomycete *Streptomyces lusitanus*. *Mar. drugs* 10(3): 668-676.
- Han, Y., Tian, E., Xu, D., Ma, M., Deng, Z. and Hong, K. 2016. Halichoblelide D, a new elaiophylin derivative with potent cytotoxic activity from mangrove-derived *Streptomyces* sp. 219807. *Molecules* 21(8): 970-972.
- Handelsman, J., Rondon, M. R., Brady, S. F., Clardy, J. and Goodman, R. M. 1998. Molecular biological access to the chemistry of unknown soil microbes: a new frontier for natural products. *Chem. & Biol.* 5(10): 245-249.
- Holguin, G., Vazquez, P. and Bashan, Y., 2001. The role of sediment microorganisms in the productivity, conservation, and rehabilitation of

- mangrove ecosystems: an overview. *Biol. and Fertil. of soils*, 33(4): 265-278.
- Hong, K., Gao, A. H., Xie, Q. Y., Gao, H. G., Zhuang, L., Lin, H. P., Yu, H. P., Li, J., Yao, X.S., Goodfellow, M. and Ruan, J. S. 2009. Actinomycetes for marine drug discovery isolated from mangrove soils and plants in China. *Mar. drugs*. 7(1): 24-44.
- Hu, H. Q., Li, X. S. and He, H., 2010. Characterization of an antimicrobial material from a newly isolated *Bacillus amyloliquefaciens* from mangrove for biocontrol of Capsicum bacterial wilt. *Biol. control* 54(3): 359-365.
- Hu, Y. and MacMillan, J. B. 2011. Erythrazoles A–B, Cytotoxic Benzothiazoles from a Marine-Derived *Erythrobacter* sp. *Org. Lett.* 13(24): 6580-6583.
- Hutchinson, C. R. 1999. Microbial polyketide synthases: more and more prolific. *Proc. Natl. Acad. Sci.* 96(7): 3336-3338.
- ISFR [Indian State of Forest Report]. 2017. Available : <https://currentaffairs.gktoday.in/india-state-forest-report-isfr-2017-released-moefcc-02201852632.html>
- Jaruchoktaweechai, C., Suwanborirux, K., Tanasupawatt, S., Kittakoop, P. and Menasveta, P. 2000. New macrolactins from a marine *Bacillus* sp. Sc026. *J. Nat. products* 63(7): 984-986.
- Joel, E.L., Bhimba, V. 2010. Isolation and characterization of secondary metabolites from the mangrove plant *Rhizophora mucronata*. *Asian Pac. J. Trop. Med.* 3: 602–604.
- Kanagasabhpathy, M., Sasaki, H. and Nagata, S. 2008. Phylogenetic identification of epibiotic bacteria possessing antimicrobial activities isolated from red algal species of Japan. *World J. Microbiol. and Biotechnol.* 24(10): 2315-2321.

- Kathiresan, K. and Bingham, B. L. 2001 Biology of Mangroves and Mangrove Ecosystems. *Adv. in Mar. Biol.* 40: 81-251.
- Katz, L. and Baltz, R.H. 2016. Natural product discovery: past, present, and future. *J. Ind. Microbiol. & Biotechnol.* 43(2-3): 155-176.
- Kavitha, R., Aiswariya, S. and Ratnavali, C. M. 2010. Anticancer activity of red pigment from *Serratia marcescens* in human cervix carcinoma. *Int. J. Pharma. Res.* 2(1): 784-787.
- Kaźmierczak, D., Ciesielski, W., Zakrzewski, R. and Żuber, M. 2004. Application of iodine-azide reaction for detection of amino acids in thin-layer chromatography. *J. Chromatography A* 1059(1-2): 171-174.
- Kim, S. Y., Kim, J. Y., Kim, S. H., Bae, H. J., Yi, H., Yoon, S. H., Koo, B. S., Kwon, M., Cho, J. Y., Lee, C. E. and Hong, S., 2007. Surfactin from *Bacillus subtilis* displays anti-proliferative effect via apoptosis induction, cell cycle arrest and survival signaling suppression. *FEBS Lett.* 581(5): 865-871.
- Kim, S. H., Ko, H., Bang, H. S., Park, S. H., Kim, D. G., Kwon, H. C., Kim, S.Y., Shin, J. and Oh, D.C. 2011. Coprismycins A and B, neuroprotective phenylpyridines from the dung beetle-associated bacterium, *Streptomyces* sp. *Bioorganic & Med. Chem. Lett.* 21(19): 5715-5718.
- Kimura, M., 1980. A simple method for estimating evolutionary rates of base substitutions through comparative studies of nucleotide sequences. *J. Mol. Evol.* 16(2): 111-120.
- Kizhakkekalam, V. K. and Chakraborty, K. 2019. Pharmacological properties of marine macroalgae-associated heterotrophic bacteria. *Archives of microbiol.* 201(4): 505-518.
- Kluge, B., Vater, J., Salnikow, J. and Eckart, K. 1988. Studies on the biosynthesis of surfactin, a lipopeptide antibiotic from *Bacillus subtilis* ATCC 21332. *FEBS Lett.* 231(1): 107-110.

- Knight, V., Sanglier, J. J., DiTullio, D., Braccili, S., Bonner, P., Waters, J., Hughes, D. and Zhang, L. 2003. Diversifying microbial natural products for drug discovery. *Appl. Microbiol. and Biotechnol.* 62(5-6): 446-458.
- Krieg, N.R. and Holt, J.G. 1984. Bergey's Manual of Systemetic Bacteriology (George, G., Boone, D.R., Castenholz, R. W., Eds.) *William and Wilkins, Baltimore, London* 1: 635- 637.
- Kucharska-Newton, A. M., Couper, D. J., Pankow, J. S., Prineas, R. J., Rea, T. D., Sotoodehnia, N., Chakravarti, A., Folsom, A. R., Siscovick, D. S. and Rosamond, W. D. 2009. Hemostasis, inflammation, and fatal and nonfatal coronary heart disease: long-term follow-up of the atherosclerosis risk in communities (ARIC) cohort. *Arteriosclerosis, thrombosis, and vascular biology* 29(12): 2182-2190.
- Kugler, M., Loeffler, W., Rapp, C., Kern, A. and Jung, G., 1990. Rhizocticin A, an antifungal phosphono-oligopeptide of *Bacillus subtilis* ATCC 6633: biological properties. *Arch. of Microbiol.* 153(3): 276-281.
- Kusuma, S., Kumar, P. A. and Boopalan, K. 2011. Potent antimicrobial activity of *Rhizophora mucronata*. *J. Ecobiotechnol.*
- Law, J. W. F., Ser, H. L., Duangjai, A., Saokaew, S., Bukhari, S. I., Khan, T. M., Ab Mutalib, N. S., Chan, K. G., Goh, B. H. and Lee, L. H. 2017. *Streptomyces colonosanans* sp. nov., a novel actinobacterium isolated from Malaysia mangrove soil exhibiting antioxidative activity and cytotoxic potential against human colon cancer cell lines. *Frontiers in microbiology* 8: 877.
- Lechevalier, H. A. and Lechevalier, M. P. 1981. Actinomycete genera "in search of a family". *The Prokaryotes: a Handbook on Habitats, Isolation, and Identification of Bacteria* 2118-2123.
- Lee, S. Y., Primavera, J. H., Dahdouh-Guebas, F., McKee, K., Bosire, J. O., Cannicci, S., Diele, K., Fromard, F., Koedam, N., Marchand, C. and

- Mendelssohn, I., 2014. Ecological role and services of tropical mangrove ecosystems: a reassessment. *Global Ecol. and Biogeogr.* 23(7): 726-743.
- Lemos, M. L., Toranzo, A. E. and Barja, J. L. 1985. Antibiotic activity of epiphytic bacteria isolated from intertidal seaweeds. *Microbial Ecology* 11(2): 149-163.
- Li Y., Xu Y., Liu L., Han Z., Lai, P. Y., Guo, Xiangrong, Zhang, X., Lin W., Qian, P. Y. 2012. Five new amicoumacins isolated from a marine-derived bacterium *Bacillus subtilis*. *Mar. Drugs.* 10: 319-328.
- Liao, H., Li, Y., Guo, X., Lin, X., Lai, Q., Xu, H., Zheng, T. and Tian, Y. 2017. *Mangrovitalea sediminis* gen. nov., sp. nov., a member of the family Alteromonadaceae isolated from mangrove sediment. *Int. J. Syst. and Evol. Microbiol.* 67(12): 5172-5178.
- Liang, J. B., Chen, Y. Q., Lan, C. Y., Tam, N. F., Zan, Q. J. and Huang, L. N. 2007. Recovery of novel bacterial diversity from mangrove sediment. *Mar. Biol.* 150(5): 739-747.
- Lin, Y., Wu, X., Feng, S., Jiang, G., Luo, J., Zhou, S., Vrijmoed, L. L. P., Jones, E. G., Krohn, K., Steingröver, K. and Zsila, F. 2001. Five unique compounds: xyloketals from mangrove fungus *Xylaria* sp. from the South China Sea coast. *J. Org. Chem.* 66(19): 6252-6256
- Liu, Y., Du, J., Lai, Q., Zeng, R., Ye, D., Xu, J. and Shao, Z. 2017. Proposal of nine novel species of the *Bacillus cereus* group. *Int. J. Syst. and Evol. Microbiol.* 67(8): 2499-2508.
- Loganathachetti, D. S., Poesakkannu, A. and Muthuraman, S. 2017. Fungal community assemblage of different soil compartments in mangrove ecosystem. *Sci. Rep.* 7(1): 8560-8561.
- Ludwig-Müller, J. 2015. Plants and endophytes: equal partners in secondary metabolite production?. *Biotechnol. Lett.* 37(7): 1325-1334.

- Luft, J. H., Zweifach, B. W., Grant, L. and McCluskey, R. T. 1965. The Inflammatory Process. New York: Academic Press. Luft121 The inflammatory process 1965 121.
- Maget-Dana, R. and Peypoux, F. 1994. Iturins, a special class of pore-forming lipopeptides: biological and physicochemical properties. *Toxicology* 87(1-3): 151-174.
- Mahmoud, M. G., Mohamed, S. S., Ibrahim, A. Y., El Awady, M. E. and Youness, E. R. 2016. Exopolysaccharide produced by *Paenibacillus lactes* NRC1: its characterization and anti-inflammatory activity via cyclooxygenases inhibitory activity and modulation of inflammation related cytokines. *Der Pharma Chemica* 8:16-26.
- Marti, M. E., Colonna, W. J., Patra, P., Zhang, H., Green, C., Reznik, G., Pynn, M., Jarrell, K., Nyman, J. A., Somasundaran, P. and Glatz, C. E. 2014. Production and characterization of microbial biosurfactants for potential use in oil-spill remediation. *Enzyme and Microbial Technol.* 55: 31-39.
- Matassa, S., Boon, N., Pikaar, I. and Verstraete, W. 2016. Microbial protein: future sustainable food supply route with low environmental footprint. *Microbial biotechnol.* 9(5): 568-575.
- May, J. J., Wendrich, T. M. and Marahiel, M. A. 2001. The *dhb* operon of *Bacillus subtilis* Encodes the biosynthetic template for the catecholic siderophore 2, 3-dihydroxybenzoate-glycine-threonine trimeric ester bacillibactin. *J. Biol. Chem.* 276(10): 7209-7217.
- Meena, K. R., Dhiman, R., Sharma, A. and Kanwar, S. S. 2016. Applications of lipopeptide (s) from a *Bacillus* sp: an overview. *Res. J. Recent Sci.* 5: 50-54.
- Mendes, L. and Tsai, S. 2014. Variations of bacterial community structure and composition in mangrove sediment at different depths in Southeastern Brazil. *Diversity* 6(4): 827-843.

- Maughan, H. and Van der Auwera, G., 2011. Bacillus taxonomy in the genomic era finds phenotypes to be essential though often misleading. *Infection, Genetics and Evolution* 11(5): 789-797.
- Miranda-Bautista, J., Bañares, R. and Vaquero, J. 2017. The Gastrointestinal System: Anatomy and Sources of Oxidative Stress. *In Gastrointestinal tissue* (pp. 3-20). Academic Press.
- Mizumoto, S., Hirai, M. and Shoda, M. 2006. Production of lipopeptide antibiotic iturin A using soybean curd residue cultivated with *Bacillus subtilis* in solid-state fermentation. *Appl. Microbiol. and Biotechnol.* 72(5): 869-870.
- Monod, J., 1949. The growth of bacterial cultures. *Annu. Rev. Microbiol.* 3(1): 371-394.
- Mulligan, C. N. 2005. Environmental applications for biosurfactants. *Environ. Pollut.* 133(2): 183-198.
- Nagao, T., Adachi, K., Sakai, M., Nishijima, M. and Sano, H. 2001. Novel macrolactins as antibiotic lactones from a marine bacterium. *J. Antibiot.* 54(4): 333-339.
- Nambudiri, S. Ernakulam has maximum number of mangrove species. *The Times of India*, 5 Aug. 2018.
- Nandakumar R., Rush M. C. Correa F. 2007. Association of *Burkholderia glumae* and *B. gladioli* with panicle blight symptoms on rice in Panama. *Plant Dis.* 91(6): 767-767.
- Naragani, K., Mangamuri, U., Muvva, V., Poda, S. and Munaganti, R. K. 2016. Antimicrobial potential of *Streptomyces cheonanensis* VUK-a from mangrove origin. *Int. J. Pharm. Pharm. Sci.* 8(3): 53-7.
- Nathan, C. 2002. Points of control in inflammation. *Nat.* 420(6917): 846.
- Nebula, M., Harisankar, H. S., Chandramohanakumar, N. 2013. Metabolites and bioactivities of Rhizophoraceae mangroves. *Nat. Products Bioprospect.* 3(5): 207-232.

- Newman, D. J., Cragg, G. M. and Snader, K. M., 2003. Natural products as sources of new drugs over the period 1981– 2002. *J. Nat. products* 66(7): 1022-1037.
- Newman, D. J. and Cragg, G. M. 2007. Natural products as sources of new drugs over the last 25 years. *J. Nat. products* 70(3): 461-477.
- Newman, D. J. and Cragg, G. M. 2012. Natural products as sources of new drugs over the 30 years from 1981 to 2010. *J. natural products* 75(3): 311-335.
- Newman, D. and Cragg, G. 2014. Marine-sourced anti-cancer and cancer pain control agents in clinical and late preclinical development. *Mar. drugs* 12(1): 255-278.
- Newman, D. J. and Cragg, G. M. 2016. Natural products as sources of new drugs from 1981 to 2014. *J. Nat. products* 79(3): 629-661.
- Nishikori T., Naganawa H., Muraoka Y., Aoyagi T., Umezawa H. 1986. Plispastins; new inhibitors of phospholopase A2, produced by *Bacillus cereus* BMG302-ff67. III. Structural elucidation of plispastins. *J. Antibiot.* (Tokyo) 39: 755-761
- Palys, T., Berger, E., Mitrica, I., Nakamura, L. K. and Cohan, F. M. 2000. Protein-coding genes as molecular markers for ecologically distinct populations: the case of two *Bacillus* species. *Int. J. Syst. and Evol. Microbiol.* 50(3): 1021-1028.
- Park H.B., Perez C. E., Perry E. K., Crawford J. M. 2016. Activating and attenuating the amicoumacin antibiotics. *Molecules.* 21: 824.
- Patel, P. S., Huang, S., Fisher, S., Pirnik, D., Aklonis, C., Dean, L., Meyers, E., Fernandes, P. and Mayerl, F. 1995. Bacillaene, a novel inhibitor of procaryotic protein synthesis produced by *Bacillus subtilis*. *J. Antibiot.* 48(9): 997-1003.

- Pathak, K. V. and Keharia, H. 2014. Identification of surfactins and iturins produced by potent fungal antagonist, *Bacillus subtilis* K1 isolated from aerial roots of banyan (*Ficus benghalensis*) tree using mass spectrometry. *3 Biotech.* 4(3): 283-295.
- Pelczar Jr, M. J., Reid, R. D. and Chan, E. C. S. 1977. *Microbiol.* 4th Edi.
- Persidis, A. 1998: Extremophiles. *Nat. Biotechnol.* 16: 593–594
- Pinchuk, I. V., Bressollier, P., Verneuil, B., Fenet, B., Sorokulova, I. B., Mégraud, F. and Urdaci, M. C. 2001. In Vitro Anti-Helicobacter pylori Activity of the Probiotic Strain *Bacillus subtilis* 3 Is Due to Secretion of Antibiotics. *Antimicrobial agents and chemotherapy* 45(11): 3156-3161.
- Plaža, G., Chojniak, J. and Banat, I. 2014. Biosurfactant mediated biosynthesis of selected metallic nanoparticles. *Int. J. Mol. Sci.* 15(8): 13720-13737.
- Poljsak, B., Šuput, D. and Milisav, I. 2013. Achieving the balance between ROS and antioxidants: when to use the synthetic antioxidants. *Oxidative medicine and cellular longevity* 2013.
- Prathiba, S. and Jayaraman, G. 2018. Evaluation of the anti-oxidant property and cytotoxic potential of the metabolites extracted from the bacterial isolates from mangrove Forest and saltern regions of South India. *Preparative Biochem. and Biotechnol.* 48(8): 50-758.
- Psenner, R. and Sattler, B. 1998. Life at the freezing point. *Sci.* 280(5372): 2073-2074.
- Public Health England, 2018 Available : <https://www.gov.uk/government/organisations/public-health-england>
- Pye, C. R., Bertin, M. J., Lokey, R. S., Gerwick, W. H. and Linington, R.G. 2017. Retrospective analysis of natural products provides insights for future discovery trends. *Proc. Natl. Acad. of Sci.* 114(22): 5601-5606.

- Rahal, A., Kumar, A., Singh, V., Yadav, B., Tiwari, R., Chakraborty, S. and Dhama, K. 2014. Oxidative stress, prooxidants, and antioxidants: the interplay. *BioMed. Res. Int.*
- Re, R., Pellegrini, N., Proteggente, A., Pannala, A., Yang, M. and Rice-Evans, C. 1999. Antioxidant activity applying an improved ABTS radical cation decolorization assay. *Free radical Biol. and Med.* 26(9-10): 1231-1237.
- Saenger, P., 2013. Mangrove ecology, silviculture and conservation. *Springer Science & Business Media.*
- Sanjivkumar, M., Babu, D. R., Suganya, A. M., Silambarasan, T., Balagurunathan, R. and Immanuel, G. 2016. Investigation on pharmacological activities of secondary metabolite extracted from a mangrove associated actinobacterium *Streptomyces olivaceus* (MSU3). *Biocatalysis and Agric. Biotechnol.* 6: 82-90.
- Sekurova, O. N., Schneider, O. and Zotchev, S. B. 2019. Novel bioactive natural products from bacteria via bioprospecting, genome mining and metabolic engineering. *Microbial biotechnol.* 12 (5): 828-844
- Sengupta, S., Pramanik, A., Basak, P. and Bhattacharyya, M. 2018. Draft Genome Sequence of Bioactive Strain *Streptomyces* sp. SMS_SU21, Isolated from Soil Sediment of the Sundarbans Mangrove Ecosystem. *Genome Announc.* 6(27): 1-7.
- Ser, H. L., Palanisamy, U. D., Yin, W. F., Abd Malek, S. N., Chan, K. G., Goh, B. H. and Lee, L. H., 2015. Presence of antioxidative agent, Pyrrolo [1, 2-a] pyrazine-1, 4-dione, hexahydro-in newly isolated *Streptomyces mangrovisoli* sp. nov. *Front. Microbiol.* 6: 854-855.
- Ser, H. L., Palanisamy, U. D., Yin, W. F., Chan, K. G., Goh, B. H. and Lee, L. H., 2016. *Streptomyces malaysiense* sp. nov.: a novel Malaysian mangrove soil actinobacterium with antioxidative activity and cytotoxic potential against human cancer cell lines. *Sci. Rep.* 6: 24247-24248.

- Shahidi, F. 2000. Antioxidants in food and food antioxidants. *Food/nahrung*, 44(3): 158-163.
- Sherris, J. C., Shoesmith, J. G., Parker, M.T. and Breckon, D., 1959. Tests for the rapid breakdown of arginine by bacteria: their use in the identification of pseudomonads. *Microbiology* 21(2): 389-396.
- Simões, M. F., Antunes, A., Ottoni, C. A., Amini, M. S., Alam, I., Alzubaidy, H., Mokhtar, N. A., Archer, J. A. and Bajic, V. B. 2015. Soil and rhizosphere associated fungi in gray mangroves (*Avicennia marina*) from the Red Sea—a metagenomic approach. *Genomics, proteomics & bioinformatics*, 13(5): 310-320.
- Sostres, C., Gargallo, C.J., Arroyo, M.T. and Lanás, A., 2010. Adverse effects of non-steroidal anti-inflammatory drugs (NSAIDs, aspirin and coxibs) on upper gastrointestinal tract. *Best practice & Res. Clin. Gastroenterol.* 24(2): 121-132.
- Souto, G. I., Correa, O. S., Montecchia, M. S., Kerber, N. L., Pucheu, N. L., Bachur, M. and Garcia, A. F. 2004. Genetic and functional characterization of a *Bacillus* sp. strain excreting surfactin and antifungal metabolites partially identified as iturin-like compounds. *J. Appl. Microbiol.* 97(6): 1247-1256.
- Srinivas, D., Mital, B.K. and Garg, S.K., 1990. Utilization of sugars by *Lactobacillus acidophilus* strains. *Int. J. food Microbiol.* 10(1): 51-57.
- Suganthi C., Mageswari A., Karthikeyan S., Anbalagan M., Sivakumar A., Gothandam K. M. 2013. Screening and optimization of protease production from a halotolerant *Bacillus licheniformis* isolated from saltern sediments. *J. Genet. Eng. and Biotechnol.* 11(1): 47-52
- Sun, J., Shao, J., Sun, C., Song, Y., Li, Q., Lu, L., Hu, Y., Gui, C., Zhang, H. and Ju, J., 2018. Borrelidins F–I, cytotoxic and cell migration inhibiting agents from mangrove-derived *Streptomyces rochei* SCSIO ZJ89. *Bioorganic & Med. Chem.* 26(8): 1488-1494.

- Sun, W., Wu, W., Liu, X., Zaleta-Pinet, D. A. and Clark, B. R. 2019. Bioactive compounds isolated from marine-derived microbes in China: 2009–2018. *Mar. drugs* 17(6): 339-340.
- Takao, T., Kitatani, F., Watanabe, N., Yagi, A. and Sakata, K. 1994. A simple screening method for antioxidants and isolation of several antioxidants produced by marine bacteria from fish and shellfish. *Bioscience, Biotechnol. and Biochem.* 58(10): 1780-1783.
- Tamehiro, N., Okamoto-Hosoya, Y., Okamoto, S., Ubukata, M., Hamada, M., Naganawa, H. and Ochi, K. 2002. Bacilysocin, a novel phospholipid antibiotic produced by *Bacillus subtilis* 168. *Antimicrobial Agents and Chemotherapy* 46(2): 315-320.
- Tan, R.X. and Zou, W.X., 2001. Endophytes: a rich source of functional metabolites. *Natural product reports* 18(4): 448-459.
- Tan, L.T.H., Chan, K.G., Khan, T.M., Bukhari, S.I., Saokaew, S., Duangjai, A., Pusparajah, P., Lee, L.H. and Goh, B.H., 2017. *Streptomyces* sp. MUM212 as a source of antioxidants with radical scavenging and metal chelating properties. *Front. in Pharmacol.* 8: 276.
- Thatoi, H. N. and Biswal, A. K. 2008. Mangroves of Orissa Coast: floral diversity and conservation status. *Spec. Habitats and Threatened Plants of India.* 11(1): 201-208.
- Thilakan, B., Chakraborty, K. and Chakraborty, R.D. 2016. Antimicrobial properties of cultivable bacteria associated with seaweeds in the Gulf of Mannar on the southeast coast of India. *Canadian J. Microbiol.* 62(8): 668-681.
- Thongjun, J., Tansila, N., Panthong, K., Tanskul, S., Nishibuchi, M. and Vuddhakul, V. 2016. Inhibitory potential of biosurfactants from *Bacillus amyloliquefaciens* derived from mangrove soil against *Vibrio parahaemolyticus*. *Ann. of Microbiol.* 66(3): 1257-1263.

- Thoppil, R. J. and Bishayee, A. 2011. Terpenoids as potential chemopreventive and therapeutic agents in liver cancer. *World J. Hepatol.* 3(9): 228-230.
- Tomlinson P.B. 2016 *The Botany of Mangroves*. 2nd ed. Cambridge University Press; Cambridge, UK: Ecology 11–28.
- Uzair, B., Ahmed, N., Ahmad, V. U., Mohammad, F. V. and Edwards, D. H., 2008. The isolation, purification and biological activity of a novel antibacterial compound produced by *Pseudomonas stutzeri*. *FEMS Microbiol. Lett.* 279(2): 243-250.
- Vanittanakom, N., Loeffler, W., Koch, U. and Jung, G., 1986. Fengycin-a novel antifungal lipopeptide antibiotic produced by *Bacillus subtilis* F-29-3. *J. antibiot.* 39(7): 888-901.
- Velho-Pereira, S., Parvatkar, P. and Furtado, I. J., 2015. Evaluation of antioxidant producing potential of halophilic bacterial bionts from marine invertebrates. *Indian J. Pharma. Sci.* 77(2): 183-184.
- Waldi, D. 1965. Spray reagents for thin-layer chromatography. In *Thin-layer chromatography* (pp. 483-502). Springer, Berlin, Heidelberg.
- Watve, M. G., Tickoo, R., Jog, M. M. and Bhole, B. D. 2001. How many antibiotics are produced by the genus *Streptomyces*?. *Arch. Microbiol.* 176(5): 386-390.
- Wiese, J., Thiel, V., Nagel, K., Staufenberger, T. and Imhoff, J. F. 2009. Diversity of antibiotic-active bacteria associated with the brown alga *Laminaria saccharina* from the Baltic Sea. *Mar. Biotechnol.* 11(2): 287-300.
- Wiese, J. and Imhoff, J. F. 2019. Marine bacteria and fungi as promising source for new antibiotics. *Drug Dev. Res.* 80(1): 24-27.
- Winter, J. M., Sato, M., Sugimoto, S., Chiou, G., Garg, N.K., Tang, Y. and Watanabe, K. 2012. Identification and characterization of the chaetoviridin and chaetomugilin gene cluster in *Chaetomium*

- globosum* reveal dual functions of an iterative highly-reducing polyketide synthase. *J. American Chem. Soc.* 134(43): 17900-17903.
- Winter, J. M., Chiou, G., Bothwell, I. R., Xu, W., Garg, N. K., Luo, M., Tang, Y. 2016. Expanding the structural diversity of polyketides by exploring the cofactor tolerance of an inline methyltransferase domain. *Org. Lett.* 15: 3774–3777.
- Wu, J., Xiao, Q., Xu, J., Li, M.Y., Pan, J.Y. and Yang, M.H., 2008. Natural products from true mangrove flora: source, chemistry and bioactivities. *Nat. Product Rep.* 25(5): 955-981.
- Yasmeen, S., Muvva, V. and Munaganti, R. K. 2016. Isolation and characterization of bioactive *Streptomyces* from mangrove ecosystem of machilipatnam, Krishna district, Andhra Pradesh. *Asian J. Pharm. Clin. Res.* 9(3): 258-263.
- Ye, F., Li, X.W. and Guo, Y. W. 2016. Recent progress on the mangrove plants: Chemistry and bioactivity. *Curr. Org. Chem.* 20(18): 1923-1942.
- Yin, H., Guo, C., Wang, Y., Liu, D., Lv, Y., Lv, F. and Lu, Z., 2013. Fengycin inhibits the growth of the human lung cancer cell line 95D through reactive oxygen species production and mitochondria-dependent apoptosis. *Anti-cancer drugs.* 24(6): 587-598.
- Young, I. M. and Crawford, J. W. 2004. Interactions and self-organization in the soil-microbe complex. *Sci.* 304(5677): 1634-1637.
- Youssef, T. and Saenger, P., 1998. Photosynthetic gas exchange and accumulation of phytotoxins in mangrove seedlings in response to soil physico-chemical characteristics associated with waterlogging. *Tree Physiol.* 18(5): 317-324.
- Youssef, T. and Saenger, P., 1999. Mangrove zonation in Mobbs Bay—Australia. *Estuarine, Coastal and Shelf Sci.* 49: 43-50.

- Zainal, N., Ser, H.L., Yin, W. F., Tee, K. K., Lee, L. H. and Chan, K.G., 2016. *Streptomyces humi* sp. nov., an actinobacterium isolated from soil of a mangrove forest. *Antonie van Leeuwenhoek* 109(3): 467-474.
- Zhang Y., Dong J., Yang B., Ling J., Wang Y. and Zhang S. I. 2009. Bacterial community structure of mangrove sediments in relation to environmental variables accessed by 16S rRNA gene-denaturing gradient gel electrophoresis fingerprinting. *Scientia Marina*. 73(3): 487-498.
- Zhao, H., Yan, L., Xu, X., Jiang, C., Shi, J., Zhang, Y., Liu, L., Lei, S., Shao, D. and Huang, Q., 2018. Potential of *Bacillus subtilis* lipopeptides in anti-cancer I: induction of apoptosis and paraptosis and inhibition of autophagy in K562 cells. *AMB Express*. 8(1): 78-79.
- Zhao H. B., Shao D. Y., Jiang C. M., Shi J. L., Li Q., Huang Q. S., Rajoka MSR, Yang H., Jin M. L. 2017. Biological activity of lipopeptides from *Bacillus*. *Appl. Microbiol. Biotechnol.* 101(15): 5951–5960.

**IDENTIFICATION AND CHARACTERIZATION OF BIOACTIVE
LEADS FROM MANGROVE SEDIMENT
ASSOCIATED BACTERIA AND ASSESSMENT OF THEIR
THERAPEUTIC POTENTIAL**

By

LAKSHMI RAJAN

(2014-09-103)

Abstract of the Thesis

Submitted in partial fulfilment of the requirement for the degree of

B. Sc. - M. Sc. (INTEGRATED) BIOTECHNOLOGY

Faculty of Agriculture

Kerala Agricultural University, Thrissur



DEPARTMENT OF PLANT BIOTECHNOLOGY

COLLEGE OF AGRICULTURE

VELLAYANI, THIRUVANANTHAPURAM - 695 522

KERALA, INDIA

2019

158

ABSTRACT

Mangrove sediment associated bacteria are of significant importance in the field of medicine and pharmaceuticals as new promising sources of biologically active pharmacophores due to extreme conditions, such as high salt concentrations and soil anoxia. This study aimed to evaluate the antimicrobial, antioxidant and anti-inflammatory properties of *Bacillus amyloliquefaciens* associated with *Acanthus ilicifolius* and *Avicennia officinalis*, collected from the Mangalavanam mangrove ecosystem of Kerala State of India. The bacteria exhibiting significant antioxidant and antimicrobial activities were isolated, identified and characterized by integrated biochemical, morphological, microbiological and 16S rRNA sequencing. Spot-over-lawn-assay was carried out to screen all the 40 isolates against various pathogens like *A. caviae*, *E. coli*, *V. parahemolyticus* and MRSA to hit upon the antibacterial compound producing microbes. The *B. amyloliquefaciens* MK765025 strain exhibiting significant antimicrobial activity against *V. parahemolyticus* and antioxidant activity against the free radicals, was selected for further extraction and purification of bioactive metabolites. The extraction of bioactive compounds was carried out using ethyl acetate to obtain the crude organic extracts and exhibited potential antioxidant activities (i.e., IC_{50} 3.5 $\mu\text{g/mL}$ and 3.9 $\mu\text{g/mL}$ to quench DPPH and ABTS radical species, respectively) coupled with 5-lipoxygenase inhibitory activity (IC_{50} 6 $\mu\text{g/mL}$). The extracellular organic extracts exhibited potential activity towards the test pathogens *V. parahemolyticus*, MRSA, *E. coli* and *A. caviae* with the inhibition zone ranging from 16-22 mm for 100 μg of the extract in disc diffusion assay. The minimum inhibitory concentration was determined by broth dilution method against different pathogenic bacteria, and was found to be lesser than 12.5 μg for all the test organisms. The crude extract of *B. amyloliquefaciens* MK765025 exhibited significant antimicrobial, antioxidant and anti-inflammatory activities, and therefore, was selected for purification on C_{18} reverse stationary phases to yield two polyketides with oxotetrahydrofuran moiety. The compound (2) displayed potential antioxidant activities (IC_{50} 0.31-0.32 mg/mL) and anti-inflammatory properties against pro-inflammatory lipoyxygenase (IC_{50} 0.90 mg/mL). Thus the compound 2, could find its utilities as valuable pharmacophore with potential antioxidant and anti-inflammatory properties.

